2016

Time-Lapse Polymerizations Triggered by pH clock Reactions

Elizabeth Jee
Louisiana State University and Agricultural and Mechanical College, liz.jee@live.com

TIME-LAPSE POLYMERIZATIONS TRIGGERED BY PH CLOCK REACTIONS

A Dissertation

Submitted to the Graduate Faculty of the
Louisiana State University and
Agricultural and Mechanical College
in partial fulfillment of the
requirements for the degree of
Doctor of Philosophy

in

The Department of Chemistry

by
Elizabeth Nicole Pohlmann Jee
B.S. Southeastern Louisiana University, 2010
August 2016

ACKNOWLEDGEMENTS

There are so many people to thank for helping me to get where I am today. My dear friends deserve a huge thank you for always being near to lend a hand or an ear, and just being great people. Without you all I would have gone crazy a long time ago. Thank you for filling my life with so many happy memories!

My chemistry journey started with the awesome faculty and staff in the department of chemistry and physics at Southeastern Louisiana University. Dr. Vogel taught me the first chemistry course and persuaded me to enroll as a chemistry major because it would give me an edge over the biology majors trying to get into med school. After the end of my second year in the program and having met the rest of the instructors I realized I did not truly want to be a medical doctor, but a chemist instead. All thanks to the wonderful instruction, encouragement, and fun I had in those classes with those people. All of the departmental faculty and staff were great but these instructors specifically had a hand in directing my path: Dr. Dolliver, Dr. Sommerfeld, Dr. Norwood, Dr. Kim, Dr. Parkinson, Dr. Temple, Dr. Voegel, Dr. Fotie, Dr. Doughty, and Dr. Allain. These are a mix of chemists and physicists and they showed me how cool and interesting science really is. I never had an interest in the scientific fields until my time as a chemistry major with these amazing instructors. Thank you for awakening something in me I never knew existed. I can never thank you enough.

My colleagues at school, the Pojman Team and Britney (especially Leah and Britney), have been very helpful with problems of research and life. As graduate students in the same department we have similar struggles and accomplishments. It's awesome to have such a great support network that truly understands this craziness we

call graduate school. Thank you for being a part of this chapter in my life and letting me be a part of yours.

My professors here at LSU have been so amazing! When people ask me why I chose LSU, one of my reasons is the great people! From my first visit I could tell how much the professors care about the students and want them to succeed. A big thank you goes to my divisional professors and committee members, Dr. Pojman, Dr. Zhang, Dr. Spivak, Dr. Russo, Dr. Cueto, and Dr. Hayes, for always demanding more than what I give. Teaching me to work hard for success and also everything I've learned about macromolecular chemistry. You each have a different set of expertise in the field and I value every one. I didn't fall in love with chemistry until I learned about polymers. Thank you for pushing me in that direction my first semester.

A special thank you goes to my major advisor, Dr. Pojman. His hands-off mentoring approach taught me how to be self-reliant and independent, yet know when to ask for help. When I started working in his lab I didn't know a single thing about polymers and he forced me to figure it out on my own. Looking back now I realize how valuable this training has been. It has given me the confidence and knowledge to tackle any research problems I may encounter, because if I don't know the answers or where to start I know how to figure it out. Thank you for helping me become an independent, free-thinking scientist.

My family deserves a huge thank you for always being a constant source of love, support, and encouragement. A special shout out goes to my parents. They instilled within me the values of kindness, sincerity, hard work, and dedication from a young age. Without which I believe I would not be successful in life. To my father, thank you for

always being a voice of comfort when I am feeling overwhelmed or sad. To my mother, I am eternally grateful for everything you have sacrificed for me and given to me to show me the true meaning of unconditional love. Without you I would not be half the woman I am today. Thank you from the bottom of my heart.

Finally, I would like to dedicate this work to my daughter, Amalie. You have been the shining light in my life since your arrival. You give me a reason to greet each day with a smile and the strength to overcome any obstacle. I thank God every day that I get to be your mother. I hope this dissertation can show you the power of hard work and dedication and what you can accomplish if you don't give up on yourself and follow through with your goals. I love you to the moon and back and moon and back and moon and back times infinity.

TABLE OF CONTENTS

ABSTRACT

The theme of this work is time-lapse polymerizations triggered by pH clock reactions. The first chapter is the introduction and gives a long overview of the different chemistries studied here. The second chapter focuses on the bromate-sulfite clock reaction. Based on some simplified and accepted reaction equations[1] for the bromate-sulfite clock, we presumed it may be possible to increase the pH of the solution via ammonia addition and hinder or significantly reduce the reactivity of the clock reagents, thus creating a storage stable reaction.

Adding a polymer system that would not crosslink until the solution became acidic would have created a storable, cure-on-demand, adhesive or coating system that could be triggered by the drop in pH of the bromate-sulfite clock reaction. However, the clock time was only tunable on a 2 hour time scale and the polymer crosslinking system was not triggered by the change in pH of the clock reaction.

Chapter 3 discusses the research performed on the urea-urease clock reaction as a trigger for the Michael-addition type polymerization of Thiocure® 1300 (ETTMP) and poly(ethylene glycol) diacrylate 700 (PEGDA). We had great success creating this time-lapse polymerization system and were even able to create the first isothermal frontal polymerization system that does not require the gel effect to propagate the polymer fronts. This work focuses on the effect changing reagent concentrations has on the clock time, gel time, storage modulus, and subsequent degradation time in the batch-cured trials. The swelling capabilities and mass loss over time of the lyophilized hydrogel were also studied. In the IFP trials front velocity and front occurrence as they were affected by the reagent concentration were investigated. It was found that the

clock reaction displayed the same trends with and without[2] monomers present. The hydrogel formed showed similar properties to the previously studied hydrogel formed without[3] a clock reaction. Finally, the polymer fronts were determined to propagate with the pH fronts.

CHAPTER 1 – INTRODUCTION

1.1 – Time-Lapse Polymerizations

A polymerizable system that can remain dormant for a predetermined amount of time and then react to form the desired product has many applications. This idea of a time-lapse polymerization is certainly not a new idea. The first time this term was coined was by Norling in his patent.[4] He developed a system that had all the necessary components to create a one pot polymerization system that could be delayed for a programmable amount of time based on the inhibitor concentrations, and after the inhibitor was completely consumed, the polymerization proceeded without a decrease in reaction rate. This inspired the development of a time-lapse polymerization system in the Pojman lab. Hu et al. were able to use the change in pH of the formaldehyde clock reaction to trigger thiol-acrylate particle formation.[5] Although this method worked well and proved a clock reaction could trigger a polymerization, the formaldehyde clock reaction is much too toxic to use in practical applications. Thus, a benign clock reaction was sought instead. This will be discussed further in *The Urea-Urease Clock Reaction* section.

1.2 – Clock Reactions

A clock reaction can be identified by the abrupt change in the concentration of a species.[6] A common type of clock reaction is the pH clock, which can be identified by the abrupt increase or decrease in pH.[5] During this abrupt change in pH the maximum reaction rate of the system is achieved and is termed as the clock time. The clock time can be measured via the inflection point of the pH curve plotted against time or the maximum peak of the first derivative of the same plot. This is usually due to either a

positive or negative feedback that causes a change in the system. Feedback is when an output signal from the system dictates what happens within the system. For example, autocatalysis is a type of positive feedback where one of the products increases the reaction rate of the system.[7] Thus, the reaction rate increases as more product is formed, so the product is catalyzing the reaction.

Figure 1-1 has an example of the bromate-sulfite clock reaction studied and discussed in Chapter 2. From this figure it can be seen that the pH starts around 7 and after an induction period, the pH abruptly shifts to a much lower pH around 2. Because the reaction is autocatalytic, there is a huge production of protons after the inhibitory steps are overcome and those protons promote the production of even more protons. Until finally, the reactants are consumed, and the reaction stops.
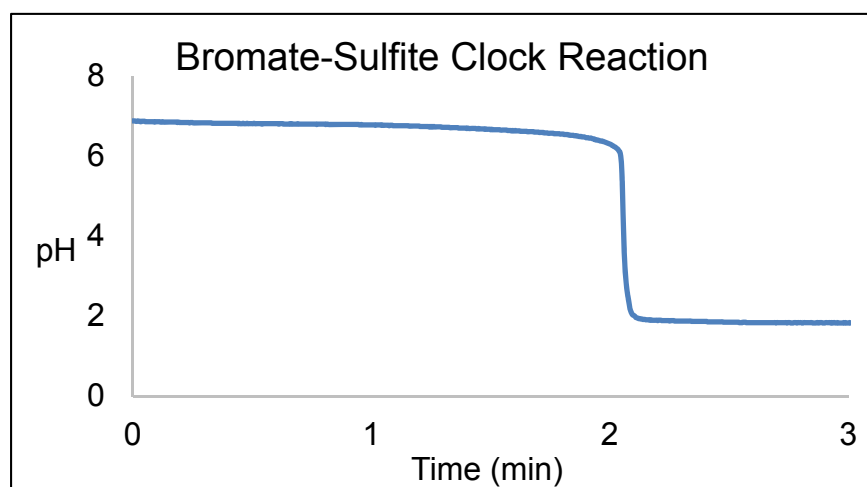

Figure 1-1. Bromate-sulfite clock reaction. This example is without the addition of ammonia.

1.3 – The Bromate-Sulfite Clock Reaction

The bromate-sulfite reaction kinetics have been well studied for over half a century now.[8] Williamson and King[8a] were one of the first groups to study this reaction. They monitored the change in pH and sulfur (IV) concentrations throughout the

experiment to determine the dependence of the second order rate coefficient on the pH. The rate coefficient, k_2, was proportional to the H^+ concentration above pH 6.4 and below pH 4.4. Since the sulfur (IV) ions had different "complexation species" in these pH ranges, Williamson and King determined there must be 2 different species responsible for the reactions with bromate. These different species were due to the different oxidation states of sulfur. They can be seen in Equation 1.

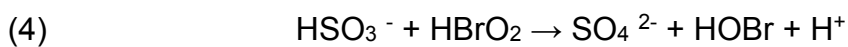(1) $$[HSO_3^- \cdot BrO_3^- + nH_2O] \text{ and } [SO_2 \cdot BrO_3^- + mH_2O]$$
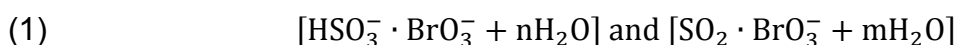
Much of the work done with the bromate sulfite system is in the area of oscillating reactions. Noyes, Field, and Körös studied the sulfuric acid-bromate-cerium-malonic acid system that produced potentiometric oscillations in both the bromate and cerium electrodes. They could not fully explain the mechanism but developed a plausible mechanism and rate equations for the system.[9] Rábai, Bazsa, and Beck also studied the bromate-ascorbic acid-malonic acid system and proposed some possible reaction equations and mechanisms.[10] Edblom, Orbán, and Epstein investigated the Landolt reaction with ferrocyanide in a CSTR. This reaction was along that same lines as the others except it replaces bromine with iodine and cerium with ferrocyanide.[11] They followed that work up with a paper about the mechanism of the same system, proposing 13 reactions and rate constants for the 7 overall reactions of the system.[12] Gaspar and Showalter elaborated on this reaction and proposed a new set of mechanisms with even more equations and divided the equations up into categories by the processes they perform in the reaction.[13] In 1980 Richard M. Noyes published a paper detailing *A Generalized Mechanism for Bromate-Driven Oscillators Controlled by Bromide*.[14] Later, Edblom et al. developed a refined chemical model of the bromate-sulfite-ferrocyanide

reaction.[15] Keresztessy, Nagy, Bazsa, and Pojman[16] went on to study convection in traveling wave propagation of the bromate-sulfite system, while Nagy, Keresztessy, and Pojman[17] also showed "Jumping" waves were possible due to periodic convection in the same system. For both papers, the mechanism of the bromate-sulfite system proposed by Edblom et al.[15] was accepted.

These are just a small handful of the oscillating bromate reactions that have been studied. The discrepancies in reaction mechanisms and rate constants goes to show how complex this system really is. There is no easy straight forward way to measure all the ions participating in the multitude of equilibria and reactions so some approximations and simplifications must be made to be able to model this system even remotely accurately.

Hanazaki and Rábai[1a] studied the *Origin of Chemical Instability in the Bromate-Sulfite Flow System* without a negative feedback and produced a pH clock reaction. They were also able to develop a simplified and accepted set of reaction equations for the bromate-sulfite system based on the original work of Williamson and King[8a] and the RKH model.[18] They believed this method better described the observed behaviors of the system and went on to further simplify the model into 2 distinct pathways, the S path and the B path.

The S path is the first to proceed and consumes the sulfite present via Equations 2- 5 below.

$$(2) \qquad H^+ + SO_3^{2-} \rightleftharpoons HSO_3^-$$

$$(3) \qquad HSO_3^- + BrO_3^- \rightarrow SO_4^{2-} + HBrO_2$$

$$(4) \qquad HSO_3^- + HBrO_2 \rightarrow SO_4^{2-} + HOBr + H^+$$

(5) $\qquad$ $HSO_3^- + HOBr \rightarrow SO_4^{2-} + Br^- + 2H^+$
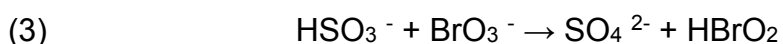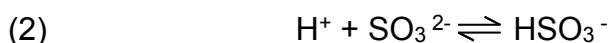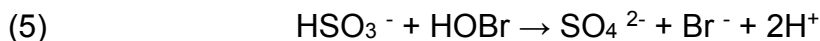
The reactions involved in path B are listed below with Equations 6- 9.

(6) $\qquad$ $H^+ + HSO_3^- \rightleftharpoons H_2SO_3$

(7) $\qquad$ $H_2SO_3 + BrO_3^- \rightarrow SO_4^{2-} + HBrO_2 + H^+$

(8) $\qquad$ $H_2SO_3 + HBrO_2 \rightarrow SO_4^{2-} + HOBr + 2H^+$

(9) $\qquad$ $H_2SO_3 + HOBr \rightarrow SO_4^{2-} + Br^- + 3H^+$
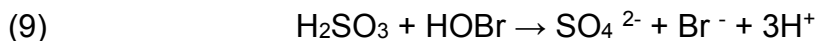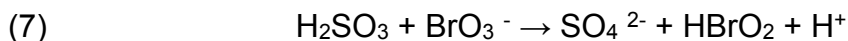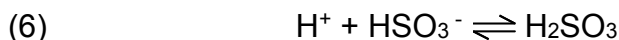
A follow up work by Okazaki, Rábai, and Hanazaki[1b] describes this reaction well; the S path equilibrium (Equation 2) lies far to the left at basic pH. As protons are produced from Equations 3 – 5 the sulfite in Equation 2 quickly consumes it to produce HSO_3^- and reduce more bromate. Therefore, the net change in $[H^+] \approx 0$. The reaction rate of Equations 2 – 5 are greater than 6 – 9 when SO_3^{2-}, H^+, and BrO_3^- are present in solution. Once the sulfite is completely consumed the bisulfite pathway can start operating. This is the induction period of the clock reaction. Up until this point there is no change in pH. Once the bisulfite pathway starts producing protons there is a rapid decrease in pH because the B path produces 3 protons. As more protons are produced Equation 6 pushes further to the right, generating more H_2SO_3 and increasing the reaction rate of Equations 7 – 9 until all the bisulfite is consumed. Combining Equations 3 – 5, gives the overall reaction of the S path (Equation 10), and combining Equations 7 – 9 gives the overall reaction of the B path (Equation 11).[8c, 19]

(10) $\qquad$ $3H^+ + 3SO_3^{2-} + BrO_3^- \rightarrow 3SO_4^{2-} + Br^- + 3H^+$

(11) $\qquad$ $3H^+ + 3HSO_3^- + BrO_3^- \rightarrow 3SO_4^{2-} + Br^- + 6H^+$
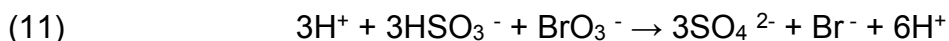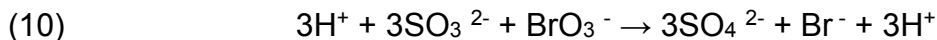
In the current investigation, the clock reaction has been perturbed by adding a "fugitive base," a base that can easily escape from the reaction system. Addition of

ammonium hydroxide has been studied because it can easily evaporate when left open to the air. Other low molecular weight amines were tested but only ammonia evaporated in a sufficient time frame without heating. When left unperturbed, the bromate-sulfite clock reaction has an initial pH around 7. Thus, with the addition of ammonium hydroxide the initial pH can be increased and the induced delay in clock time studied. The idea is that the increase in pH will sufficiently delay the clock reaction and if the solution remains sealed so ammonia cannot evaporate, then the clock reaction will be halted long enough to create a storage stable system. This would prove useful to create a storage stable time-lapse polymerization system if combined with a polymerization reaction that is water soluble and will remain dormant until the pH decreases. Optimally reacting between pH 3 – 5, depending on initial reagent concentrations.

1.4 – Polycarbodiimides

Polycarbodiimides (PCDIs) are a type of polymer that contains carbodiimide (CDI) functionalities. Lloyd and Burns extensively studied the optimum reaction conditions[20] and coupling mechanism[21] of water-soluble CDIs. They discovered that the optimum pH for the reaction is about pH 4, and the CDIs are inactive at high pHs because the carboxylic acid is not protonated. CDIs have found their way into the coatings industry shortly after Lloyd and Burns' studies. Many patents[22] have been issued for systems using CDIs and PCDIs as either a crosslinker (CDIs) for a resin or the resin (PCDIs) to be crosslinked. All of these examples are for coatings but that is not the only use of CDIs and PCDIs. Han et al. have recently studied the reaction of PCDIs with poly(acrylic acid) (PAA) for use in a Li-ion battery negative electrode.[23] They proposed a mechanism for the reaction. A drawing based on their mechanism, using the compounds studied in this research can be seen in Figure 1-2.
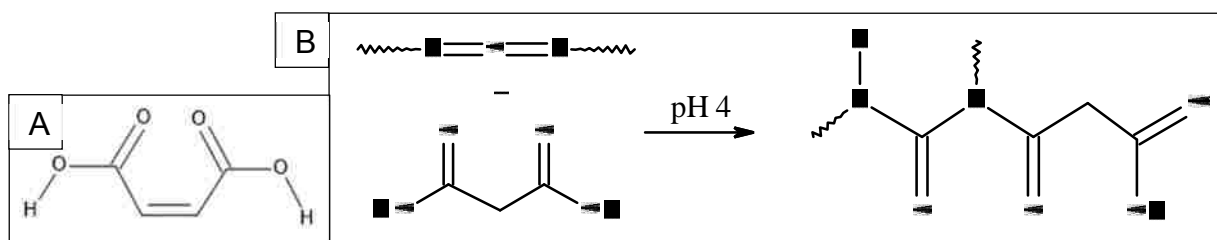
Figure 1-2. A) Maleic acid, one of the crosslinkers used. B) PCDI and malonic acid react readily at pH 4 to form an N-acyl urea type compound.

In this work PCDI resins obtained from Picassian Polymers were crosslinked by dicarboxylic acids, specifically maleic or malonic acid. The idea was to study the crosslinking of the resins as it was triggered by reduction in pH from the bromate-sulfite clock reaction.

Since PCDIs are unreactive at high pH and the bromate-sulfite clock reaction will not proceed at high pHs, our ultimate goal between these two systems was to have a time-lapse polymerization occur after the fugitive base escaped the reaction medium and the pH dropped below 5. After the switch in pH from the bromate-sulfite clock reaction, the solution will be acidic enough for the PCDI to react with the dicarboxylic acid and form a crosslinked network.

1.5 – The Urea-Urease Clock Reaction

Another system that exhibits autocatalysis is the urea-urease clock reaction. This is another clock reaction that was studied in hopes of triggering a time-lapse polymerization. Urease has been studied for almost a century now, and the crystal structure was just recently elucidated by Balasubramanian and Ponnuraj.[24] In 1926 James B. Sumner published an article on the crystallization of Jack Bean urease[25]. This was the first enzyme to ever be crystallized, proving that enzymes are proteins and that

7

the crystallization of proteins was possible. Sumner's feat was rewarded with a Nobel Prize in 1946.[24]

Urea is also a well-studied molecule. In 1828 Wohler was the first to synthesize an organic compound, urea.[26] Since both of these compounds are naturally occurring biological molecules, it makes sense that people would want to study them and employ them for new applications in chemistry. The decomposition of urea by urease has been studied in buffers[27] and without buffers[28]. Purification methods of urease[29] and investigation into the function of the nickels in the active site[30] have been popular areas of study with the enzyme as well. Inhibitors of urease[31] and pH dependence on structure[32] are two more well studied areas. The hydrolysis of urea by urease can be seen in Figure 1-3.
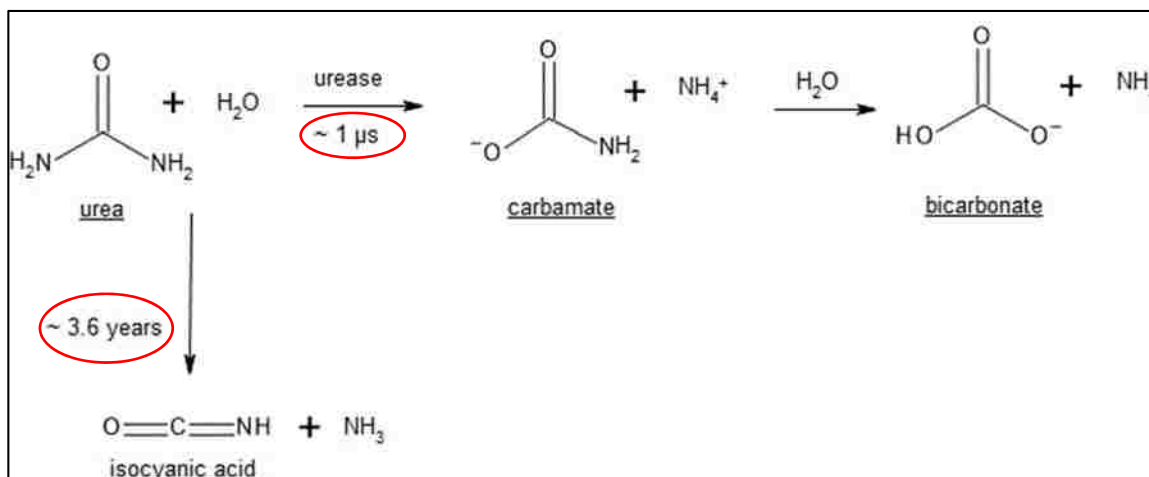

Figure 1-3. Urea decomposition with and without urease presence adapted from Krajewska et al.[32]

Figure 1-3 shows how urease aids in the quick decomposition of urea in water as reported by Krajewska et al.[32] With urease present at its optimal pH the enzyme can break down urea in about 1 microsecond to form carbamate and an ammonium ion.

After that, another water molecule breaks down the carbamate to make bicarbonate and ammonia. The bicarbonate is eventually reduced to carbon dioxide. Thus, the entire process generates 2 ammonias and 1 carbon dioxide in a matter of seconds. However, without urease, urea is stable in water for about 3.6 years and does not make the desired products but rather isocyanic acid.[32]

Figure 1-4 from our work[33] shows the pH dependent reaction rate of urease in Figure 1-4A. The enzyme is most active between pH 5.5 – 8.5, and the maximum rate is at pH 7. Therefore, we can see how the typical clock reaction graph in Figure 1-4B is possible. If a solution of urea has enough acid added to decrease the initial pH to about 4, then when the urease is added it will have a very low reaction rate. As urea is degraded and ammonia is produced the pH of the solution will rise and in turn increase the reaction rate of the urease. Once the pH gets around 5.5 the enzyme's activity is very high and there is an abrupt increase in pH because the rate of ammonia production increases significantly. Once the pH reaches about 8.5 the activity of enzyme starts to dwindle, and the solutions pH eventually plateaus somewhere around pH 9.
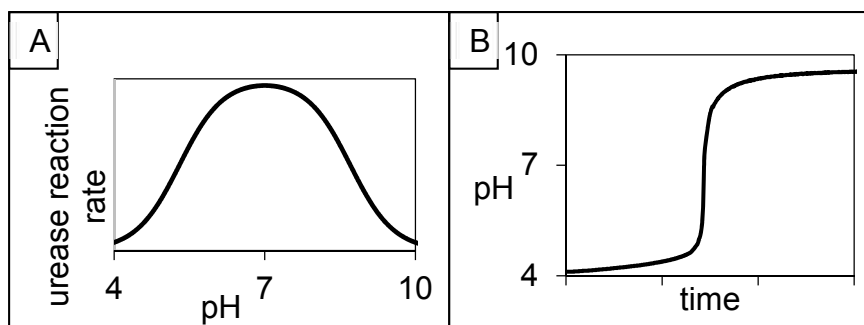

Figure 1-4. A) Urease reaction rate as a function of pH. B) Typical urea-urease clock reaction pH profile over time. Adapted from Jee et al.[33]

The first attempt at creating a clock reaction with the urea-urease system was performed by Hu et al.[2a] The studied the effect of adding a weak acid versus a strong

acid to the system and also how changing the concentration of the reagents affected the system. They found that a weak acid, like acetic acid, creates a buffer in the solution and dampens the sharpness of the pH switch. While adding sulfuric acid, a strong acid, did not produce a buffer, and a sharp pH switch was observed around the clock time. They also discovered that increasing the urea or urease concentrations decreased the clock time because more ammonia was produced in a shorter amount of time. Thus, the pH increased faster and increased the reactivity of the urease. Although, as expected, increasing the acid concentration increased the clock time because more ammonia had to be produced before the pH would rise and increase urease activity.

In this same work by Hu et al., a mathematical model of the urea-urease clock reaction was developed from the Michaelis-Menten kinetics of the reaction and the appropriate acid/base equilibria. Computer simulations were performed and compared well with experimental results.

In a follow up paper by Wrobel et al.[2b] pH wave fronts were studied in thin layers. They found that if the reaction mixture is sandwiched between an inverted petri dish cover and the bottom, creating a thin layer ≤ 1 mm, and preventing ammonia evaporation from the system, that changes in pH occur in a 2-dimensional zone and propagate outward from their point of initiation. An example of a pH front in thin layers can be seen in Figure 1-5. This picture is an example of the urea-urease fronts studied in this work with universal indicator added. The solution starts out acidic (red/orange), and the basic fronts (blue spots) appear randomly throughout the dish. As the fronts propagate, there is a pH gradient along the edge of the front. In Figure 1-5 it is seen as a yellow band around the front, this indicates a pH of about 6 - 7.

Wrobel et al. found that increasing either urea or urease concentration increased the front velocity and number of spontaneous fronts that occurred. The fronts were observed to travel with constant velocity. Wrobel also goes on to explain that inorganic pH wave front systems such as the bromate-sulfite system, which demonstrate acid autocatalysis, have faster fronts (1-20 mm/min) than the base autocatalysis driven urea-urease fronts (0.1-1 mm/min) that were observed. Autocatalysis is the driving force behind these clock reactions discussed.

Figure 1-5. Petri dish with urea-urease clock reaction and universal indicator. Red/orange color (pH <5.5), yellow (~pH 6.5), blue green (pH >8). Blue green fronts spontaneously occur and propagate throughout the dish.

The interesting patterns produced in these autocatalytic reaction-diffusion systems are caused by spatial inhomogeneities that can occur in unstirred thin layer reaction vessels. These fronts are a delicate balance between the reactivity of the reagents and the diffusion of the products.[34] Fronts have been studied with many types of biological reactions; glucose oxidase,[35] DNA catalyzers,[34] DNA oligonucleotides,[36] and self-replicating RNAs,[37] to name a few. Some interesting applications of these types of reactions are to make smart materials[38], synthetic mechanical pumping systems[39], and a pH responsive nanoparticle coating[40].

Work that has been done with the oscillating reactions discussed in the bromate-sulfite section, and most of the other works not discussed as well, require chemical compounds that possess multiple oxidation states and can easily switch between them. Namely, halogens, sulfur compounds, and transition metals have been the subjects of interest.[41] However, these compounds tend to be extremely oxidizing and a potential health hazard. Thus, the desire to create a non-toxic system for many potential biological applications in adhesives, drug delivery, tissue engineering, stimuli responsive sensors, etc. is understandable.

Since urea and urease are both biological compounds, it seems feasible that if the clock reaction parameters are finely tuned it could be combined with a biocompatible polymer system to create a tunable reaction system. The urea-urease clock reaction starts at a low pH and then switches to a high pH through autocatalytic ammonia production and this change in pH could trigger another reaction. A Michael-addition type polymerization would be a good candidate because it remains inactive at acidic pH. It has already been observed that the urea-urease clock time can be tunable,[2a] and the system is capable of producing pH wave fronts that are also tunable[2b]. Therefore, adding a polymerization reaction that should be unreactive with any component in the solution until the pH is sufficiently basic could produce a programmable batch-cured polymerization system that may also be capable of isothermal frontal polymerization.

1.6 – Isothermal Frontal Polymerization

Frontal Polymerization (FP) is a method of converting a monomer system into a polymer via a propagating reaction zone, or front.[42] In Thermal Frontal Polymerization, hereafter referred to as simply FP, an external heat source, such as a soldering iron, is

applied to the monomer system as the energy source to initiate polymerization.[43] The point of initiation will have the fastest reaction rate because the energy source is being directly applied. Due to the exothermic nature of the polymerization reaction, the front propagates through the monomer increasing the reaction rate thus leaving polymer behind.[44] Once a front has been initiated the external energy source can be removed. If too much heat is lost during propagation there will not be enough energy to overcome the activation energy of the polymerization, and the front will be quenched.[45]

In 1972 Chechilo and Enikolopyan discovered FP[46] and studied the wave front structure and propagation[47]. Later, polymerizations of methyl methacrylates and how initiator type and concentration affected front velocity were explored[48] as well as the effects of pressure on FP.[49] Pojman and coworkers have extensively studied FP of acrylates and also epoxy resins,[50] urethane-acrylate copolymerizations,[51] thiol-ene chemistry,[42] and many other systems and applications of FP. Mariani et al. have also done research in the area of frontal polymerization with systems such as dicyclopentadiene,[52] polyurethanes,[53] interpenetrating polymer networks[54], and unsaturated polyester/styrene.[55] FP is useful to produce strong polymer materials and composites for adhesives and fillers. However, the high temperatures (> 200 ºC) required for curing limit its range of application.[56]

Isothermal Frontal Polymerization (IFP) is a type of frontal polymerization that occurs at a constant temperature. IFP systems have typically been made by addition of a polymer seed to a solution of monomer and possibly initiator. This required that the polymer be soluble in the monomer solution. When the monomers diffuse into the polymer seed a viscous area is produced. Polymerization begins in both the monomer

solution and the polymer seed, but the greater viscosity of the monomer solution in the polymer seed leads to a quicker polymerization rate. This is known as the Trommsdorff or gel effect.[57] Because of this gradient in viscosity that is formed, optically[58] and functionally[59] gradient polymers can be produced.

1.7 – Thiol-Acrylate Hydrogels

In this work, ethoxylated trimethylolpropane tri(3-mercaptopropionate) (ETTMP or Thiocure® 1300 or thiol) and poly(ethylene glycol) diacrylate (PEGDA) monomers were used to create a time-lapse polymerization hydrogel triggered by the urea-urease clock reaction. The reaction scheme of the monomers and subsequent polymer can be seen in Figure 1-6.

Once the solution is above pH 7, the thiols are deprotonated and become good nucleophiles for the electron deficient double bond of the acrylate. The thiol anion attacks the acrylate, and the negatively charged acrylate then grabs a proton from solution to neutralize itself.[60] This produces the structure seen at the bottom of Figure 1-6. Since the thiol is trifunctional and the acrylate is difunctional, they were kept in a 2:3 molar ratio to ensure a 1:1 functional group ratio.

Polymer networks are ubiquitous in synthetic products made for commercial use today. With advances in medicine being made every day, a significant area of polymer use and research is for medical purposes like drug delivery, tissue scaffolding, and wound dressings, to name a few.[61] Some of these applications require the *in situ* formation of the polymer network, in which case the mechanical properties of the system and its biocompatibility must be well understood.
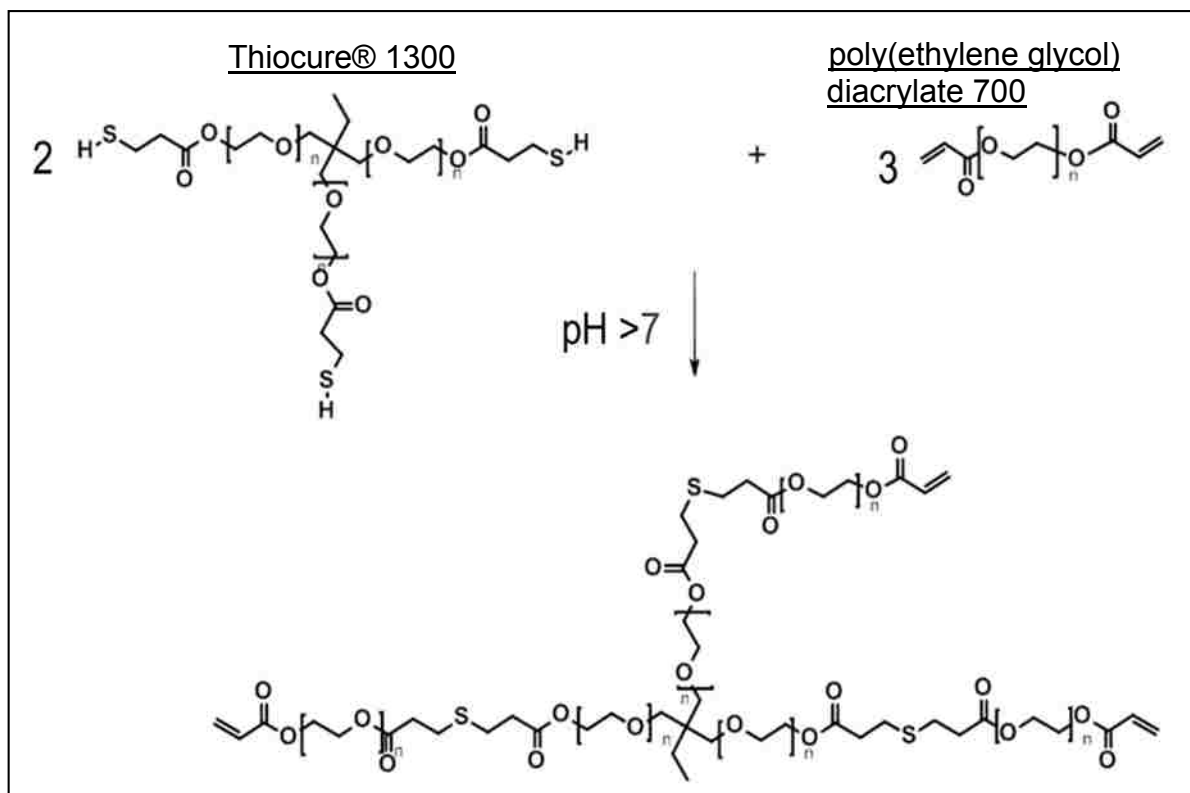
Figure 1-6. Michael-addition type reaction of Thiocure® 1300 and PEGDA and resulting polymer.

A common, commercially available area of medical hydrogels is with the application of surgical tissue adhesives and sealants, of which poly(ethylene glycol) is a major component of the polymeric hydrogels used. This is because it is biocompatible and does not elicit an immune response from the body. It can also be passed quite easily through the kidneys once it hydrolyzes back into a liquid.[62] These PEG based hydrogels on the market today have some sort of functionalization that can produce a crosslinked network like some combination of acrylate, thiol, or amine derivatives that can undergo either a photopolymerization or a base-catalyzed reaction by simply mixing the reagents together. The most common uses of these hydrogels are for air or fluid leakage prevention and soft tissue adhesion. For example, preventing suture line bleeding, postsurgical cerebrospinal fluid leakage, pulmonary air leakage, corneal

15

lacerations and transplant bandages, retina reattachment, and vascular closures among many others.[63]

Some other great applications of PEG hydrogels pertain to tissue engineering. Xu et al. developed a hydrogel that could deliver stem cells to cutaneous wounds while keeping the cells hydrated and nourished.[64] Lutolf et al. found a way to incorporate collagenous extracellular matrices into PEG based hydrogels for repairing bone defects.[65] Young and Engler developed a PEGDA-thiolated hyaluronic acid system that could undergo a stiffening process after so many hours (>100 hours) post polymerization. They realized the heart muscle cells do this during development and to create a better scaffold for heart tissues in vitro, a hydrogel that could do the same was needed. Since the stiffening time was dependent upon PEGDA molecular weight, they stated the system could be tuned to other tissue scaffold stiffening needs as well.[66]

Another useful application of PEG based hydrogels is for therapeutic delivery because of their high load capacity and biocompatibility. The wide range of drugs or therapeutics used today may include synthetic or natural pharmaceuticals, proteins, or living cells. In the case of living cells, the cytotoxicity of the hydrogel and gelation method is very important to ensure viability of the therapeutic. For this reason, click chemistries have emerged as a leading contender for hydrogel formation. Some of the most common are copper(I)-catalyzed azide-alkyne click hydrogels, thiol-ene photocoupling, Diels-Alder reactions, oxime reactions, and pseudo-click reactions like the thiol-Michael addition and aldehyde-hydrazide coupling.[67] To allow release of the cargo these compounds must have a degradation method that can be completed in the body like hydrolysis of an ester, enzymatic cleavage, or light activated degradation.[68]

With these click chemistries, gelation begins upon mixing of the materials. To allow working time with the hydrogel, a delay in curing may be desired. To induce this induction time in gelation, a control over the gel rate must be employed.[69] Lutolf et al. studied how changing the amount and type of charge on amino acids surrounding a cysteine thiol affected the reactivity of the thiol in a Michael-addition reaction to a PEG diacrylate.[70] Lutolf and Hubbell also investigated the effect pH had on the gelation time of a thiol to a vinyl sulfone, which underwent a Michael-addition reaction.[71] Chatani et al. from the Bowman group was able to produce an induction time with the thiol-click polymerization by adding methanesulfonic acid as an inhibitor.[72]

The thiol-acrylate hydrogel used in this work has been previously characterized by Pritchard et al.[3] They determined the hydrogel and monomers to be biocompatible and tested the hydrogel's ability to be a drug delivery vehicle of methylprednisolone sodium succinate. Because the hydrogel contains many pH sensitive ester bonds, it is degradable over time in water. That is a property specifically needed for biomedical applications to ensure removal of the polymer system after it has performed its job.[73]

1.8 – Conclusions

In the next two chapters, I will describe how we attempted to develop two separate time-lapse polymerization systems. The first involves the bromate-sulfite clock reaction. Based on some computer simulations, we believed it would be possible to add ammonia to the clock solution and significantly delay the clock reaction. This would result in a storage stable solution for a few months as long as the container remained sealed to halt ammonia evaporation. By coupling a polymerization to the clock reaction that would only react at acidic pH (the final pH after completion of the clock reaction) it might be possible to create a time-lapse polymerization system with storage stable

capabilities. The polymer selected, polycarbodiimides (PCDIs), once crosslinked with a dicarboxylic acid would create a good waterproof coating after evaporation of the water in the clock reaction. Thus, after the time-lapse crosslinking system was opened, it could be applied to a surface, the ammonia would evaporate, the clock reaction reduce the pH, and then the dicarboxylic acid would crosslink the PCDI creating a coating. However, this was not the observed results. We found the system to be much more complex than anticipated. All of this will be discussed in chapter 2.

The other system studied was the trithiol-diacrylate time-lapse polymerization system triggered by the urea-urease clock reaction. With this system we built upon the works of Hu et al. and Wrobel et al. Hu and coworkers developed the urea-urease clock reaction and studied the effect of acid type and concentration on the clock time. Wrobel and coworkers furthered the research by creating the first thin layer wave fronts with the urea-urease clock reaction. They studied how changing the reagent concentration affect front occurrence and front velocities.

From these works we wanted to further the study and create the first Isothermal Frontal Polymerization (IFP) system that did not rely on the gel effect to propagate fronts and also develop a time-lapse polymerization system triggered by the change in pH of the clock reaction. Unlike the bromate-sulfite research, these endeavors were extremely successful and we were able to produce a hydrogel from a clock reaction/monomer solution. We studied how changing reagent concentrations of both the clock reaction and the monomers affected the clock time, gel time, degelation time, and swelling of the hydrogel from a dry state in batch-cured trials. We studied the effect of reagent concentrations on front occurrence and front velocities in the IFP trials. Other

questions answered from the IFP studies were whether or not any convective effects were present during propagation of the fronts and do the polymer fronts travel with the pH fronts? All of these results will be discussed in Chapter 3.

CHAPTER 2 – BROMATE-SULFITE CLOCK REACTIONS

2.1 – Chapter Summary

The bromate-sulfite clock reaction has been studied with addition of ammonia in hopes of inducing a delay in the clock time. It was found that changing the ammonia concentration can produce a delay in the clock time but does not actually affect the reaction rate of the clock reaction. Rather, the internal ammonia-ammonium buffer formed increases with increasing ammonia concentration, which requires more acid to be produced from the clock reaction to see an abrupt change in pH. The delay in clock time could not surpass 2 hours. Thus, a storage stable time-lapse polymerization system could not be developed.

Attempts at creating a non-storable time-lapse polymerization system triggered by the bromate-sulfite clock reaction were also not successful. This may be due to the harsh oxidizers used in the reaction that destroyed the polymer frameworks, or more probably reaction of malonic/maleic acid (the polymer crosslinkers) with bromate generated a brominated compound that was too sterically hindered to react with the polycarbodiimides (PCDI). Never the less, due to time constraints attempts at creating a time-lapse polymerization system with the bromate-sulfite clock were abandoned, and efforts were directed to the urea-urease system discussed in Chapter 3.

This chapter will describe the experiments performed with the clock reaction and the small range of tunability of the clock time based on ammonia concentration. Also to be discussed is the complexity of the clock reaction studied, the polymers tested for use in the time-lapse polymerization system, and why the selected systems were chosen.

2.2 – Introduction

2.2.1 – Bromate-Sulfite Clock Reaction

The kinetics of bromate-sulfite reaction have been well-studied.[8a, 8b, 74] The reaction starts at pH 7, and after all the sulfite is consumed switches abruptly to pH 2. This happens in a matter of about 2 minutes when ammonia is not present (Figure 2-1). This behavior is exemplary of a pH clock reaction. A pH clock reaction is a reaction that abruptly switches pH after a calculated amount of time based on reagent concentrations. The inflection point of the graph is the point where the maximum reaction rate has been reached and is termed the "clock time" of the plot.[6]
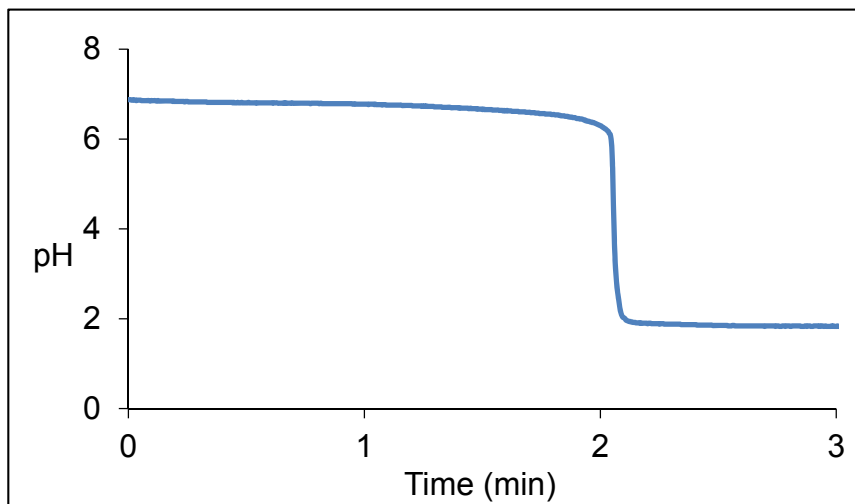

Figure 2-1. Typical bromate-sulfite clock reaction without ammonia.

A majority of the work that has been done with the bromate-sulfite system is with oscillating clock reactions. By changing the metals used in the system different oscillators can be created.[9-14] With each of these works the mechanisms of the bromate-sulfite reaction and the reactions with the metals incorporated have been

difficult to elucidate. There has been much debate over the true mechanisms because there are so many ions present in the system at any given time.

More recently, several works[1a, 1c, 19] have emerged with what seem to be valid simplified mechanisms of the bromate-sulfite clock reaction. These are by no means the complete list of mechanisms but the major ones that produce the change in pH observed over time with this system. As shown with Equations 2- 9 in the bromate-sulfite section of the introduction, there are two distinct paths taken in this clock reaction: the sulfite (S) path and the bisulfite (B) path. The S path is the first to proceed and consumes all the sulfite present. As seen below in Equation 10 from the introduction, there is no net change in pH with this pathway. The time it takes for the sulfite to be consumed is the induction time of the clock reaction because the B path takes over after that. As seen in Equation 11 below, the B path has a net change of $[H^+]$ ≈ 3. As protons are produced the solution pH decreases and the reaction rate of the B path increases, reaching the maximum reaction rate during this drop in pH. After all the bisulfite is consumed the pH levels off and the clock reaction ceases. Okazaki et al. explain this reaction very well in their recent work.[1b]

(10) $3H^+ + 3SO_3{}^{2-} + BrO_3{}^- \rightarrow 3SO_4{}^{2-} + Br^- + 3H^+$

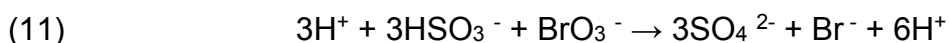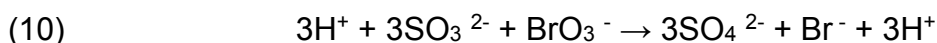(11) $3H^+ + 3HSO_3{}^- + BrO_3{}^- \rightarrow 3SO_4{}^{2-} + Br^- + 6H^+$

Figure 2-2 shows the change in reagent concentrations in the unaltered clock reaction. The sulfite, $SO_3{}^{2-}$, is consumed first with the S path. After which the B path kicks in and consumes the remaining bisulfite, $HSO_3{}^-$. This results in a large production of protons, which can be seen at 300 seconds in the pH graph of Figure 2-2. In the

bottom plot the bisulfite is quickly consumed, and it is also apparent that not all of the

bromate is consumed.
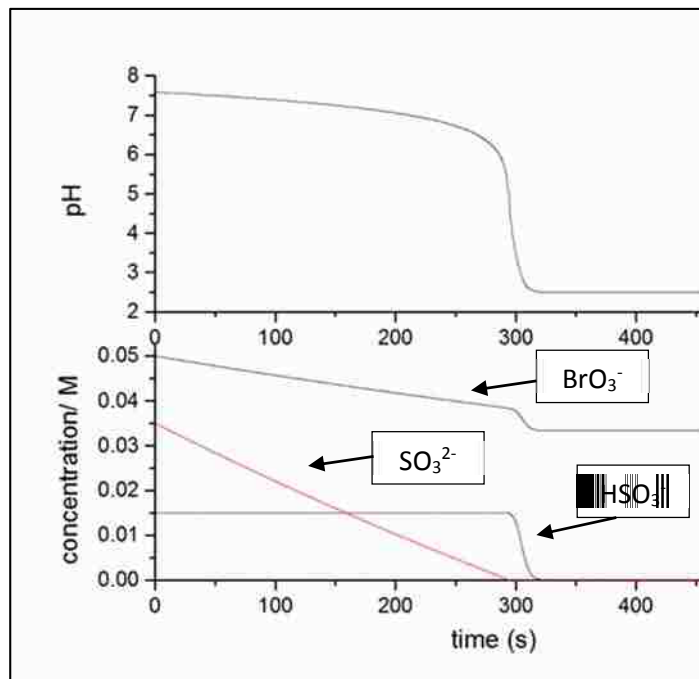
Figure 2-2. pH vs time of the bromate-sulfite clock in the top plot. The bottom plot shows the change in concentrations associated with the change in pH seen in the top plot. Image courtesy of Dr. Annette F. Taylor.

2.2.2 – Attempts to Create a Time-Lapse Polymerization

The crosslinking system chosen was a polycarbodiimide (PCDI) crosslinked by a

dicarboxylic acid. This was chosen because it was readily available for purchase, was

water soluble, proven to be non-reactive at basic pH and crosslink at mildly acidic pH

(~4).[75] In addition, PCDIs have proven to be useful polymers for coatings and many

patents have been issued for them.[22] PCDI and malonic acid readily react at pH 4 to

form the N-acyl urea form of crosslinked polymer [Figure 2-3(B)]. The other crosslinker

used was maleic acid [Figure 2-3(A)].

As mentioned, with this work we wanted to create a time-lapse polymerization system by coupling the clock reaction to an acid-catalyzed reaction. Ideally, the polymer chains and crosslinkers would remain unreactive until the pH dropped low enough and triggered the acid-catalyzed crosslinking reaction. Based on the computer simulation done by our collaborator, Dr. Annette F. Taylor at the University of Sheffield, it was predicted that this system could have optimum concentrations that would allow for a storage stable solution to create a one pot cure-on-demand adhesive.
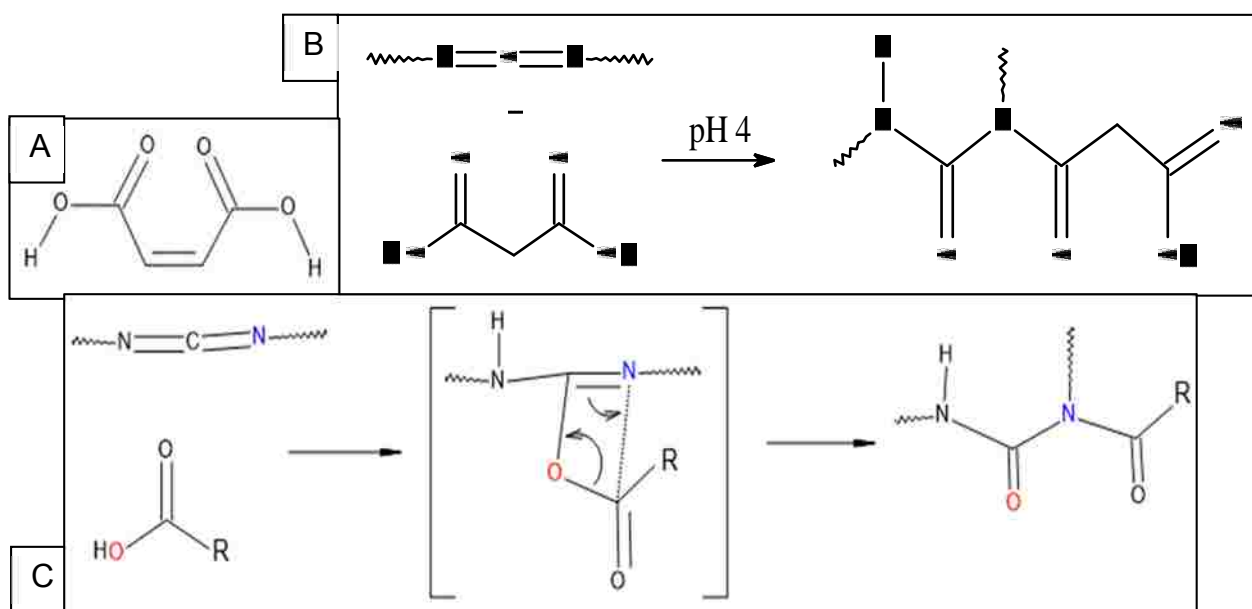
Figure 2-3. A) Maleic acid, one of the crosslinkers used. B) PCDI and malonic acid react readily at pH 4 to form an N-acyl urea type compound. C) Internal rearrangement mechanism of PCDI with a generic carboxylic acid. Adapted from Llyod and Burns.[75a]

Based on Figure 2-4, the solution would have a very low rate of reaction on the shelf for a few months. After removing the lid and applying the solution to a surface the ammonia would evaporate, the clock reaction should proceed if enough sulfite and bromate remain, and then once the solution was acidic the crosslinking could occur. However, this was not proven to be the case.

Figure 2-4. Using lower initial clock reagent concentrations, a delay of 100 days is theoretically possible if SO_3^{2-} and BrO_3^- are still present after ammonia evaporation. The top plot shows the pH change (solid black line) and change in rate of ammonia evaporation (k8, red dashed line). The bottom plot shows the change in clock reagent concentrations over time. Image courtesy of Dr. Annette F. Taylor.

2.3 – Methods, Materials, and Reactions

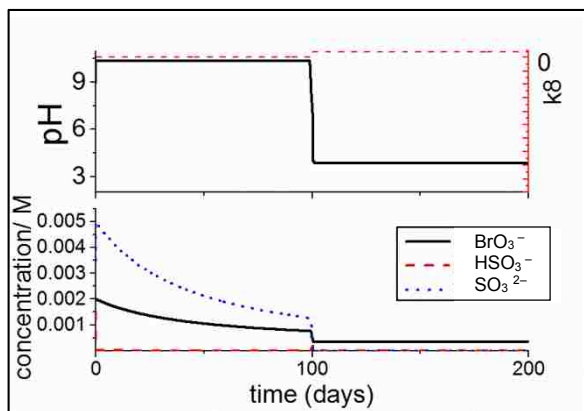Reagent grade sodium sulfite, sodium bromate, malonic acid, and maleic acid were obtained from Sigma-Aldrich and used as received. Sodium metabisulfite, reagent grade, came from Acros Organics, and 30% Ammonium Hydroxide Solution came from Macron Chemicals. Both were used as received. Sodium sulfite and sodium metabisulfite were stored in a vacuum sealed desiccator to prevent oxidation. Polycarbodiimide XL-702 was donated by Picassian Polymers and used as received. Vernier pH sensors and Logger Lite software were used to record the change in pH as a function of time during the clock reactions.

For every trial, the appropriate amounts of solids were weighed to make 0.1 M sodium sulfite and sodium bromate solutions, while 0.05 M sodium metabisulfite solutions were used. The sulfite and bisulfites were dissolved in one beaker and the bromate in another. The two solutions were not mixed until the appropriate amount of ammonium hydroxide was added to the bromate solution. Once mixed, the pH probe

25

started recording the change in pH vs. time until the clock reaction was complete. The magnetic stir plate was set between 1500 - 1700 rpms for all trials and a small stir bar (1 cm width) was used in a 50 mL beaker at room temperature (22 ºC). Each trial had a total solution volume of 30 mL and initial pH after ammonium hydroxide addition ranged from 7 to 10. After the clock reaction switched and the pH remained relatively constant, data collection was terminated.

2.4 – Results and Discussions

A typical bromate-sulfite clock reaction with and without ammonium hydroxide addition is depicted in Figure 2-5. Without ammonium hydroxide the initial pH is about 7, the solution clocks in 2 minutes, and the final pH is about 2. With enough ammonium hydroxide to raise the initial pH to just over 8, the solution does not clock until about 70 minutes, and the final pH is around 3. With increasing initial pH there was an increased delay in clock time of up to 5 hours, as shown in Figure 2-6. However, the final pH increased too. Furthermore, if the initial pH of the solution was above pH 9 there was a complete loss of clock behavior all together, Figure 2-7.

It was also observed that when the clock solution was stored in a vial with no headspace of air for ammonia to evaporate, once the vial was opened the clock reaction never happened. Rather than seeing the typical sharp decrease in pH, a curve similar to the one seen in Figure 2-7 was observed, and the final pH was around 4- 5, depending on the concentrations of reagents. Another interesting feature was the linear decrease in pH from 10.5 to 8 and then a titration style hump observed from pH 8 to 6. These changes in the rate of pH decrease are indicative of ammonia evaporation. From pH 10.5 to 8 the equilibrium is mostly on the aqueous ammonia side of the equation with ammonium hydroxide. Therefore, evaporation is easy because it does not need to be

deprotonated to enter the gaseous state. However, from pH 8 – 6 the ammonium ion is more prevalent than the aqueous ammonia. So evaporation slows down because this internal buffer between the aqueous ammonia and ammonium hydroxide is formed, decreasing the rate of conversion form aqueous ammonia to gaseous ammonia. This indicates that the trend observed with pH was simply ammonia evaporation and not the clock reaction.[76]
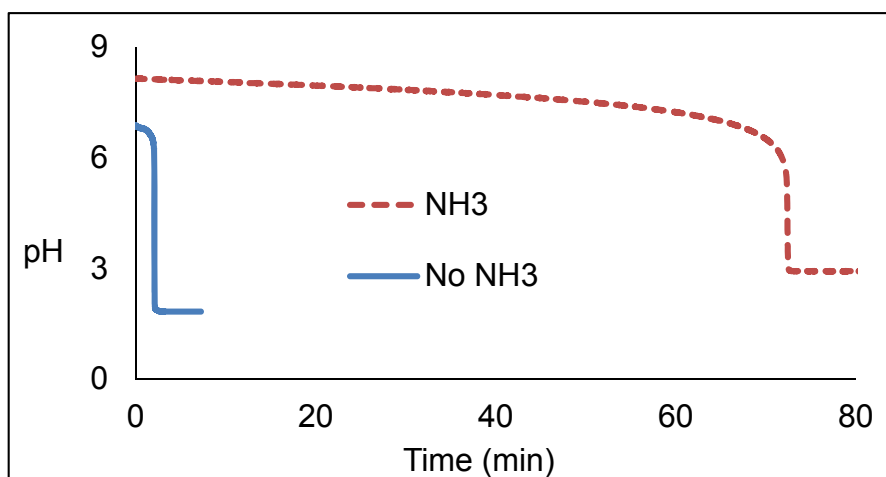

Figure 2-5. Bromate sulfite clock with and without 18 M ammonium hydroxide present.
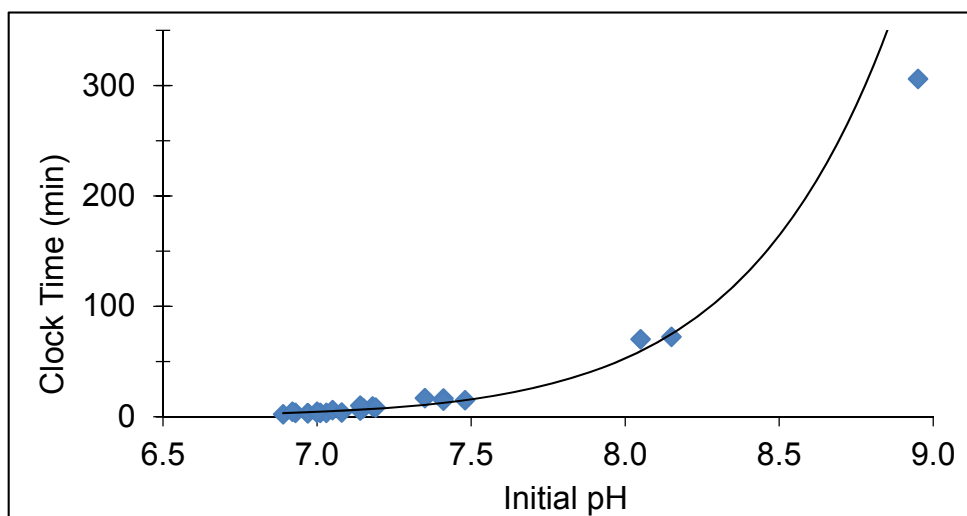
Figure 2-6. Clock time as a function of initial pH, altered by 18 M ammonium hydroxide.
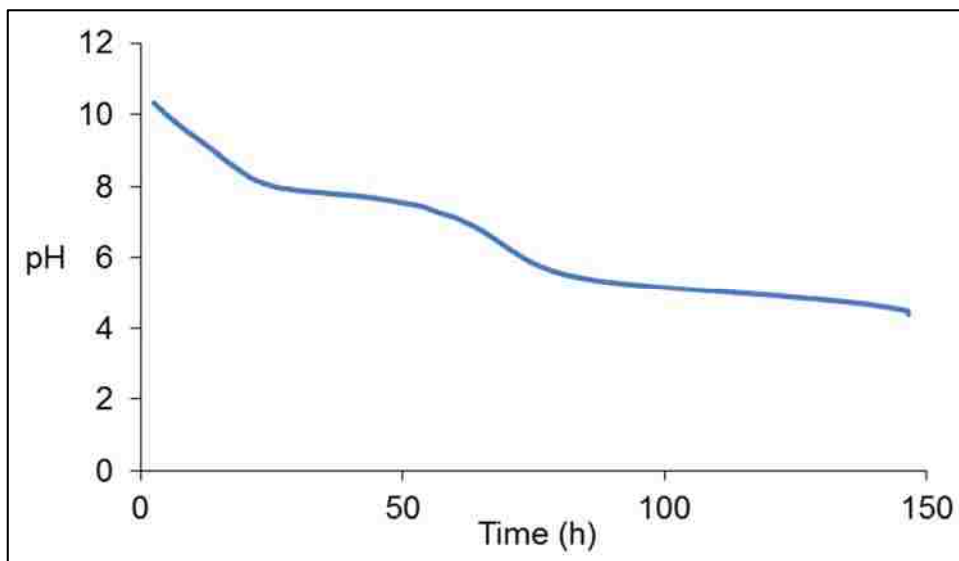
Figure 2-7. pH time plot of bromate-sulfite reaction with enough 18 M ammonium hydroxide to raise the pH above 10.

Going back to the computer simulations it is apparent that the clock reaction still proceeds in the presence of ammonia, but at a much slower rate. Looking at Figure 2-8, the bisulfite is essentially non-existent at high pHs because the system is lying far on the sulfite side of the equilibrium. Thus, when sulfite reacts with bromate there is no significant change in pH because the number of protons produced equals the number of protons consumed. So when the ammonia is finally allowed to evaporate the change in pH we see is just that: Ammonia evaporation because the sulfite has already been consumed. This is further indicated by the higher final pH between 4- 5 that is typically observed, as in Figure 2-7. From these results and the numerous studies and conflicting mechanisms and rate constants presented in the literature, it is easy to see how complex this system really is. There are so many ions reacting in solution at any given moment that a straight forward set of reactions and rate constants are difficult to

elucidate because only a small number of ions can actually be measured with indicator solutions and electrodes.
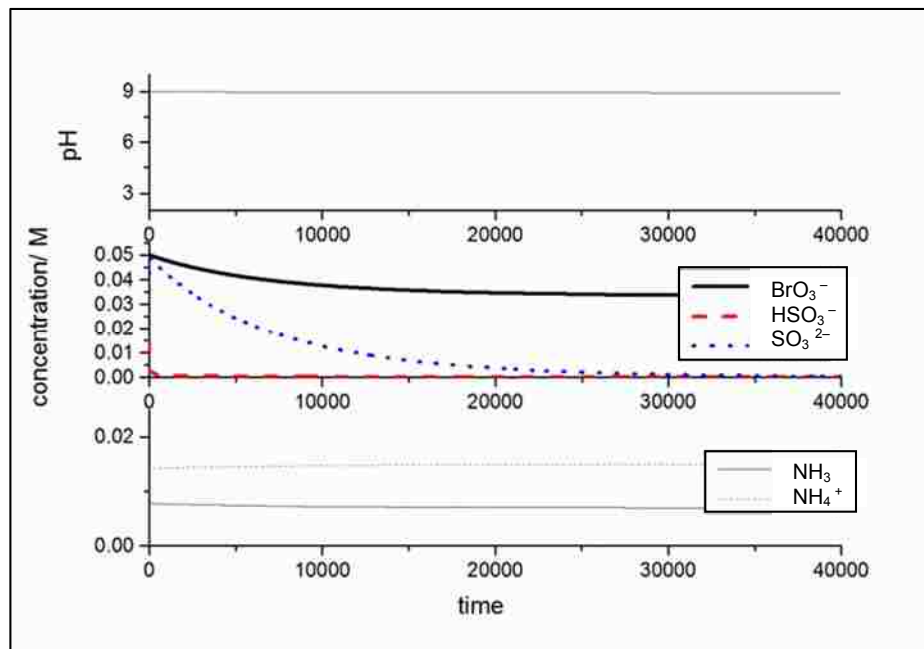
Figure 2-8. Effect of ammonia on reagent concentrations in a closed system, time in seconds. Image courtesy of Dr. Annette F. Taylor.

Even though we could not generate a storage stable system we still tried to create a time-lapse crosslinking system. Figure 2-9 shows the preliminary tests of PCDI with malonic and maleic acid (the two different dicarboxylic acids chosen as the crosslinkers). The images below show the PCDI mixed with malonic and maleic acid dissolved in a small amount of water and universal indicator. The acids lowered the pH to 4, as indicated by the red color, and the chemicals readily reacted over the course of a few hours.

Even though the malonic and maleic acids are very similar in structure, only differing by 1 carbon and 1 double bond, they yielded very different polymers. The

maleic acid polymer was textured and had mechanical properties similar to dried up

Silly String. It almost resembled a brain. This is due to the limited mobility of the carbon

backbone because of the double bond in the middle of the molecule. The malonic acid

has one more carbon and no double bond so it can move more to form the bonds. This

sample had more of a gummy, squishy texture, like a fruit gummy snack.
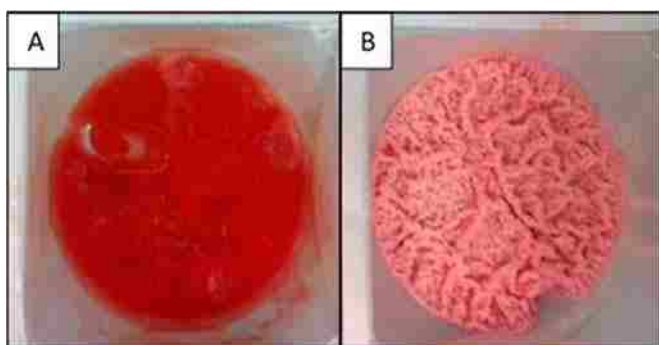
Figure 2-9. XL-702 (PCDI) polymerized with (A) malonic acid and (B) maleic acid

After a reaction was observed the samples were added to the clock reaction to

try and induce time-lapse crosslinking. However, the gelation of the media was never

observed. Many different polymer and clock reaction concentrations were tested but a

polymerization never occurred. This may be due to the malonic and maleic acids being

brominated in a Belousov-Zhabotinsky (BZ) type reaction.[77] This probably would cause

some steric hindrance or some electronic effects by removing electron density from the

reaction zone, prohibiting the internal cyclic rearrangement that is necessary to form the

N-acyl urea compound to complete the crosslinking (Figure 2-10). Another possibility is

the reaction of sulfuric acid with the CDI functional group, creating a sulfate ester

(Figure 2-11). [78] Since the attempts at creating both a storage stable system and a time-

lapse crosslinking system with the bromate-sulfite clock reaction were unsuccessful we

quit wasting time and moved on to the urea-urease clock reaction system discussed in Chapter 3.
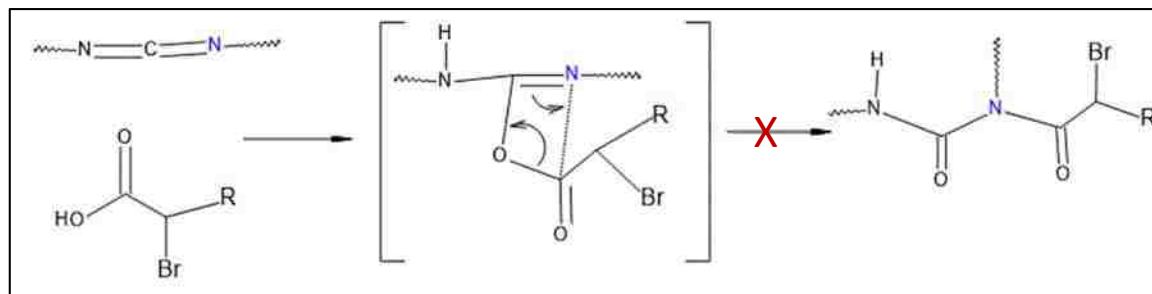
Figure 2-10. Depiction of how a brominated carboxylic acid could affect the reaction of the PCDI with a malonic or maleic acid.
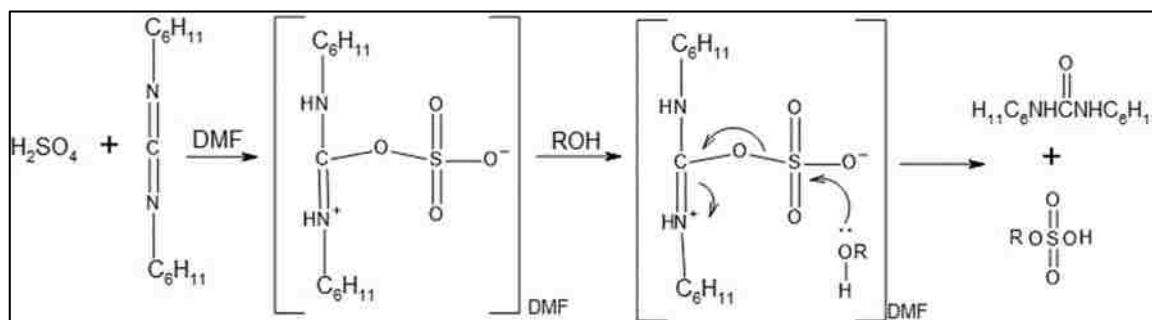
Figure 2-11. Reaction of PCDI with sulfuric acid. Adapted from Hoiberg et al.[78]

2.5 – Conclusions

In this work the bromate-sulfite clock time dependence on initial pH as altered by 18 M ammonium hydroxide was investigated. It was determined that the clock time could be delayed up to 2 hours with an initial pH < 9. However, an initial pH ≥ 9 resulted in the loss of clock reaction behavior. This because the bisulfite is not present at high pH, so the sulfite species is the one participating in the reaction with bromate. Because the S path is the only one reacting there is no net change in proton concertation. Therefore, the final pH does not drop drastically as it does when bisulfite reacts. To

further support this theory, the pH versus time plots when the initial pH is above 9 show characteristics of simple ammonia evaporation.

Even though the computer simulations show low initial reagent concentrations should be able to halt the clock reaction long enough to be stored that is not what was observed experimentally. These results demonstrate how complex this clock reaction is and even though we can mimic the overall reaction fairly well, predicting minute changes in the reaction mechanisms are not so straight forward.

In addition to failed attempts at creating a storage stable solution, creating a time-lapse crosslinking system was not successful either. The PCDI and malonic and maleic acids were shown to react readily without additional reagents at room temperature within a few hours. However, once incorporated into the bromate-sulfite clock reaction gelation was not observed over various reagent concentrations. This is most likely due to the reaction of the malonic and maleic acids with bromate in a BZ type reaction or reaction of PCDIs with sulfuric acid. With these results, the research of this system was concluded, and the urea-urease time-lapse polymerization system was pursued instead.

CHAPTER 3 – UREA-UREASE CLOCK REACTIONS

3.1 – Chapter Summary

This chapter will discuss the development of a new time-lapse polymerization system triggered by a pH clock reaction and the investigation of how changing reagent concentrations of the urea-urease clock reaction or thiol-acrylate hydrogel affected the final pH, clock time, gel time, degelation time, front velocities, storage modulus, and swelling ratio. Increasing the clock reagents' concentrations increased the initial rate of ammonia production and the urea concentration affected the final pH of the solution. This resulted in decreased clock times, gel times, degelation times, and storage moduli, while increasing front velocities and swelling ratios. Increasing monomer concentrations lowered the initial pH by increasing the 3-mercaptopropionic acid buffer content and produced more effective crosslinking bonds. This had the opposite effect of the increased urea concentration trials. In addition, the first isothermal frontal polymerization system that does not rely on the gel effect to propagate polymer fronts was produced. With Schlieren imaging it was observed that polymer fronts travel with pH fronts. This system has been proven to be highly tunable as a time-lapse polymerization system.

3.2 – Introduction

There are many applications for a cure-on-demand biocompatible and/or degradable polymer systems, such as adhesives[62], tissue engineering scaffolds[79], drug delivery systems[68], and in vitro cell differentiation platforms,[66] which can benefit from having an induction or working time before polymerization. To achieve this goal one must determine the external trigger that induces self-assembly and disassembly, like pH, temperature, chemical agents, etc. then find a way to insert or remove the stimulus

on an appropriate time scale.[69] Some work has been done using catalysts[80] or clock reactions[40] as triggers in self-assembly/disassembly. The urea-urease reaction specifically has been studied to produce self-mineralizing composites,[81] trigger the gelation of peptides,[82] create enzyme logic gates,[83] and program the gelation of chitosan for delivery of cells.[84]

Reaction-diffusion systems that produce chemical waves are of much interest to those studying biological processes and origins of life because these kinds of autocatalytic reactions are believed to be the methods by which the first organisms developed.[85] They are also a convenient method to develop a polymerization that can propagate along with the chemical waves in a system. Some of the systems that have been shown to produce fronts and induction times utilize inorganic reactions[39, 41], DNA catalyzers[34], and self-replicating moieties.[36-37, 86] These impressive and interesting systems unfortunately are either non-biocompatible or cannot easily be linked to other reactions.

The time-lapse polymerization system studied here was used to create the first isothermal frontal polymerization (IFP) system that does not rely on the gel effect to propagate the polymer fronts. Frontal Polymerization (FP) was first discovered by Chechilo et al.[46] and is a way to polymerize a solution or mixture by initiating the polymerization at one specific point and then the products of the polymerization promote further polymerization. The interesting part is that even after the external initiating stimulus is removed, the polymerization fronts can travel throughout the entire system. The most common type of FP is thermal FP. With this method a heat source is applied to one area of the reaction mixture, the heat produced from the exothermic reaction will

propagate through the system until it is fully polymerized even though the heat source was removed just after initiation.[57b] Although thermal FP can be very useful to create adhesives[87], wood fillers[57b], and endoskeletons for flexible materials[88], the temperatures of the reactions are well above 100 ºC. So it is not useful for most biological applications.

IFP is different from thermal FP in that the temperature remains constant throughout the system and is much lower than typical thermal FP systems. Previously, IFP required that the monomer solution be able to dissolve a small piece of polymer and could only be used with free-radical polymerizations. Once dissolved, the monomer solution has an increased viscosity in the polymer and polymerization will occur faster than in the less viscous monomer solution without polymer. This is referred to as the Trommsdorff or gel effect.[57a] IFP has been used to create optically gradient materials if a dopant is added.[89]

Unlike IFP systems studied previously which utilize the gel effect and free-radical mechanisms[59], we were able to develop an aqueous system that undergoes a Michael-addition type polymerization mechanism to form a hydrogel and does not require the gel effect to propagate the polymer fronts. The change in pH induced by the urea-urease clock reaction triggers the reaction between ethoxylated trimethylolpropane tri(3-mercaptopropionate) (ETTMP, Thiocure® 1300, or thiol) and poly(ethylene glycol) diacrylate (PEGDA). The solution is acidic upon addition of the thiol because there is residual 3-mercaptopropionic acid in each batch left over from the synthesis process which is difficult to remove. This was a useful happenstance because acid is needed to lower the pH of the solution to create a clock reaction with the urea-urease system.[2a]

Jack Bean Urease was the first enzyme to be crystalized almost a century ago.[25] Since then it has been well studied however, its complete crystal structure was just recently elucidated.[24] The reaction of urea with urease in water produces 2 ammonia molecules and 1 carbon dioxide molecule. Because urease has a pH dependent bell-shaped rate curve, a pH clock reaction can be produced if a small amount of acid is added to the solution before urease is added. Figure 3-1 shows the reaction mechanism of urea and urease, the pH dependent urease rate, a typical clock reaction pH plot, the pH dependent thiol-acrylate gelation rate, and the reaction ETTMP and PEGDA in basic solution.

In the figure below, the enzyme activity rate of the reaction can be seen in Figure 3-1(B). At pH 4 the urease is only mildly reactive. If urea and urease are in an acidic solution (between pH 3- 4 for this study), the urease will slowly start to decompose urea and produce ammonia [3-1(A)]. As the ammonia is produced the pH slowly starts to rise. With the increase in pH comes an increase in urease reaction rate, thus producing ammonia at a faster rate. We can see the autocatalytic rise in pH in Figure 3-1(C), yielding a typical urea-urease clock reaction graph. After the solution surpasses pH 7 the thiol monomers are more easily deprotonated and begin to react with the acrylate monomers. The pH dependent polymerization rate is shown in Figure 3-1(D) and the reaction of the monomers above pH 7 is shown in 3-1(E).

The urea-urease clock reaction was first studied by Hu et al.[2a] They determined the effect reagent concentrations had on the clock time and the difference between using a weak versus a strong acid had on the clock time. It was determined that a weak

acid dampens the abrupt switch in pH because a buffer is formed, increasing urea or

urease decreases clock time, and increasing acid concentration increases clock time.[2a]
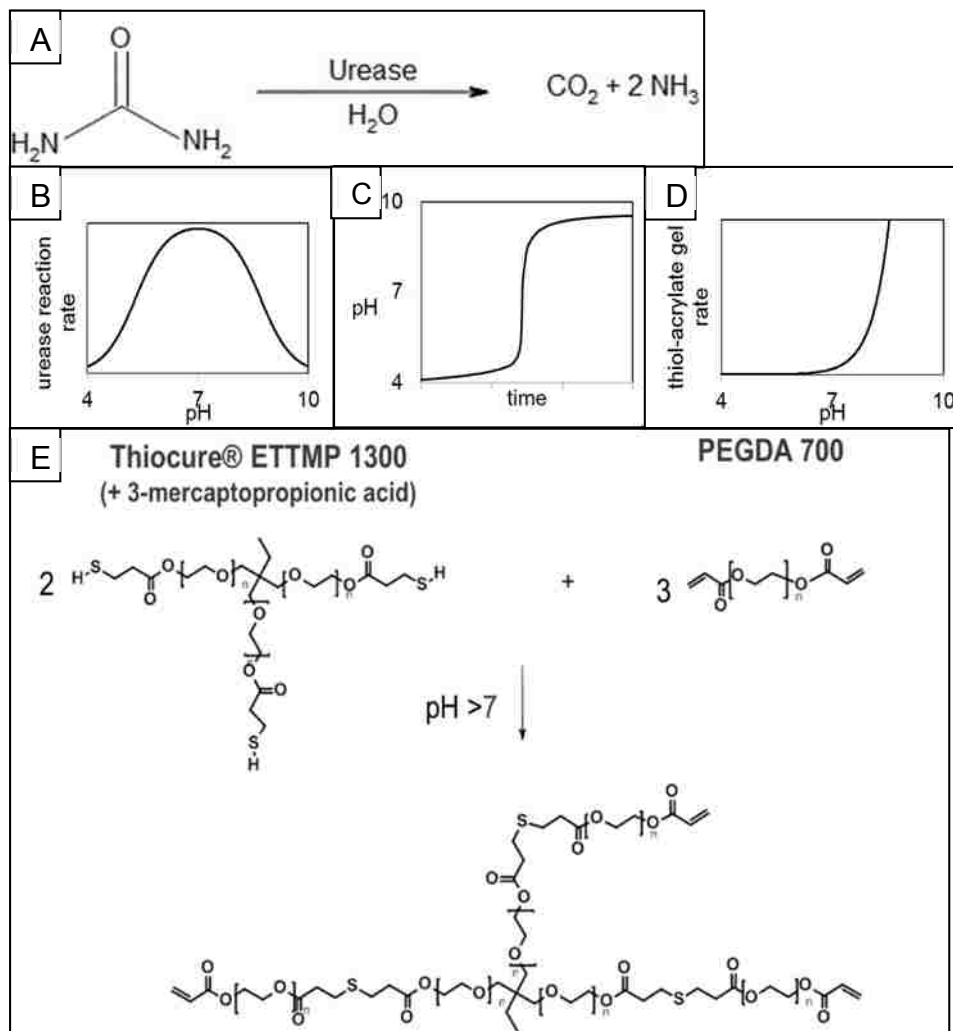
Figure 3-1. A) Urea decomposition by urease in water to produce carbon dioxide and 2 ammonia molecules. B) Urease enzyme activity graph. The maximum activity is at pH 7. C) Typical clock reaction graph for the urea-urease clock reaction. D) Polymerization rate of thiol-acrylate hydrogel made. These are adapted from Jee et al.[33] E) Michael-addition reaction of ETTMP to PEGDA and resulting bonds. The reaction does not stop here but rather continues to form a fully crosslinked network.

Following up that work, Wrobel et al.[2b] studied pH wave front propagation in the

urea-urease system. They found that increasing urea or urease concentrations

increased the front velocities and decreased the induction time before fronts appeared.

Also, the number of fronts that appeared increased. They also found that fronts propagated with a constant velocity. This is expected[34] from autocatalytic fronts that do not rely on diffusion alone to propagate.

These two works by Hu et al. and Wrobel et al. were the foundation of the work presented here. We studied how adding thiol and acrylate monomers to the urea-urease clock reaction to trigger a time-lapse polymerization affected the clock time, gel time of the polymer, and subsequent degradation time of the polymer in batch-cured systems. We also investigated the change in rheological behavior and swelling ratios in the batch-cured polymers. Polymer and pH wave front propagation in the IFP system was also studied. These monomers were selected because they have already been well characterized in aqueous buffered solution and proven to be biocompatible.[3] In addition to these features, the most important feature (besides being water soluble) was that they readily undergo a Michael-addition reaction in basic solution, while remaining unreactive at pH < 7.[60] This would allow for the entrapment of therapeutics or cells, which could then release the entrapped moieties in the body after a predetermined time of degradation. Also, PEG hydrogels are well studied entities in the biomedical field because of their diverse range of possible functionalities, biocompatibility, tunability of degradation rates, hydrophilicity, and porosity.[61, 67, 73b]

In this work, we explored the development of the time-lapse polymerization of ETTMP-PEGDA hydrogels triggered by the change in pH of the urea-urease clock reaction. The dependence of clock time, gel time, degradation time, front velocities, and front occurrence on reagent concentrations is discussed. Evidence that polymer fronts occur simultaneously with pH fronts is presented, and the gel times of stirred batch trials

are compared to the clock times. The swelling ratio of the hydrogel in DPBS at 20 ºC and 37 ºC were also investigated.

3.3 – Materials, Reactions, and Methods

The chemicals used for these experiments were: Jack Bean urease type III U1500 (34,310 Units/g solid) lyophilized powder from Sigma-Aldrich, extra pure (>98%) urea pearls from Acros Organics, Poly(ethylene glycol) diacrylate (PEGDA) (M_n = 700 g/mol, ρ= 1.12 g/mL) from Sigma-Aldrich, ethoxylated trimethylolpropane tri(3-mercaptopropionate) (ETTMP, Thiocure® 1300, or "thiol") (M_n = 1300 g/mol, ρ= 1.15 g/mL) from Bruno Bock Chemicals, and Universal Indicator (pH 2- 11) from Fischer Scientific. The pH probes used were purchased from Vernier and the accompanying Logger Lite software for data collection was utilized. For frontal polymerization experiments, 60 X 15 mm polystyrene Falcon® disposable petri dishes were obtained from VWR. The stir plates were VWR brand.

In these experiments clock time and gel time were measured as a function of initial reagent concentrations. For each concentration variation 50 mL of solution was made to perform triplicate trials of both the batch-cured tests and thin layer IFP tests. 1 mL of universal indicator was included in every trial. The batch-cured tests were the stirred trials in 50 mL glass beakers with a 5/8" X 5/16" Teflon stir bar. The stir plate was set to 4, which was later determined to be between 1500 – 1700 rpm depending on which stir plate was used. A Vernier pH probe was inserted into the liquid for all stirred trials. Unfortunately, the stroboscope tachometer, which was used to determine stir plate rpm, was not purchased until after the experiments were completed. Even though the setting of 4 on each stir plate varied by about 100 rpm, the results proved to be

reproducible in that range. The gel time was defined as the point when the stir bars

ceased to spin because of sufficient gelation of the solution.

In the thin layer experiments, 1.5 mL of the mixed solution from a batch trial was

withdrawn and dispensed between the inverted petri dish lid and bottom. The bottom

was placed carefully on the lid so no air bubbles were trapped. A Pentax Optio W80

camera with time-lapse image shooting capability was anchored directly above the petri

dish to record the propagating pH fronts. An illustration of the experimental set up can

be seen in Figure 3-2 below.
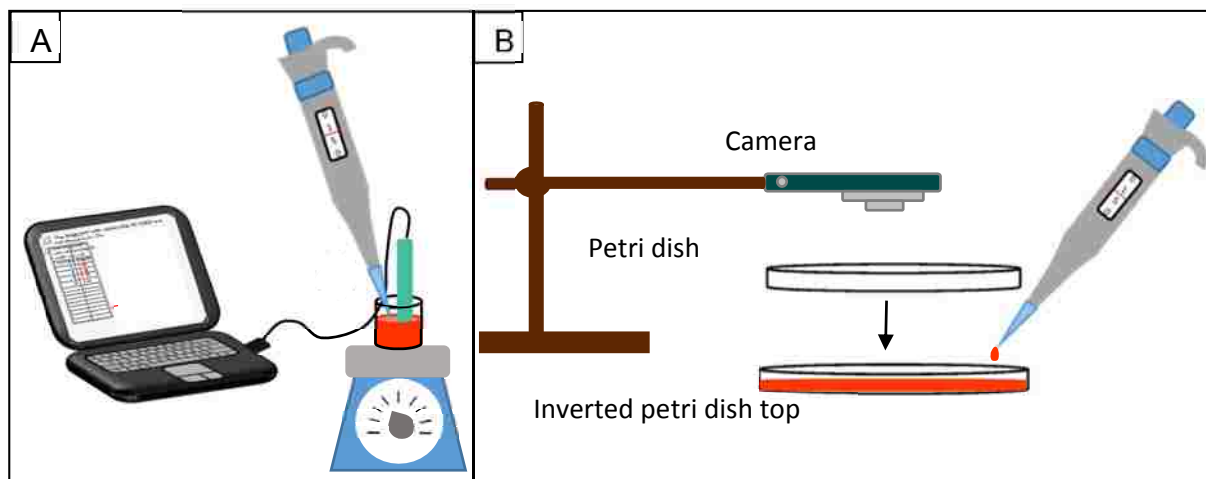
Figure 3-2. A) All reagents for the clock reaction were mixed together in a beaker. The pH probe was inserted and data collection commenced. A pipette was used to remove 1.50 mL of the reaction mixture. B) The 1.50 mL removed was dispensed into the inverted petri dish top. The petri dish bottom was placed on top the solution and time-lapse photography of the fronts began.

The pH of the solution was recorded by the probe at a rate of 1 data point every

3 seconds. Data collection continued until the switch in pH from acidic to basic was

observed, and the pH remained constant over several minutes. The gel time of the

solution was the time when the stir bar quit stirring. It was measure with a stop watch.

Time-lapse images of the wave fronts in the petri dish apparatuses were recorded until the entire dish switched from red (acidic) to blue (basic). Images were taken every 10 seconds. Image sequences were analyzed with ImageJ. The diameter growth of 3 different spots per image sequence were measured using the straight line measuring tool. The distance-to-pixel ratio of each image sequence was calibrated at the beginning of every new trial. Four measurements were taken of each chosen spot at each time interval to average and account for error in measurement. The measured diameters for each spot and time were imported to an Excel file. Plots of the radial distance traveled versus time were made for each spot measured. The front velocity was determined from the slope of the line made by those plots and were then averaged for each petri dish. Those averages were then used to calculate the average and standard deviation of each reagent concentration variation.

Some trials did not produce wave fronts so switch time alone is reported. Switch time is the time needed for the entire system to switch from acidic to basic; similar to the clock time in the batch systems. The switch time was measured from the start of the video until the entire solution turned blue. The recorded times were plotted as a function of reagent concentration.

Rheological experiments were also performed using a TA AR200ex rheometer with the aid of Dr. Qinglin Wu, Renewable Natural Resources Professor at LSU, and his graduate student, Kunlin Song. Solutions were made in a similar fashion as the batch studies. One solution containing the desired urea, thiol, and acrylate concentrations was made with a total volume of 3 mL. Then a 1 mL urease solution of desired concentration was made. The vials were transported to the rheometer lab, and the urease solution

41

was poured into the urea/thiol/acrylate solution. The resulting mixture was shaken for ~30 seconds before 1.50 mL was withdrawn with a syringe and dispensed onto the Peltier plate. A 40 mm steel plate was lowered onto the solution at a set height of 1.0000 mm. Any extraneous liquid that was expelled from between the plates was wiped up from the Peltier plate. The changes in storage and loss moduli were recorded over time as the sample was sheared at a fixed angular frequency of 0.628 rad/s, with a constant 1% strain, at ambient temperatures (typically 22- 24 ºC).

In the gelation/degelation experiments in vials, 15 mL of solution was prepared for a given concentration set and dispensed into 4 mL vials until full. If an air bubble happened to be trapped in the solution it was monitored for movement. If an air bubble was not trapped during filling of the vials, then ammonia and carbon dioxide gases produced from the reaction of urea and urease were formed and those bubbles were monitored. Gelation was defined as the time when bubbles stopped moving upon inversion of the vials and degelation was defined as the time when movement was allowed again after sufficient hydrolysis of the gel.

Shadowgraph experiments were performed to observe the propagating polymer fronts and elucidate if the fronts traveled with the pH fronts. Dr. Patrick Bunton, Physics Professor at William Jewel College, captured the shadowgraph images.

Swelling studies were performed with discs made in a 1 cm diameter silicone mold with a volume of 0.60 mL solution per well. Discs were made in batches of 12 per concentration variation and allowed to cure for 24 hours before lyophilization for 48 hours. After freeze drying the dry weights were measured, and the discs were placed in Dulbecco's phosphate-buffered saline (DPBS) for swelling. The discs were weighed

several times the first day and then once daily after that. For each measurement, the discs were removed from the DPBS, lightly blotted on a paper towel to remove excess liquid, and then the wet weight was recorded. After weighing the discs were returned to the jar of DPBS and either left on the bench top or placed back in the incubator. Swelling was monitored for at least a week, in some cases longer.

3.4 – Results and Discussion

3.4.1 – Batch Reaction Polymerizations

The original idea, to create a hydrogel from poly(ethylene glycol) diacrylate (PEGDA) and ammonia produced from the decomposition of urea by urease, was not successful. Initial tests were performed with just PEGDA and concentrated ammonium hydroxide and also PEGDA mixed with some water and ammonium hydroxide. Theoretically, this should work because it is a simple base catalyzed Michael-addition reaction[90] between the ammonia and an acrylate. To make sure it was possible we tried it first before coupling it to the clock reaction. Figure 3-3 shows the tests with two sets of vials. Figure 3-4 shows the reaction of the ammonia and PEGDA.

When the PEGDA was added to the clock reaction, polymerization did not occur. The clock reaction still proceeded as normal but no gelation of the PEGDA was observed. The first thought was to look at the amount of ammonia being produced in a given reaction. With the higher urea concentrations used (0.1 M) the pH plateaus around 9.3. Since these systems are mostly water, and do not contain buffers or significant amounts of strong acids and bases, the pH should theoretically be much higher if all of the urea is converted to ammonia.
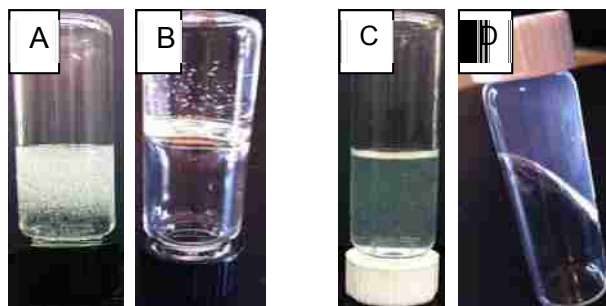
Figure 3-3. Images A & B show the mixing and subsequent gelation of 2.0 g PEGDA and 20 µL 18 M NH4OH. Images C & D show the mixing and subsequent gelation of 2.0 g PEGDA, 2.0 g H2O, and 20 µL 18 M NH4OH.
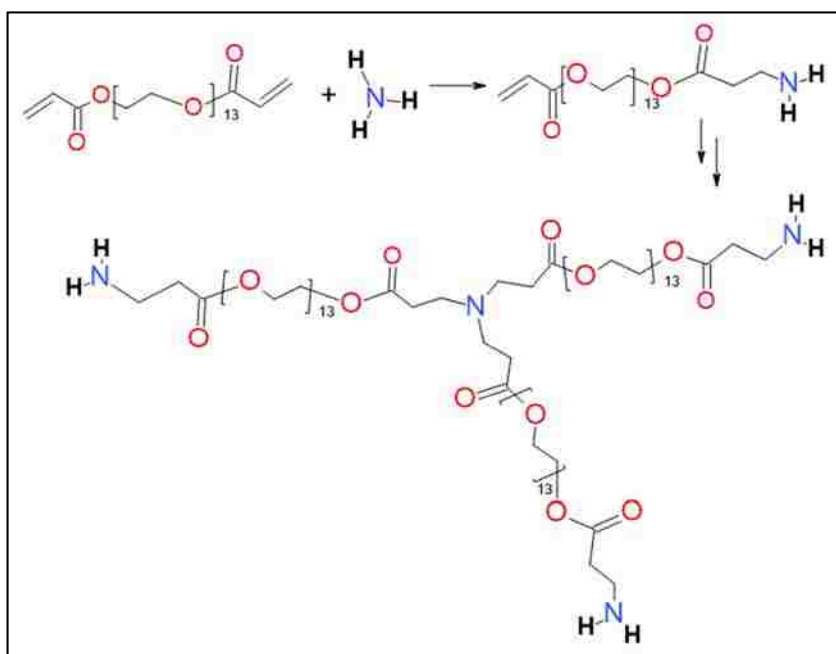
Figure 3-4. PEGDA and NH3 Michael addition type polymerization method leading to a completely crosslinked network.

Using simple acid/base equilibrium equations (Equations 1-11) it can be seen that only 0.224 µM NH3 is produced if the pH stops at 9.3. From Equations 12 – 19 we can see that to produce enough ammonia to crosslink a 0.05 M PEGDA solution the pH must reach almost 11.

$$(1) \qquad 14 = pOH + pH$$

$$(2) \qquad 14 - 9.3 = pOH$$

(3) $\qquad$ $4.7 = \text{pOH}$

(4) $\qquad$ $[\text{OH}] = 10^{-4.7} = 1.995 \times 10^{-5}$

(5) $\qquad$ $\text{pK}_{\text{b,NH}_3} = 4.75$

(6) $\qquad$ $10^{-\text{pK}_\text{b}} = 10^{-4.75}$

(7) $\qquad$ $\text{K}_{\text{b,NH}_3} = 1.778 \times 10^{-5}$

(8) $\qquad$ $\text{K}_\text{b} = \dfrac{[\text{OH}^-][\text{NH}_4^+]}{[\text{NH}_3]}$

(9) $\qquad$ $[\text{NH}_3] = \dfrac{[\text{OH}^-][\text{NH}_4^+]}{\text{K}_\text{b}}$

(10) $\qquad$ $[\text{NH}_3] = \dfrac{\left(1.995 \times 10^{-5}\,\text{M}\right)^2}{1.778 \times 10^{-5}\,\text{M}}$

(11) $\qquad$ $[\text{NH}_3] = 2.24 \times 10^{-5}\,\text{M}$

(12) $\qquad$ $\text{K}_\text{b} = \dfrac{[\text{OH}^-][\text{NH}_4^+]}{[\text{NH}_3]}$

(13) $\qquad$ $[\text{NH}_3] \times \text{K}_\text{b} = [\text{OH}^-][\text{NH}_4^+]$

(14) $\qquad$ $(0.05\,\text{M NH}_3)(1.778 \times 10^{-5}) = [\text{OH}^-][\text{NH}_4^+]$

(15) $\qquad$ $[\text{OH}^-] = \sqrt{8.89 \times 10^{-7}} = 9.429 \times 10^{-4}$

(16) $\qquad$ $pOH = -\log_{10} 9.429 \times 10^{-4}$

(17) $\qquad$ $14 - pOH = pH$

(18) $\qquad$ $14 - 3.02 = pH$

(19) $\qquad$ $pH \cong 11$

Remembering the urease enzyme activity graph in Figure 3-1B, it is obvious that the enzyme does not work above pH 10. This graph is theoretical and more practically it is seen that the enzyme will not produce enough ammonia for the solution to go above 9.3- 9.5. Therefore, this clock reaction can never produce enough ammonia to make a

hydrogel network using ammonia as a crosslinker between PEGDA monomers. Thus, a different set of monomers must be chosen.

Some lab members were using ETTMP and PEGDA as monomers to make a hydrogel. The monomers are water soluble and undergo a Michael-addition type reaction. Below pH 7 they are unreactive, so they seemed like the perfect candidate. After the first time mixing them in with the clock reaction they polymerized when the solution turned basic.

In this section, 3.4.1- Batch Polymerization Reactions, I will describe how changing the initial reagent concentrations of monomers, urea, and urease affected the clock time, gel time, and degradation time of the hydrogel. Since the two monomers needed a stoichiometric ratio of functional groups to optimally react, they were kept in a 2:3 molar ratio of ETTMP:PEGDA throughout all experiments. For ease and to abate confusion, changes in the monomer concentration will be referenced in terms of ETTMP concentration. For example, if it is said that 0.05 M ETTMP was used, it is implied that the corresponding 0.075 M PEGDA was used to keep the appropriate ratio of monomers.

Figure 3-5 shows the clock time, gel time, and final initial pH as a function of urea concentration. As urea concentration increases, the clock time and gel time decrease. This is the same trend observed in the experiments without the monomers.[2a] The initial pH does not change much with increasing urea concentration for the 0.01 M and 0.03 M trials because the urea does not have a direct effect on the pH of the solution. However, in the 0.05 M and the 0.10 M urea trials there is a large amount of experimental uncertainty associated with the initial reagent concentration. This is due to the ammonia

produced during initial mixing of the urea/ETTMP/PEGDA and urease solutions. With high urea concentrations the solutions begin producing ammonia within microseconds upon insertion of the urease solution which causes local variances in the initial pH. After about 30 seconds the solution is well mixed and homogeneous. This is further supported by the 0.1 - 0.2 increase in pH observed after complete mixing.

Figure 3-5. Average clock time, gel time, and initial pH as a function of urea concentration. Initial concentrations were $[urease]_0$ = 0.5 mg/mL (17 units/mL) and $[ETTMP]_0$ = 0.05 M, T = 25 °C. Error bars are from 3 repeat trials.

Figure 3-6 shows the dependence of clock time, gel time, and initial pH on urease concentration. As urease concentration increases, the clock and gel times decrease. It is also interesting to note that because of the short clock times observed in these trials, the trend between clock time and gel time is easily discernible in this graph. Because of the large time scale associated with the other 2 reagent variation graphs, the gel time appears to happen around the same time of the clock time but the amount

of time between the two is not noticeable. They are all within 2-5 minutes of each other. This indicates that the polymer fronts should propagate closely behind the pH fronts in thin layers. This will be discussed further in the next section.
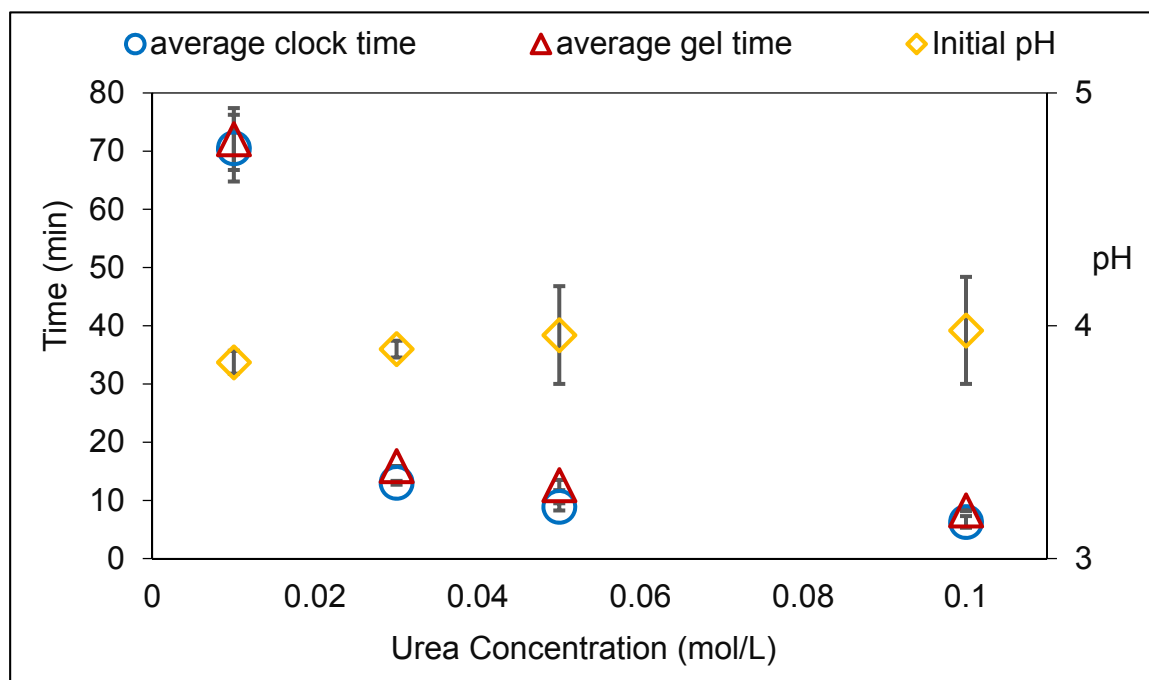

Figure 3-6. Average clock time, gel time, and gel pH as a function of urease concentration. Initial concentrations were $[urea]_0$ = 0.03 M and $[ETTMP]_0$ = 0.05 M, T = 25 °C. Error bars are from 3 repeat trials.

The other information that can be gleaned from this graph is the initial pH dependence. The initial pH increases with increasing urease concentration, and the uncertainty associated with the largest concentration is much larger than the two lower concentrations. This is for the same reason as the experimental uncertainty seen in the largest urea concentrations. Upon mixing, the urease is most concentrated at the point of addition and starts reacting very quickly, thus increasing the pH instantly in that area. However, after thoroughly mixing the two solutions the urease concentration is homogenous throughout the beaker, and the rate of ammonia production slows down.

Within experimental uncertainty, the trend with urease concentration and clock time is similar to that observed in the monomer-free studies.[2a]

Figure 3-7 shows the clock time, gel time, and initial pH dependence on ETTMP concentration. As expected, with increasing monomer concentration there was an increase in clock and gel time, and a decrease in initial pH. With the addition of monomer there is an addition of 3-mercaptopropionic acid. As with the previous work by Hu et al. an increase in acid concentration leads to a decrease in initial pH and an increase in clock time.[2a]
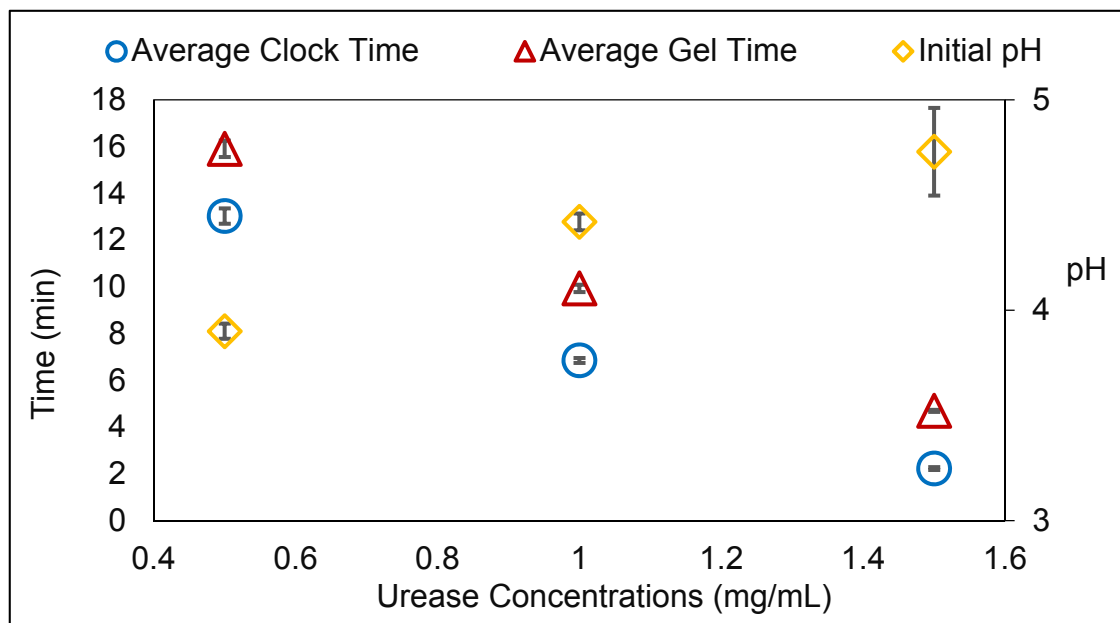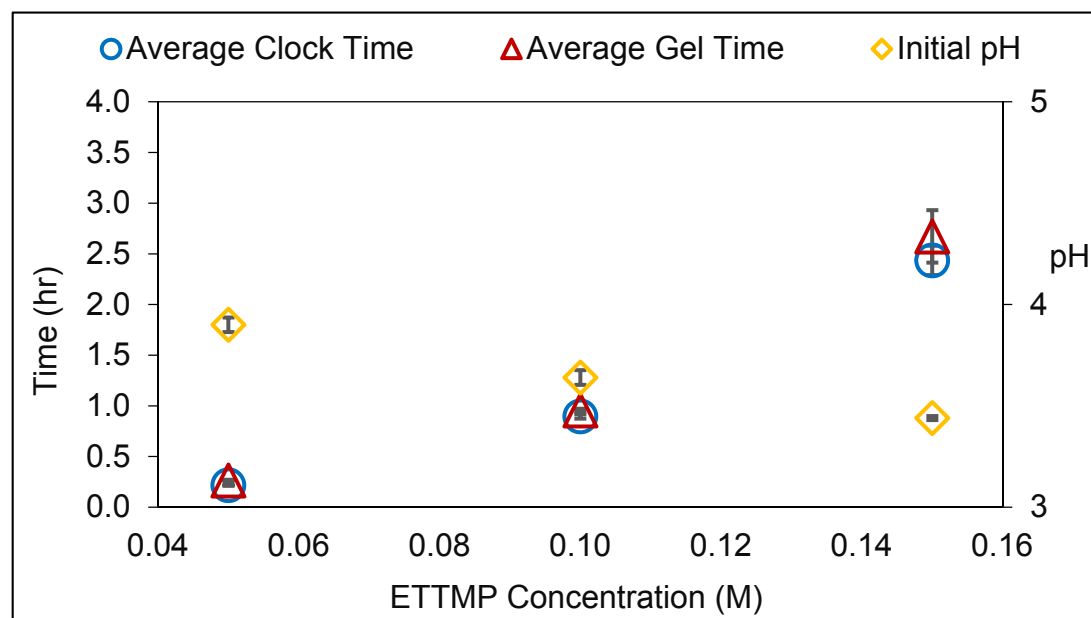

Figure 3-7. Average clock time, gel time, and gel pH as a function of ETTMP concentration. Initial concentrations were $[urea]_0$ = 0.03 M and $[urease]_0$ = 0.5 mg/mL (17 units/mL), T = 25 °C. Error bars are from 3 repeat trials.

Figure 3-8 shows the final pH as a function of reagent concentration. Increasing urea concentration increases the amount of ammonia produced which raises the final pH. Increasing the urease concentration increases the rate that the ammonia is produced and therefore does not affect the final pH. Increasing ETTMP concentration

lowers the initial pH of the solution, which not only delays the clock time, but also decreases the final pH when the same amount of ammonia is produced for each lower initial solution pH.
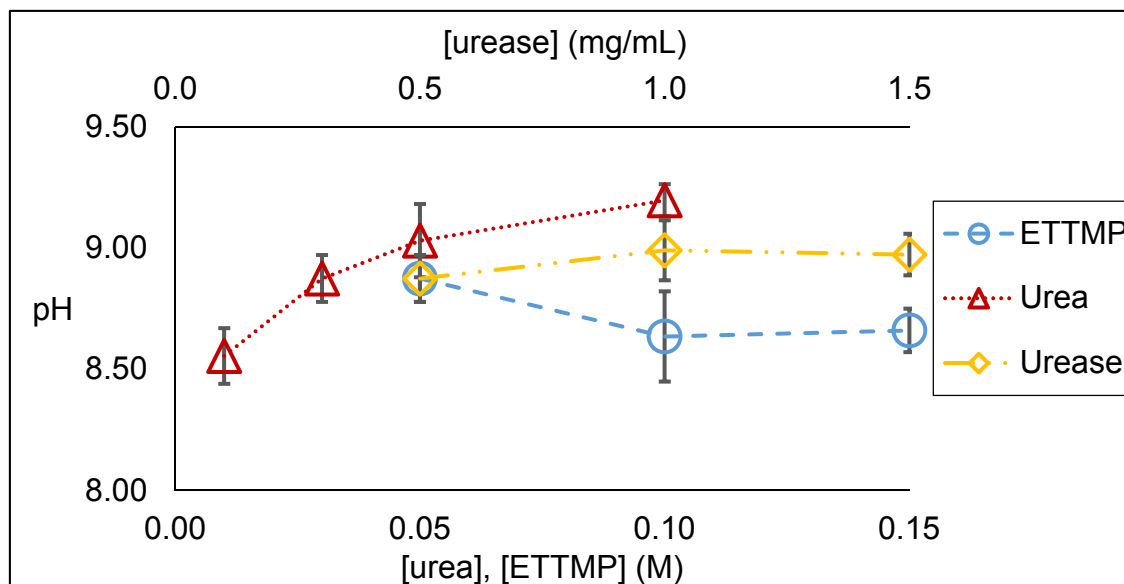
Figure 3-8. Average final pH as a function of reagent concentration. Initial concentrations of the unvaried reagents were $[urea]_0$ = 0.03 M, $[urease]_0$ = 0.5 mg/mL (17 units/mL), $[ETTMP]_0$ = 0.05 M, and T = 25 °C. Error bars for 3 replicate trials of each variation.

Figure 3-9 shows the degelation times of the batch-cured samples as a function of urea and ETTMP concentrations. During the first day, time was recorded starting with when the solutions were made and when any returned to liquid that time was recorded for the sample. After the first day the time to return to the liquid state was counted by days rather than hours and solutions were checked daily. There are 2 factors in this system that can be manipulated by changing the reagent concentrations to affect the hydrolysis rate. The final pH of the water present and the amount of water present in the hydrogel will determine the rate at which the hydrolysis occurs.[91] Changing the number of carbons between the thiol group and the ester linkage could also alter the hydrolysis

rate[92], but for this study we used the same monomers and only varied the reagent concentrations. As would be expected, decreasing the urea concentration increased the time required for the gel to revert back to a liquid. This is because the amount of ammonia formed was greater, producing a higher final pH. Increasing the ETTMP concentration led to a decrease in the amount of water present in the same volume of solution. This resulted in a decrease in the amount of hydroxide present to cleave the esters and also an increase in the number of bonds that would need to be cleaved in order to allow flow of the chains.
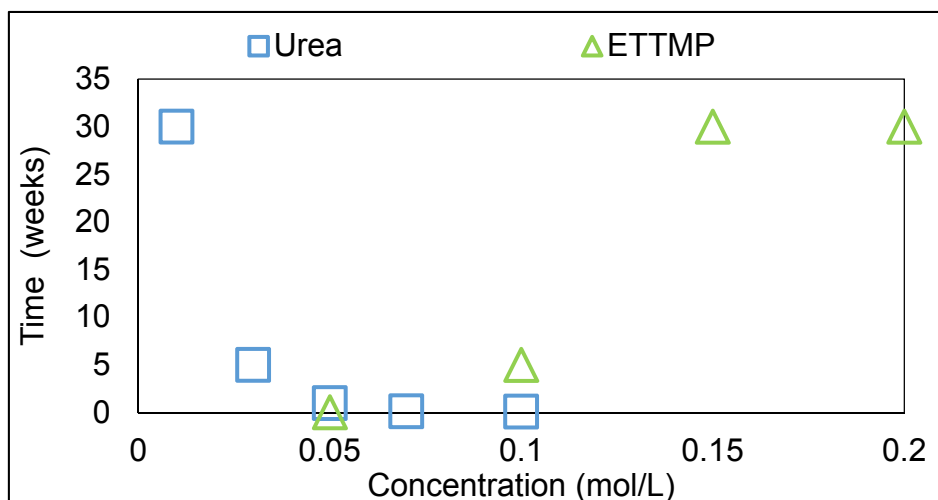
Figure 3-9. Degelation time of samples based on urea and ETTMP concentrations is defined as the time it took the sample to return to the liquid state. Initial concentrations of unvaried reagents were $[urea]_0 = 0.03$ M, $[ETTMP]_0 = 0.10$ M, $[urease]_0 = 0.5$ mg/mL (17 units/mL). Three replicate trials were prepared for each concentration and no discernible difference in degelation time was observed

Figure 3-10 shows gelation and subsequent degradation of 0.05 M ETTMP hydrogels as triggered by two different urea concentrations in the urea-urease clock reactions (0.01 M urea and 0.1 M urea). As was seen with the urea concentration variation batch trials and the degradation study shown in Figures 3-5 and 3-9, using less urea resulted in an increase in gel time and degradation time. Comparing the black solid

line (0.1 M urea) and the blue dashed line (0.01 M urea) a difference in gel time, degradation time, and storage modulus can be seen. Since the monomer concentration is constant in both trials, these are all due to the difference in urea concentration, which affects the amount of ammonia produced. The 0.1 M urea trial polymerizes before the 0.01 M urea trial because more ammonia is produced in the same amount of time initially, which increases the rate of ammonia production in the autocatalytic urea decomposition, and the buffer effects of the 3-mercaptopropionic acid are quickly overcome. Also, the final pH of the solution/hydrogel is higher with the greater urea concentration so the rate of hydrolysis of the ester groups is competitive with the rate of polymerization of the monomers. This is most likely why there is a difference in storage modulus between the two trials, even though the monomer concentrations are equal. And it is most definitely the reason the subsequent degradation of the 0.1 M urea trial is faster than the 0.01 M urea trial.
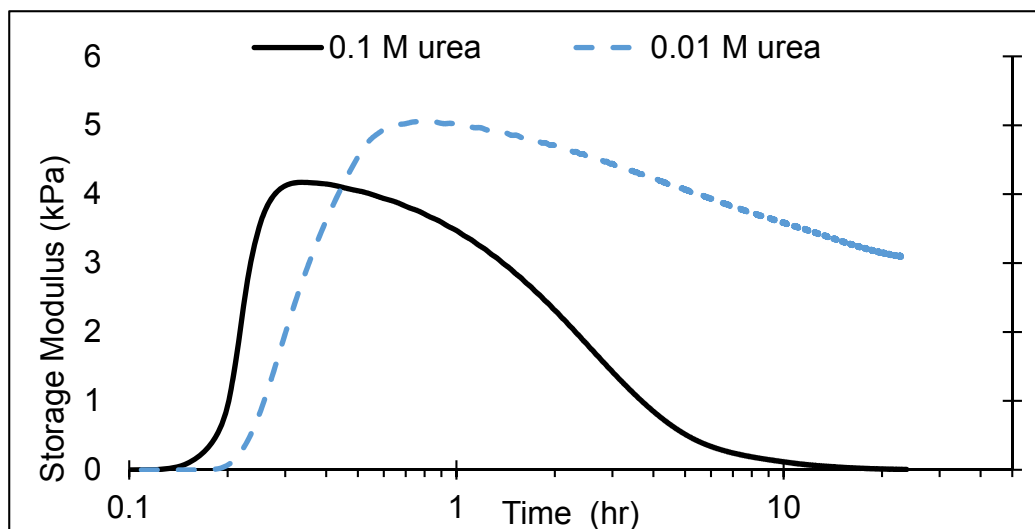
Figure 3-10. Rheological measurements of hydrogels. Initial concentrations were [ETTMP]$_0$ = 0.05 M, [PEGDA]$_0$ = 0.075 M, [urease]$_0$ = 0.5 mg/mL (17 units/mL), [urea$_1$]$_0$ = 0.1 M (black solid line), and [urea$_2$]$_0$ = 0.01 M (blue dashed line). Graph adapted from Jee et al.[33]

In Figure 3-11, once again, the urea concentration is varied with 0.01 M and 0.1 M, but now the ETTMP concentration is raised to 0.1 M. Looking at this graph, the same trends as in Figure 3-10 can be seen with the difference in urea concentration: the higher urea concentration led to shorter gel times, shorter degradation times, and lower storage modulus of the hydrogel. However, the difference in gel time between the two trials with the 0.1 M ETTMP is greater than with the 0.05 M ETTMP because there is more 3-MPA buffer to overcome. Starting from a lower pH the rate of urea consumption by urease is lower and also, more ammonia must be produced to raise the pH above the buffered pH.[2a]
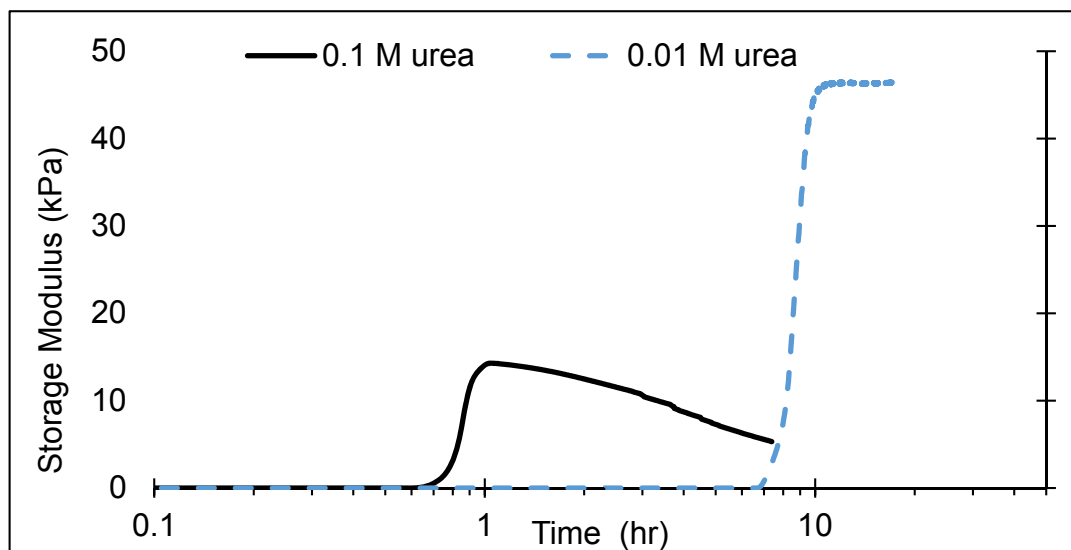
Figure 3-11. Rheological measurements of hydrogels. Initial concentrations were [ETTMP]$_0$ = 0.1 M, [PEGDA]$_0$ = 0.15 M, [urease]$_0$ = 0.5 mg/mL (17 units/mL), [urea$_1$]$_0$ = 0.1 M (black solid line), and [urea$_2$]$_0$ = 0.01 M (blue dashed line). Graph adapted from Jee et al.[33]

The large difference in storage modulus between the two trials is most likely due to ester hydrolysis during polymerization, just like with the lower ETTMP concentrations. However, it is more pronounced with the increased ETTMP concentrations because

there are more ester groups that can be broken and more effective bonds in the hydrogel that can be made. With the more dilute 0.05 M ETTMP trials, there is a greater chance of ineffective bonds forming.[91] Meaning, active chain ends are more likely to react intramolecularly and produce defects in the hydrogel network via self-looping bonds, cyclic oligomers, or just leave unreacted ends dangling. With the more concentrated 0.1 M ETTMP hydrogel, there are more unreacted acrylate monomer ends around the active thiol anions, and it is less likely for intramolecular reactions to happen. Also, with the increased concentration comes the increased chance of entanglements, which also adds to the storage modulus of a hydrogel.[91] The increase in effective bonds is also the reason the 0.1 M ETTMP trials took longer to degrade. With the 0.01 M urea/0.1 M ETTMP trial, it did not degrade over the 24-hour rheological study and was also the same concentration of one of the trials in the degelation study (Figure 3-9) that still has not degraded over the course of the year. The data shown here in Figures 3-10 and 3-11 matches that explained in Figure 3-9. The gel times, degradation times, and gel strength can be tuned by adjusting urea or ETTMP concentrations.

3.4.2 – Thin Layer pH Wave Front Experiments

The thin layer IFP experiments were conducted alongside the batch-cured experiments. As mentioned in the materials and methods section, 1.5 mL of each solution was withdrawn from the preliminary batch sample trials and dispensed in a petri dish for wave front observation. The Pentax camera was mounted above the petri dish for imaging. After the IFP experiments were performed it was realized that all the concentrations should be lowered to allow a greater range between front speeds and switch times in the concentration ranges chosen. So there would be a direct comparison

between batch-cured and IFP trials it was decided to re-do the batch-cured experiments with the new range of concentrations chosen for IFP studies. So the batch-cured trials presented in the previous section, 3.4.1, are not the same concentrations as the IFP trials presented in this section, 3.4.2.

Also, our collaborators had the shadowgraphy equipment set up to accurately measure the polymer wave fronts alongside the pH wave fronts and determine they were indeed propagating concurrently.[33] Thus, after a new set of reagent concentrations was established, they performed the more accurately recorded experiments. Therefore, these wave front experiments cannot be directly compared to the batch experiments described in the previous section. However, the same general trends were observed: increasing clock reagent concentrations increases front velocities and clock times, while increasing monomer concentrations decreases front velocities and clock times.

The universal pH indicator changes color according to the pH of the solution as follows: red < 3.0, orange-red (3.0 – 4.0), orange (4.0- 5.0), orange-yellow (5.0- 5.5), yellow (5.5- 6.0), green-yellow (6.5), yellow-green (7.0), light green (7.5), dark green (8.0), blue-green (8.5), blue (9.0), and purple ≥10. However, the clock reaction never reached pH 10. Determining the pH of the solution is not as accurate with the indicator as it is with the pH probe, but an estimation can be made. The switch times of the trials can be seen in Figure 3-12. The switch time of the petri dish trials were defined as the time when the entire petri dish turned blue, signifying the end of the pH change.

From Figure 3-12 it is apparent that increasing the urea and urease concentrations results in a decrease in switch time. As expected, the opposite trend is observed with increasing monomer concentrations from 0.13 M thiol (18.3 min switch) to

0.27 M thiol (21.7 min switch). When monomer concentrations were increased the amount of 3-MPA increased and creates a larger buffer to be overcome. This requires more ammonia to be produced before seeing a large increase in pH. Only two different monomer concentrations were tested so an official trend cannot be stated. However, the constant ETTMP concentration was 0.067 M, which is lower than the lowest data point for the monomer variations, and the urea concentration was 0.06 M. There were urea concentrations of 0.05 M and 0.08 M tested, and they switched at 1.9 and 1.3 min, respectively. Therefore we can estimate that the 0.067 M ETTMP concentration with a constant urea concentration of 0.06 M would switch around 1.6 min. This is significantly lower than the 0.13 M and 0.27 M ETTMP concentrations.
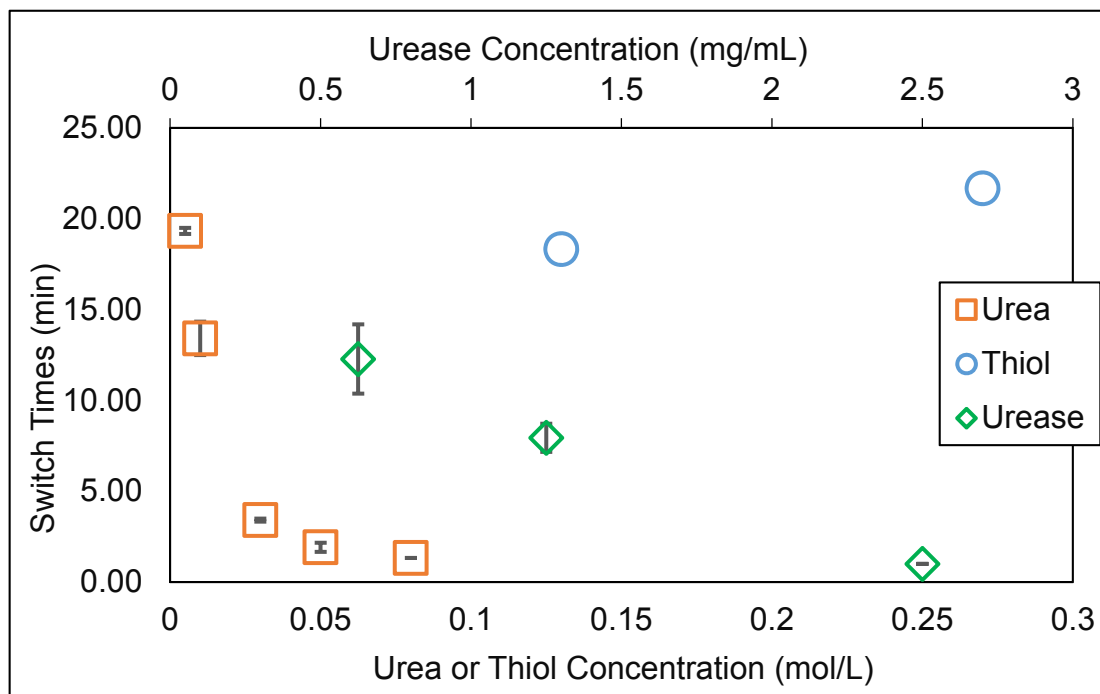
Figure 3-12. Switch times of various reagent concentration samples in petri dishes. Switch times were measured as the time when the entire petri dish turned blue (basic). Initial concentrations of unvaried reagents were $[urea]_0 = 0.06$ M, $[urease]_0 = 1.25$ mg/mL, $[ETTMP]_0 = 0.067$ M, and $[PEGDA] = 0.10$ M, T = 22 °C.

Front velocities were determined by measuring the change in diameter of a front spot over time. The diameter was then divided in half and plotted versus the time measured. A typical plot to determine front velocity can be seen in Figure 3-13. Each growing spot was kept as its own series of data points, and a line was fitted to it. Then the slope from each spot's line was averaged with all the slopes for a given concentration set and the error was determined. After the front velocities were determined for all the concentration variations, a plot showing the trend between changing concentrations was made and can be seen in Figure 3-14.
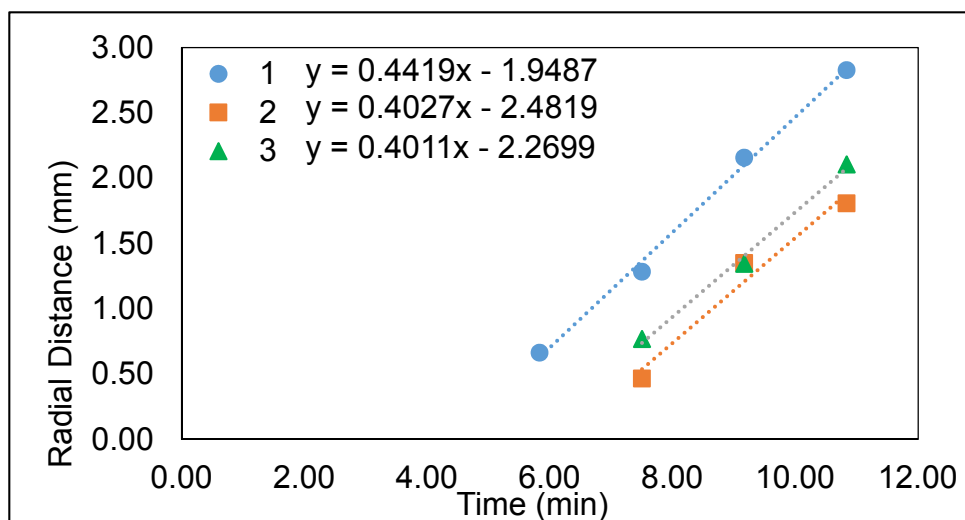
Figure 3-13. Radial distance traveled as a function of time for 3 different fronts in a single petri dish. Initial concentrations were [urease]$_0$ = 1.25 mg/mL and [ETTMP]$_0$ = 0.067 M.

A summary of the front velocities calculated from all the trials can be seen in Figure 3-14. Front velocities increased with increasing clock reagent concentrations. No trend can be deduced from the increasing monomer concentrations because only 2 different concentrations were successfully recorded and only the lower monomer concentration trials actually produced fronts. The higher monomer concentration trials changed pH uniformly across the petri dish. The figures below will illustrate the

experiments performed to obtain front velocity and total switch time. The same trends are observed as were seen in the batch polymerization trials. An increase in urea or urease produces an increase in front velocity and switch time, because the clock reaction produces ammonia more quickly, thus increasing the autocatalytic response in urease activity. Also, an increase in monomer concentration led to a decrease in front velocity and switch time, because more 3-MPA was present and a larger buffer capacity was formed.
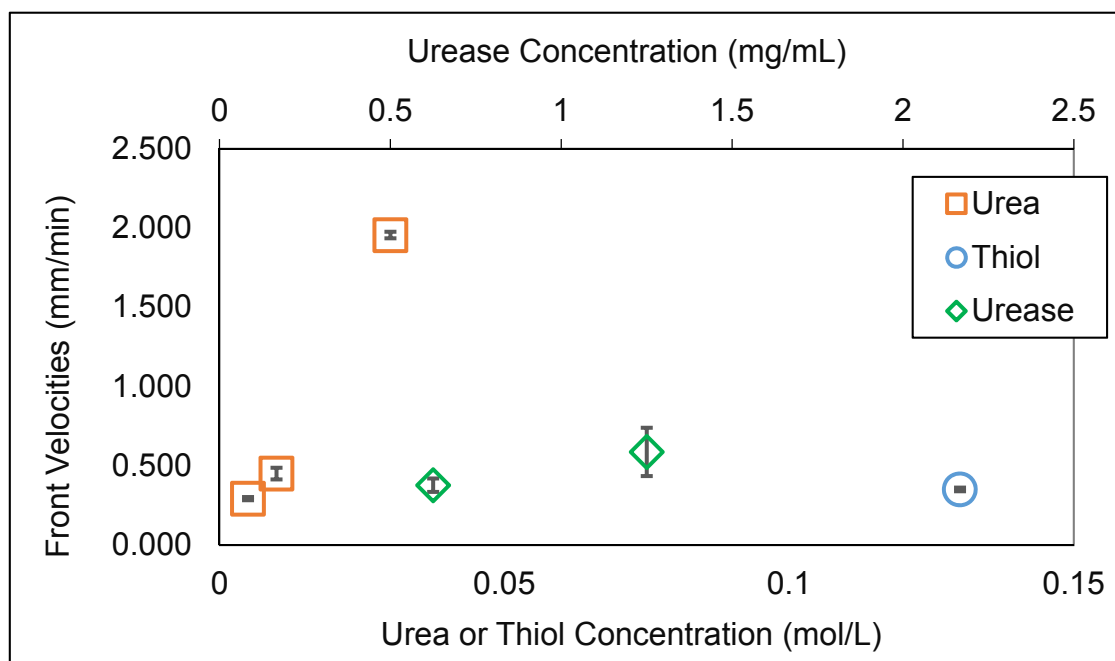
Figure 3-14. Front velocities averaged over 3 trials per set of reagent concentrations. Initial concentrations of unvaried reagents were $[urea]_0$ = 0.06 M, $[urease]_0$ = 1.25 mg/mL, $[ETTMP]_0$ = 0.067 M. Monomers always kept in a 1:1 functional group ratio.

In Figure 3-15 (0.13 M thiol) the first fronts appeared around 12 minutes, and the switch time was about 18 minutes. In 3-17 (0.27 M thiol) the first fronts take longer to appear (around 18 minutes), there are significantly fewer fronts than 3-15, and the entire system switched around 21 minutes (3 minutes slower than 3-16). Thus, with less monomer, there were more fronts that occurred about 6 minutes sooner and propagated

for about 6 minutes before the entire dish switched. However, with the doubled

monomer concentration, it could be argued that no true fronts occurred, and the entire

system switched from acid to base rather uniformly except for the few fronts that

showed up towards the end, after the acid buffer was overcome throughout the petri

dish.

Time = 13.17 min	Time =14.00 min	Time = 14.83 min	Time = 15.67 min
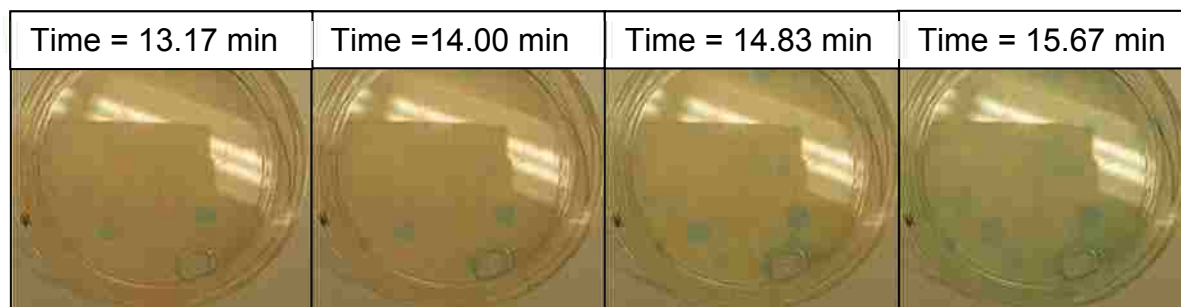
Figure 3-15. Time-lapse images of fronts. Petri dish diameter = 60 mm, solution height = 1 mm. $[ETTMP]_0 = 0.13$ M, $[PEGDA]_0 = 0.2$ M, $[urease]_0 = 1.25$ mg/mL, and $[urea]_0 = 0.06$ M.

Time = 16.83 min	Time =19.50 min	Time = 20.50 min	Time = 21.33 min
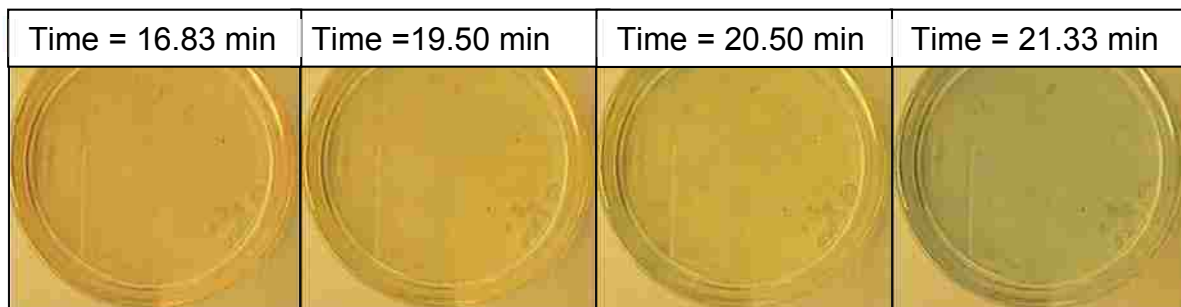
Figure 3-16. Time-lapse images of fronts. Petri dish diameter = 60 mm, solution height = 1 mm. $[ETTMP]_0 = 0.27$ M, $[PEGDA]_0 = 0.4$ M, $[urease]_0 = 1.25$ mg/mL, and $[urea]_0 = 0.06$ M.

From these Figures (3-15 and 3-16) it can be seen that the increase in acid

content does affect the fronts produced. The speed of the fronts with the higher ETTMP

concentration could not be measured because the entire system switched before any

true fronts appeared. This can be explained by the large amount of ammonia present in

the system after 3-MPA buffer is overcome,[2a] allowing the system to increase in pH quickly.

Figure 3-17 shows the 0.63 mg/mL urease, Figure 3-18 shows 1.25 mg/mL urease, and Figure 3-19 shows 2.0 mg/mL urease. With the increase in urease concentration there was an increase in front velocity and the number of fronts that appeared and a decrease in both the time needed for fronts to occur and the length of propagation before the entire system switched. The 0.625 mg/mL urease solution started producing fronts around 4 minutes, and they propagated for about 6 minutes before the entire system switched. The 1.25 mg/mL system had fronts appear around 3.5 min and propagated for about 3.5 min before the entire dish switched. The 2.5 mg/mL dish had no fronts appear and the entire system switched in just over 1 minute. These results are easily visualized in Figures 3-17 through 3-19.

| Time = 4.67 min	Time = 6.33 min	Time = 8.00 min	Time = 9.67 min

Figure 3-17. Time-lapse images of fronts. Petri dish diameter = 60 mm, solution height = 1 mm. [urease]$_0$ = 0.63 mg/mL, [urea]$_0$ = 0.06 M, [ETTMP]$_0$ = 0.067 M, and [PEGDA]$_0$ = 0.1 M.

We can see from these results that the increase in urease concentration had a large effect on the number of fronts that occurred and also the length of time the fronts propagated before switching. The number of fronts doubled with the increase in urease

concentration from 0.625 mg/mL to 1.25 mg/mL. There was a smaller effect on the front

velocity, which only increased from 0.38 mm/min to 0.59 mm/min.

| Time = 3.83 min	Time = 4.67 min	Time = 5.50 min	Time = 6.33 min
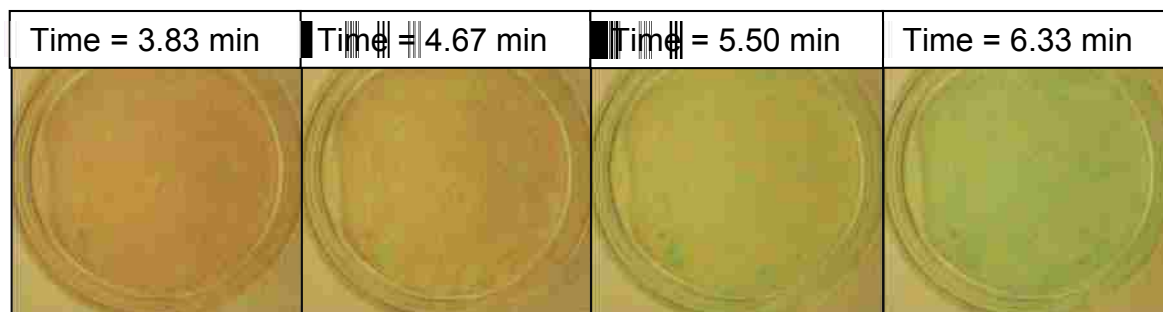
Figure 3-18. Time-lapse images of fronts. Petri dish diameter = 60 mm, solution height = 1 mm. $[urease]_0$ = 1.3 mg/mL, $[urea]_0$ = 0.06 M, $[ETTMP]_0$ = 0.067 M, and $[PEGDA]_0$ = 0.1 M.

Time = 0.00 min	Time = 0.33 min	Time = 0.67 min	Time = 1.17 min
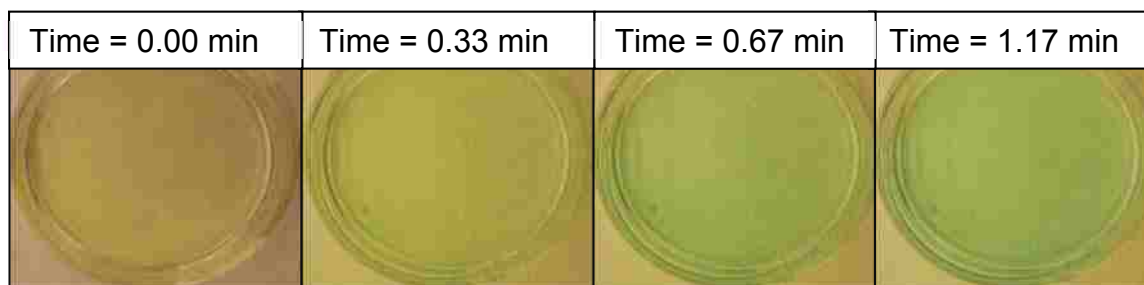
Figure 3-19. Time-lapse images of fronts. Petri dish diameter = 60 mm, solution height = 1 mm. $[urease]_0$ = 2.5 mg/mL, $[urea]_0$ = 0.06 M, $[ETTMP]_0$ = 0.067 M, and $[PEGDA]_0$ = 0.1 M.

Figures 3-20 and 3-21 show the difference between 0.005 M and 0.01 M urea

trials. 3-21, shows 0.005 M urea trials where the first fronts appeared around 10

minutes, propagated until a total switch at 19 minutes, and the front velocity was 0.29 ±

0.01 mm/min. Upon increasing the urea concentration to 0.01 M, the first fronts

appeared around 7 minutes, propagated until total switch at 13 minutes, and had a front

velocity of 0.45 ± 0.04 mm/min. Also, the number of fronts that appeared increased

slightly with increasing urea concentration.

Time = 12.00 min	Time = 13.67 min	Time = 15.13 min	Time = 17.00 min
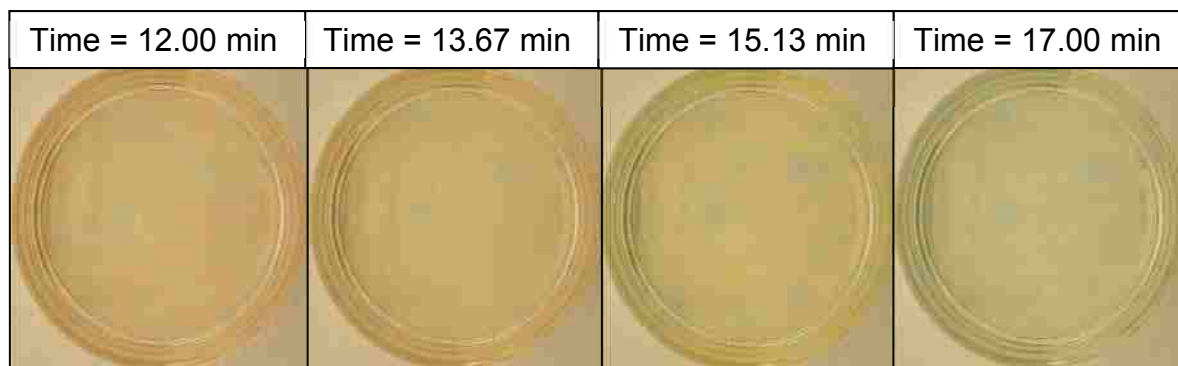
Figure 3-20. Time-lapse images of fronts. Petri dish diameter = 60 mm, solution height = 1 mm. $[urea]_0$ = 0.005 M, $[urease]_0$ = 1.3 mg/mL, $[ETTMP]_0$ = 0.067 M, and $[PEGDA]_0$ = 0.1 M.

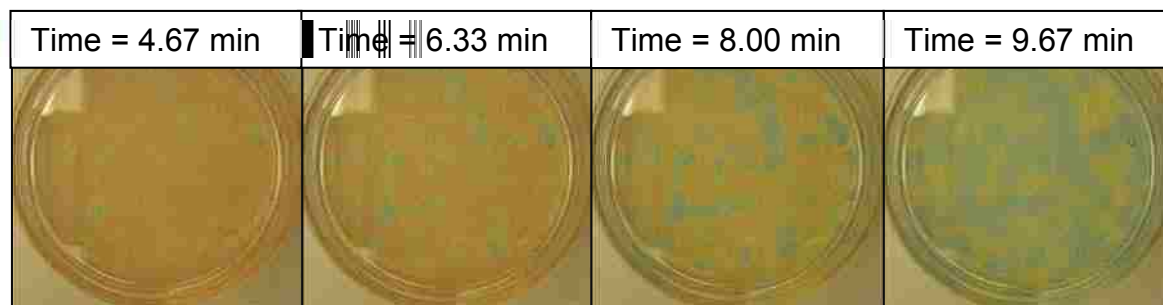| Time = 8.83 min	Time = 9.67 min	Time = 10.50 min	Time = 11.33 min
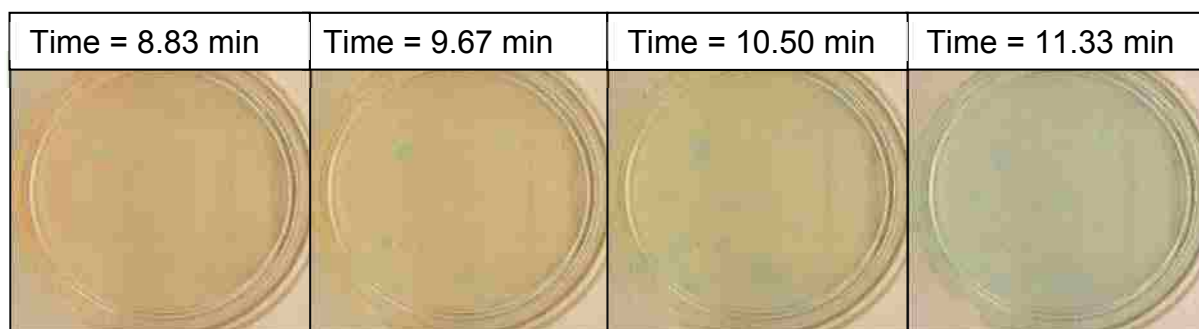
Figure 3-21. Time-lapse images of fronts. Petri dish diameter = 60 mm, solution height = 1 mm. $[urea]_0$ = 0.01 M, $[urease]_0$ = 1.3 mg/mL, $[ETTMP]_0$ = 0.067 M, and $[PEGDA]_0$ = 0.1 M.

When the urea concentration is increased again to 0.03 M the number of fronts that appeared significantly decreased, and the entire petri dish began to switch pH uniformly. With this trial there were a few fronts that appeared after the entire dish switched to ~pH 6 but that was it. The same thing happened to the rest of the urea variations, 0.05 M and 0.08 M, the pH of the entire petri dish increased uniformly. Because of this, only switch times can be recorded and are represented in the graph in Figure 3-12. Thus, these images are not shown here because no fronts were seen. As expected, increasing the urea concentration led to decreased switch times because more ammonia was being produced more quickly.

From these results, it can be seen that increasing the urease concentration had the greatest effect on the number of fronts that occurred and the switch time. It probably would have had the greatest effect on front velocity as well, however, this cannot be verified since the highest urease concentration switched before fronts could occur. Thus, leaving only 2 data points on the graph, which is not enough to form a trend. Although, the results in regards to the urea and urease reagents are similar to those observed in the system without monomers present.[2b]

3.4.3 – Polymer Fronts Imaged with Shadowgraphy and Schlieren Imaging

The images recorded and discussed in the previous section measured the change in pH of the solution with a visual aid from the universal pH indicator. However, this could not help with measuring the polymer fronts. The first attempts at using shadowgraphy to measure the polymer fronts were underwhelming. However, the right tools were not present in our lab so the images seen in Figure 3-22 are what were observed. Our collaborators did have the right equipment to perform the shadowgraph experiments so they handled those experiments for our manuscript. Although, there were still some important discoveries in our preliminary endeavors.

In Figure 3-22(A), a light was shone under the petri dish apparatus to see the differences in refractive indices of the solution within. A hole was drilled in the center of the petri dish cover so a drop of basic solution could be added to initiate the fronts. The basic solution added was some urea-urease clock reaction without monomers that had already clocked; the pH was about 9.2. The drop added was gently placed on top of the hole and capillary action pulled it into the petri dish. The addition was added in this way

so the front propagation could not be attributed to the force of injecting an aliquot of solution with the syringe.
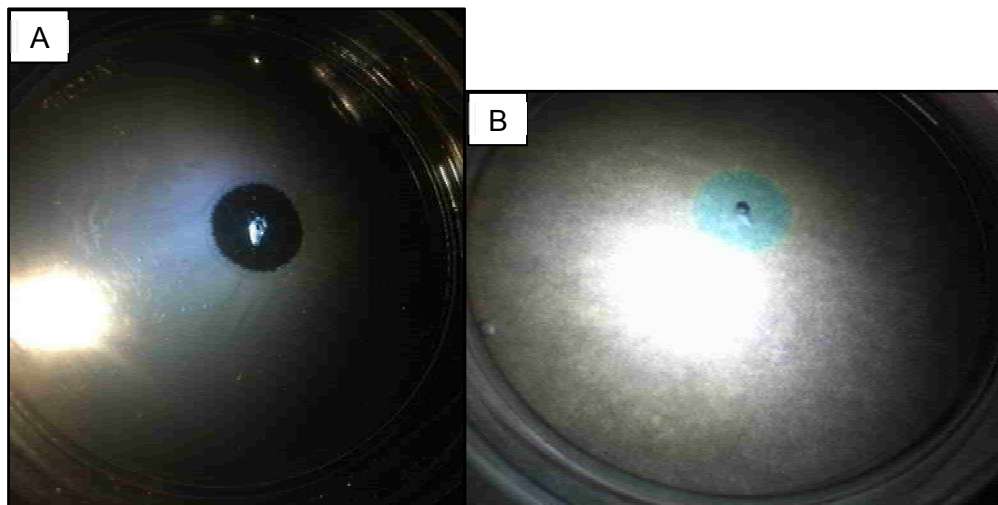
Figure 3-22. Shadowgraphs of a thin layer urea-urease clock reaction with ETTMP and PEGDA monomers and universal pH indicator. A) Shows the petri dish without a piece of white paper between the light and the dish so the change in turbidity can be seen. B) Shows the Petri dish with a piece of white paper between the light and dish so the universal indicator colors can be seen.

Shortly after the addition of the drop, the front began to propagate. As can be seen in Figure 3-22(A), the reacted section of solution in the center of the petri dish is clear, while the outskirts of the petri dish where the clock reaction has not switched yet is still cloudy. This is because the thiol functional group was deprotonated and became more soluble in the aqueous media once it became charged and more polar. This can be understood by looking at the work by Pritchard et al.[3] They determined the solubility of these ETTMP monomers in solution to be dependent on temperature and monomer concentration. At 4 °C ETTMP was most soluble below 10 weight percent and above 40 weight percent monomer in water. They also determined the pKa of ETTMP to be 9.87, which means at the basic pH observed in these experiments (pH 7.8 – 9.5) about 40 – 50% of the thiols were deprotonated.

In Figure 3-22(B), a white piece of paper was placed in between the petri dish and the light so the pH indicator colors could be seen. The propagating front is the yellow ring (pH 6- 7) in between the reacted basic blue (pH > 8) circle in the middle and the unreacted acidic red (pH < 4) area in the outside of the dish. This image was taken within 10 seconds of 3-23A. If Figure 3-22(B) is compared to Figure 3-22(A), the propagating front can be seen in both. In 3-22(A) the front is the ring around the clear center that has fingering occurring and both clear and cloudy areas can be seen within the ring. By comparing the two images it can be determined that the propagating front is around pH 6, and there is some dissolution of thiol within it. Since there are some clear fingers in the propagating front there could be some polymer formation. The change in turbidity of the solution indicates the thiol is dissolved but does not give us any information about the polymerization status.

The next course of action was to attempt to get some images with the aid of someone who has the equipment to perform the experiments. So with assistance from Dr. Patrick Bunton, Physics Professor at William Jewell College, some Schlieren images of the polymer fronts were obtained. Figures 3-23 through 3-26 show some representative Schlieren images taken in time-lapse mode of 4 petri dish experiments.

Figure 3-23 shows Schlieren images of a petri dish set up with 0.20 M ETTMP, 0.30 M PEGDA, 0.03 M urea, 0.63 mg/mL urease, and 4% (v/v) universal indicator. From these images it is apparent that the polymer fronts travel concurrently with the pH fronts. The monomers can react above pH 7 and increase in reactivity as pH increases. The basic center of each front area has already gelled and the reaction spreads out with the propagating fronts. Since the pH fronts travel relatively slowly (0.25 – 1.0 mm/min),

the polymer fronts have time to form with the pH fronts where the solution is between pH 6- 7. Even though this pH is rather low, the slow propagation of the pH fronts allows time for the gel to form, as is seen in the Schlieren images below.

The polymer front propagation of this trial can be seen in Figure 3-23 below. The blue/green textured circles are the basic gelled region, while the smooth red/orange area is the acidic liquid solution. As the neutral pH fronts propagate out slowly the polymer fronts do too. The entire petri dish was gelled at 20 minutes. To shorten the time of the experiment and reduce the amount of spontaneous front occurrence it was decided to initiate the solution in the petri dish with a drop of reacted urea-urease solution without monomers present (pH 9.2). In these trials the concentration of reagents was slightly altered as well. So none of the remaining trials can be compared to Figure 3-23. This trial was shown because it displays the polymer front propagation with the pH front propagation most clearly.

Time = 10.00 min	Time = 13.33 min	Time = 20.00 min

Figure 3-23. Schlieren images of Exp. 1. This experiment contained 0.2 M ETTMP, 0.3 M PEGDA, 0.03 M urea, 0.63 mg/mL urease, 4 % (v/v) universal indicator, no initiation of fronts.

Figure 3-24 shows the Schlieren images of the sixth experiment in the series 0.05 M ETTMP, 0.075 M PEGDA, 0.03 M urea, 0.93 mg/mL urease, and no universal indicator. The solution was initiated with a syringe needle by placing a drop of reacted

solution on top of the hole in the petri dish, allowing capillary action to insert the drop. This way, any fronts that appear cannot be attributed to the force of injection. Many spontaneous fronts can be observed in the first image of the sequence and propagate until the entire dish gelled at 8.50 minutes. The increase in the number of spontaneous fronts from the previous trial is due to the increase in urease concentration, decrease in monomer concentration, and possibly the removal of universal indicator from solution. The effect of urease and monomer concentration was shown to affect this system in this way in our published work.[33] However, the effect of universal indicator was not studied. It is not extensively studied in this work either, but could be a source of future work for someone interested in the effects. The components of universal indicator are an assortment of weak acids and bases and could have a buffering effect on the clock reaction.

Time = 0.25 min	Time = 6.08 min	Time = 8.50 min
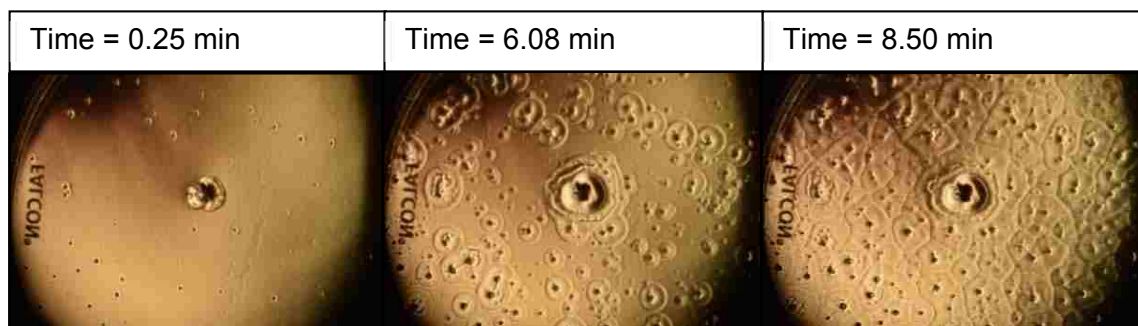
Figure 3-24. Schlieren Images of Exp 6. This experiment contained 0.05 M ETTMP, 0.075 M PEGDA, 0.03 M urea, 0.93 mg/mL urease, no universal indicator, and initiation of fronts in center with already reacted urea-urease solution (pH 9).

Figure 3-25 shows an experiment with all the same reagent concentrations as the previous experiment. The difference is the glass plate holding the petri dish was tilted to a 10° angle. The first image shows the syringe needle being removed from the petri dish after initiation. Many fronts are not visual for several minutes after initiation.

After 12.50 minutes the entire dish had gelled. This is 4 minutes (or 1.5 X) longer than

the untilted experiment present in Figure 3-24, possibly indicating a delay effect caused

by the tilt.
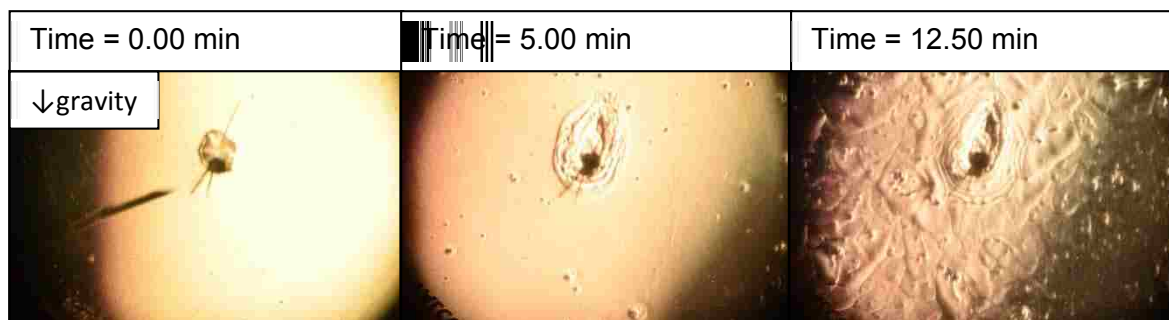
Figure 3-25. Schlieren Images of Exp. 8. This experiment contained 0.05 M ETTMP, 0.075 M PEGDA, 0.03 M urea, 0.93 mg/mL urease, no universal indicator, and initiation of fronts in center with already reacted urea-urease solution (pH 9). Also, the petri dish was tilted 10º.
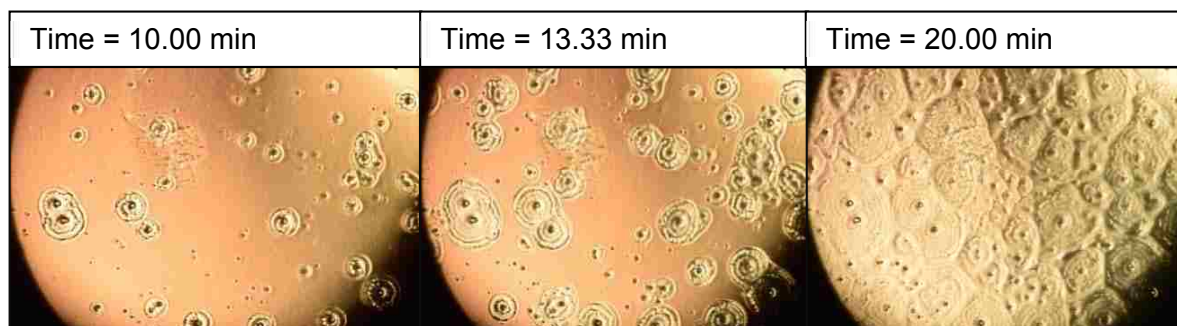

Figure 3-26: Schlieren Images of Exp. 7. This experiment contained 0.05 M ETTMP, 0.075 M PEGDA, 0.03 M urea, 0.93 mg/mL urease, 9% (v/v) universal indicator, and initiation of fronts in center with already reacted urea-urease solution (pH 9). Also, the petri dish was tilted 10º.

Another interesting observation is the apparent difference in front velocity

between the upward and downward propagating fronts. This is indicative of buoyancy

driven convective effects.[93] The reacted solution containing ammonia and carbon

dioxide is less dense than the unreacted solution containing urea. Thus, the reacted

solution floats up and raises the pH, triggering reaction of the monomers. In addition to

the convective effects of the solution, the polymerized monomer adheres to the petri dish. Thus, it cannot sink in solution to affect the pH in the unreacted solution below.

Figure 3-26 shows an experiment with the same reagent concentrations as 3-25 except 9% (v/v) universal indicator is used to observe pH fronts and see if there is a difference in reaction time with the indicator present. As before, the glass plate holding the petri dish was tilted to a 10° angle to see if any convective effects were present in the reaction. These images show that the fronts travel faster in the upward direction than in the downward direction, demonstrating buoyancy-driven convection again. The entire gel time of this experiment is 15.3 minutes, 3 minutes longer than the previous experiment without indicator and 7 minutes longer than the one without indicator and no tilt. This indicates the universal indicator plays a part in the delay of the reaction but more experiments would have to be performed to determine that definitively.

Based on these results the polymer fronts propagate with the pH fronts. By comparing the experiments with and without universal indicator it would appear the indicator delays the gel time of the system. This could be from the weak acids and bases present in the universal indicator creating a low concentration buffer in solution. We did not investigate this effect but it would be easy to test by varying the concentration of universal indicator and running a control without indicator. From that it could be determined if there was a trend between indicator concentration and clock time. If there is a buffer formed it would delay the clock time as we saw with increasing 3-MPA buffer concentration induced by increasing ETTMP concentration in the batch polymerization trials.

From the tilt it was also shown that the upward propagating fronts traveled faster than the downward propagating fronts. This is due to the change in solution density after urea is converted to carbon dioxide and ammonia. The reacted solution is less dense than the unreacted solution and subsequently rises up against gravity in the tilted apparatus. This causes the solution it diffuses into to become more basic and react more quickly than the solution below the initiation point. This is called buoyancy driven convection.

Another effect of the tilt was the delay in total gel time of the petri dish. Figures 3-24 through 3-26 showed increasing gel times of the entire petri dish with adding a 10° tilt to the petri dish and then adding universal indicator to the solution. This indicates the tilt and ions in the universal indicator may affect the clock reaction and polymerization but more precise studies would have to be done to say yes or no with certainty. We did not focus on those effects.

These experiments gave some insight into the nature of the propagating polymer fronts but is in no way a conclusive study of front velocities as the experimental parameters are altered. It can be said with certainty by looking at the images that had both indicator and polymer that the polymer fronts form with the pH fronts. However, more extensive and carefully prepared experiments are necessary to determine the effect reagent concentrations have on front velocities. More results from the front velocity experiments associated with this work can be read in our publication.[33]

3.4.4 - Swelling Studies of Hydrogel Discs

The swelling studies were performed to determine the rate of water uptake, the amount of water uptake, and the degree of degradation that occurs over time with water

present. Hydrogel discs were formed in flexible molds with varying ETTMP concentrations. After 24 hours of curing the discs were removed from the molds and lyophilized for 48 hours. After lyophilization the dry discs were weighed to determine the dry weight before possible degradation in the swelling studies. Swelling was performed with Dulbecco's phosphate-buffered saline (DPBS) (+Ca/+Mg) and DPBS (-Ca/-Mg) at 20 °C to see if there was a difference in swelling between the two saline buffers. The difference between the two buffers is the presence (+Ca/+Mg) and absence (-Ca/-Mg) of calcium and magnesium ions. These ions may affect certain proteins, like trypsin, from performing correctly by binding to the protein. Since the urease is not an active component in the hydrogel crosslinks and the hydrogel functional groups are not known to cause a reaction or complexation with the calcium and magnesium ions, there is no reason to believe that the presence or absence of calcium or magnesium would affect the swelling or degradation of the hydrogel. However, both were tested to ensure no difference was found between them. As can be seen in Figure 3-27, there was not a difference between discs from the same batch at 20 °C. Therefore, only DPBS (+Ca/+Mg) was used for future studies because it was readily available in the lab.

The equation to determine percentage swelling can be seen in (20).[94]

(20) $$\% \ swelling = \left(\frac{W_s - W_d}{W_d}\right) \times 100$$

W_s refers to the swollen weight at the time of measurement, and W_d is the dry weight after lyophilization. To determine the amount of mass erosion after swelling the same equation was used except the dried weight after the second lyophilization (after swelling for 225 hours) was used in place of W_s. This resulted in a negative number so the absolute value was taken.
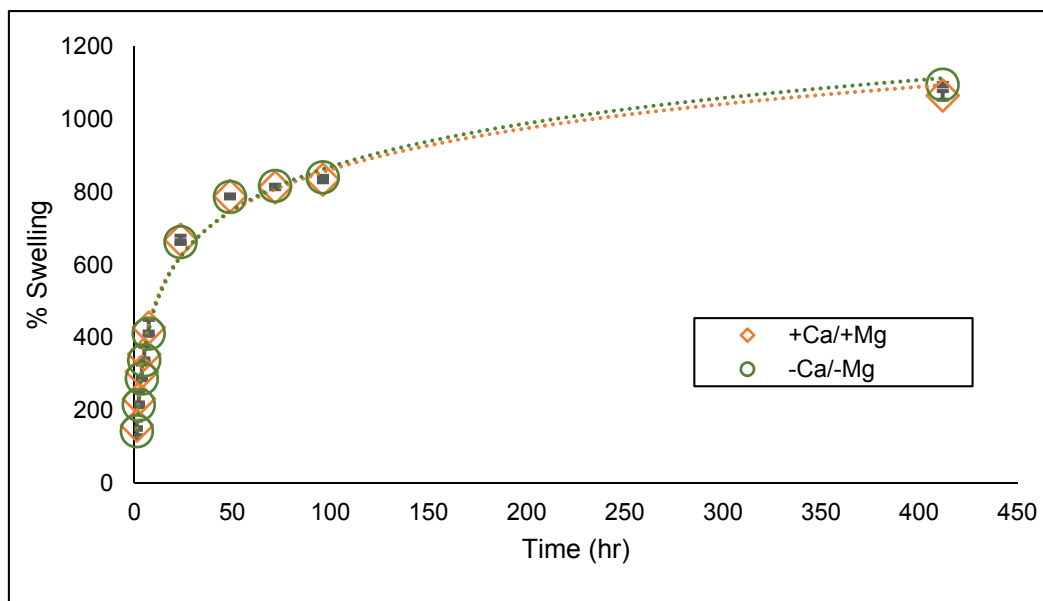
Figure 3-27. Comparison of DPBS +Ca/+Mg and DPBS -Ca/-Mg effect on swelling ratio at 20 °C. Initial concentrations were $[\text{urea}]_0 = 0.03$ M, $[\text{ETTMP}]_0 = 0.10$ M, and $[\text{urease}]_0 = 0.5$ mg/mL (17 units/mL).

The effect of temperature on swelling was also studied. Discs were swollen in DPBS (+Ca/+Mg) at 37 °C and 20 °C. The two temperatures were studied because PEG based polymers exhibit a lower critical solution temperature (LCST) that affects solubility in water.[95] The solubility of these monomers in water at various temperatures has been previously studied by Pritchard et al.[3] They determined the PEGDA (Mn = 400) was completely soluble from 4 – 37 °C; but, ETTMP (Mn = 1300) was not completely soluble at 37 °C. The concentration of monomers in water affected the solubility as well. They were least soluble at 25 wt% ETTMP. Above and below 25 wt.% they increased in solubility, being most soluble below 10 wt% and above 40 wt%.[3] For these experiments PEGDA (Mn = 575) was used but there was no noticeable change in solubility. Figures 3-28 and 3-29 show the swelling of various monomer concentrations at 37 °C and 20 °C, respectively.
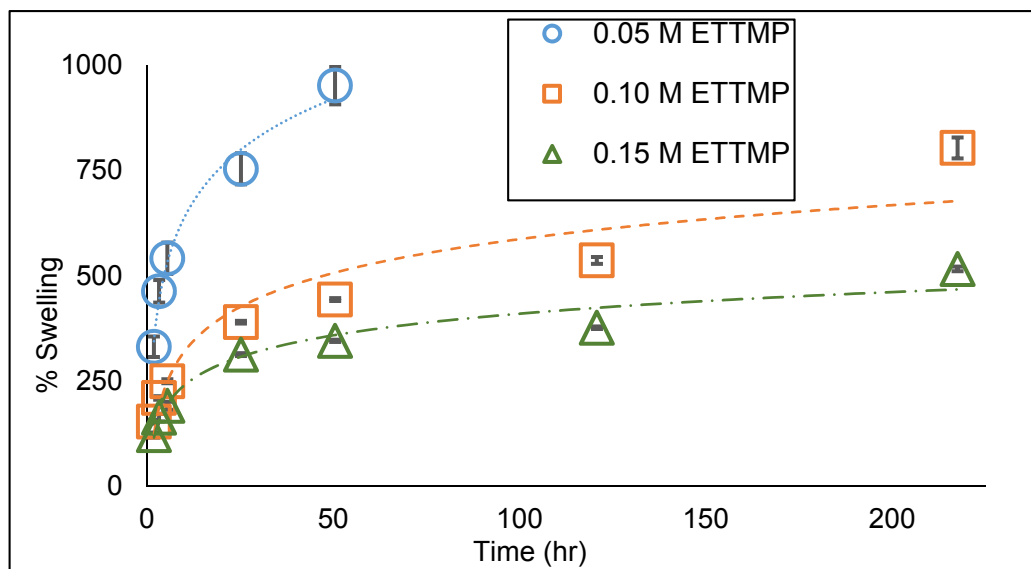
Figure 3-28. Swelling of discs in DPBS +Ca/+Mg at 37 °C. Initial concentrations were [urea]$_0$ = 0.03 M, [urease]$_0$ = 0.5 mg/mL (17 units/mL). 0.05 M discs were too degraded to weigh by 120 hr.
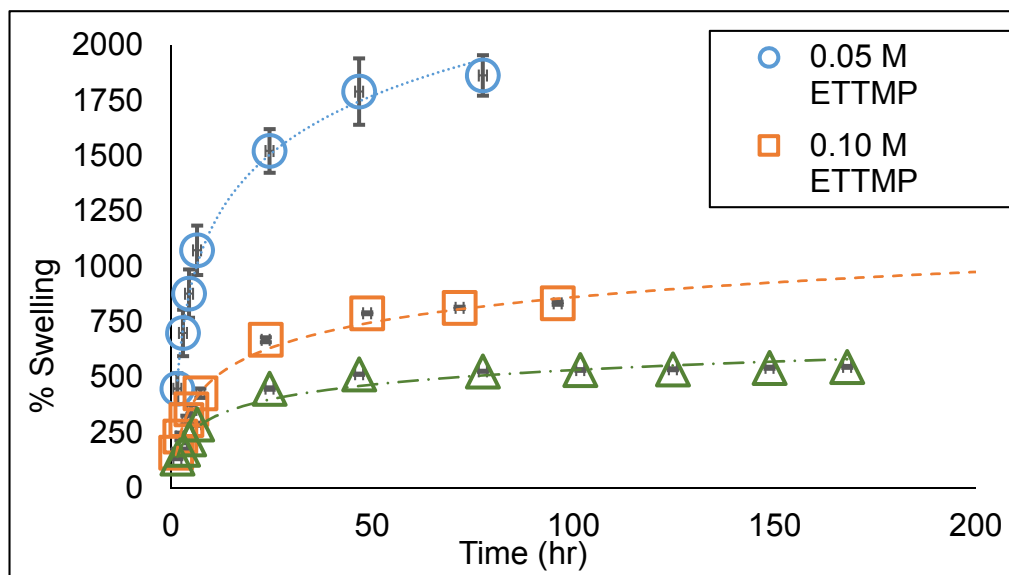
Figure 3-29. Swelling of discs in DPBS (+Ca/+Mg) at 20 °C. Initial concentrations were [urea]$_0$ = 0.03 M, [urease]$_0$ = 0.5 mg/mL (17 units/mL). 0.05 M discs were too degraded to weigh by 102 hr.

In both figures it is apparent that the 0.05 M ETTMP discs allowed for the most swelling and as monomer concentration increased swelling decreased. This is due to a change in the effective crosslink density.[71, 91, 96] When monomers are more dilute in the

73

solution during polymerization, this leads to more defects in crosslinking. For example, monomer chains can loop back on themselves, oligomer chains can form cyclic compounds not connected to the rest of the hydrogel, and unreacted chain ends are more likely to form. Conversely, a decrease in swelling seen with the increase in monomer concentration was not only do to effective crosslink formation, but also an increase in entanglements. These concentration dependent behaviors indicate that a defect-free hydrogel is not being formed. In an ideal network, the monomers would react equally with each other regardless of concentration.[71]

The 0.10 and 0.15 M discs in Figure 3-28 were lyophilized, and the dry weight was obtained at the end of the swelling study to determine the amount of mass erosion. The 0.10 M discs lost 33% ± 2% of dry mass after 225 hours in DPBS at 37 ºC. The 0.15 M discs lost 16% ± 2% of dry mass after 225 hours in DPBS at 37 ºC. Since fewer crosslinks need to be broken in the lower concentration gels it makes sense that gel degradation and mass erosion happen faster than in the higher monomer concentration gels.

Another interesting difference between the incubated and room temperature trials is that the incubated trials did not swell as much as the room temperature trials. This is due to the LCST of PEG containing monomers. Specifically, in this case, the ETTMP segments of the hydrogel. While PEGDA has an LCST well above the incubated temperature (37 ºC), the ETTMP has an LCST below 37 ºC.[3] That means the ETTMP portions of the hydrogel shrink up because they are less soluble in the water. This reduces the volume of water that can be present in the hydrogel, which was found by

Metters and Hubbell to reduce the rate of ester hydrolysis in thiol-acrylate hydrogels.[91] They developed Equation 21, the rate equation for ester linkage hydrolysis in hydrogels.

(21) $$\frac{d([Ester])}{d(t)} = k_0[H_2O][Ester]$$

This states that the change in ester concentration over time is dependent upon k_0 (the true second-order rate constant of ester degradation), water concentration, and ester concentration. Thus, water concentration plays an important factor in the degradation of ester linkages. This explains why the less swollen hydrogel studied in the incubator does not degrade as quickly as the more swollen discs at room temperature.

3.5 - Conclusions

In this chapter it was shown that the urea-urease clock reaction could be used to trigger a Michael-addition thiol-acrylate hydrogel polymerization. By changing the urea concentration the clock time, gel time, degradation time, storage modulus of the hydrogel, and front velocities could be tuned. With increasing urea concentrations came increased ammonia concentrations. This affected the rate of ammonia production, which decreased the clock and gel times and increased the front velocities. Increasing the ammonia concentration also increased the pH of the final solution and hydrogel, which increased the degradation time and lowered the storage modulus, both because the rate of ester hydrolysis was higher. Increasing the urease concentration increased the clock time, gel time, and front velocities by producing more ammonia faster.

An increase in ETTMP concentrations had the opposite effects. With the clock time, gel time, and front velocities, an increase in ETTMP meant an increase in 3-MPA buffer concentration. Therefore, the initial pH was lower (decreasing the urease activity) and more ammonia needed to be produced to exceed the buffer capacity. This led to

longer clock and gel times and slower front velocities. With respect to the degradation time, storage modulus, and swelling, an increase in ETTMP concentration meant an increase in the number of bonds that could be formed and a decrease in ineffective bond formations. This led to longer degradation times, higher storage moduli, and less water uptake during swelling.

This system has proven to be tunable for all parameters tested by one or more reagents used. The monomers have been well studied as biomedical hydrogel compounds and are known to be biocompatible. Since the urea and urease are compounds found naturally in the body, it would lead one to believe that this system can operate in a biocompatible manner for use as a tunable, biodegradable hydrogel adhesive or therapeutic delivery vehicle. However, without specific cytotoxicity tests for this system specifically, it cannot be said for sure. The time-lapse polymerization capabilities of this system also afford the ability to have a benign, tunable cure-on-demand adhesive system capable of IFP applications. Furthermore, this is the first IFP system produced that does not rely on the gel effect to initiate or propagate the polymer fronts.

CHAPTER 4 – CONCLUSIONS

The bromate-sulfite clock reaction was not an achievable choice for creating a time-lapse crosslinking system. Not only was the clock reaction unable to be suppressed for a sufficient length of time, but the polymer crosslinking network chosen to accompany it was not successful either. The bromate-sulfite clock reaction has proven to be too complex to accurately model all the reactions present in solution. Based on the accepted reaction mechanisms and rate constants[1], computer simulations predicted that there were optimum concentrations of the clock reagents that would produce a storable solution for 3 months. However, experimental results proved that the longest delay in clock time achievable with addition of 18 M ammonium hydroxide was 2 hours.

Increasing the initial pH does not seem to halt the reaction kinetics of the clock reaction as drastically as predicted. This was apparent from the pH versus time plots collected when the initial pH was raised above 9 and the final pH of the solution. The decrease in pH when the solution was above 7 matched the time frame and trend of ammonia evaporation. Particularly, the linear decrease in pH from pH 10.5 to 8 represents the abundance of aqueous ammonia in solution that can easily volatize to gaseous ammonia and then the more gradual decrease in pH from 8 to 6 depicts the pH range where ammonia and ammonium create an internal buffer. In this range ammonium hydroxide is favored in the equilibrium and very little aqueous ammonia is present to evaporate, causing a delay in the decrease in pH.

This extended clock time would have been acceptable if the clock reaction still proceeded after ammonia evaporation. However, there was never an abrupt change in

pH as there should be with a pH clock reaction. Also, the final pH ranged from 4 – 5, instead of 2 – 4 as it should have with the autocatalytic production of protons in the bromate-sulfite reaction. This indicated that the sulfite was being completely consumed at a high pH where bisulfite is not present, causing no net change in pH.

Even though a storage stable system was not developed, creation of a time-lapse crosslinking system was attempted. The polycarbodiimides (PCDIs) were crosslinked with either maleic or malonic acid in a test run before addition to the clock reaction system. They proved to be reactive with one another, yet, after addition to the clock reaction system no gelation was seen after the drop in pH. This is most likely due to either the reaction of bromate with the malonic and maleic acids in a BZ type reaction or the reaction of sulfuric acid with the PCDIs[78, 97]. Either of which could hinder the crosslinking of PCDI by malonic or maleic acid. With the conclusion of these tests efforts were redirected to the urea-urease system.

There were many successful results with the urea-urease research. In the batch-cured experiments the reagent concentrations were altered to study the effect on clock time, gel time, degelation time, storage modulus, and percentage swelling of the dried hydrogel samples. Increasing the urea concentrations resulted in an increase in ammonia produced and a decrease in clock and gel times. Another effect of the increased ammonia concentration was a higher final pH. The higher pH resulted in a decrease in degelation times and storage moduli, while increasing the percentage swelling observed. This is because the higher final pH caused hydrolysis of the ester compounds present in the hydrogel.[98]

Increasing the urease concentrations resulted in an increase in reaction rate with urea and decreased the clock and gel times. However, urease concentration had no effect on the hydrogel formation or resulting mechanical properties of the hydrogel.

The monomers used, Thiocure® 1300 (ETTMP) and poly(ethylene glycol) diacrylate 700 (PEGDA) were always kept in a 2:3 molar ration to ensure a 1:1 functional group ratio. The ETTMP contained residual 3-mercaptopropionic acid (3-MPA) from synthesis of the monomers. This acid proved useful in creating the time-lapse polymerization system because acid is needed to create the urea-urease clock reaction. By using the 3-MPA, no additional chemicals were needed because the varying monomer concentrations used in this study reduced the pH of the solution to an appropriate range (pH 3.25 – 3.75) to create the clock reaction.

Increasing the monomer concentrations resulted in an increase in 3-MPA concentration, an increase in the number of effective crosslinks formed in the hydrogel, and a decrease in the amount of water present in the hydrogel. The increase in 3-MPA caused a decrease in the initial pH and a larger buffer capacity of the system that needed to be overcome by the clock reaction.[2a] This caused an increase in clock, gel, and degelation times. The degelation time increase was due to the decrease in the final pH because the initial pH was lower, thus reducing the hydrolysis rate of the ester groups.[91, 99] An increase in the effective crosslinks resulted in higher storage moduli, an increase in degelation time (because more crosslinks had to be broken), and a decrease in percentage swelling (because the polymer chains did not have as much room to allow water uptake). The reduction in water content of the hydrogel also

resulted in a decrease in degelation time because there was less hydroxide present to hydrolyze the esters.

The swelling studies were performed on lyophilized hydrogel discs in DPBS at 20 ºC and 37 ºC. The discs displayed greater swelling capacity at 20 ºC than 37 ºC because of the LCST associated with the ETTMP monomer. 37 ºC is above the LCST of the ETTMP monomer, causing that portion of the polymer to become less soluble and shrink up.[3] This leaves less volume for the water to occupy within the discs. Since less water is present, the discs degrade slower than in the room temperature swelling studies. The difference between DPBS with and without calcium and magnesium ions was also investigated and there was no difference between the two.

Isothermal frontal polymerization experiments were also performed with this system. We were able to successfully create an IFP system that does not rely on the gel effect to propagate the polymer front. We were also able to show that the polymer fronts travel with the pH fronts. Also the front velocities do not decrease with time, signifying a true autocatalytic reaction-diffusion system was created.[57b] As expected from previous works on pH wave front propagation in the urea-urease system,[2b] increasing the clock reagents resulted in an increase in front occurrence and front velocities. Conversely, increasing the monomer concentrations meant an increase in 3-MPA, resulting in a decrease in front occurrence and front velocities. This system also displayed some buoyancy driven convective effects as a result of the decrease in density of the solution after urea is decomposed and ammonia is formed. The basic reacted solution rose up and catalyzed the polymerization of the solution above the front faster than the solution below the front.[93c]

Even though we were not able to create a storage stable time-lapse crosslinking system with the bromate-sulfite clock reaction, the urea-urease system proved to be a valuable reaction that has many applications in the biomedical and reversible adhesive fields. The hydrogel has already been proven to be biocompatible but its combination with the urea-urease system has not been studied. Since urea and urease are natural compounds found in the body it seems logical they could produce a biocompatible system. However, cytotoxicity tests would have to be done to ensure its safety.

Cytotoxicity tests are one area of future research for this system. After which, biomedical applications such as drug delivery or wound dressings could be explored. To further this study the mechanical properties of the hydrogels should be determined using dynamic mechanical analysis (DMA) at room and biological temperatures, and also the change in properties over time. The change in modulus over time would give a correlation to the change in crosslink density and a hint to its applicability in the swollen state. Knowing the mechanical properties in the dehydrated state would be useful for use it's as an adhesive.

REFERENCES

1.   (a) hanazaki, I. R., G., Origin of chemical instability in the bromate-sulfite flow system. *J. Chem. Phys.* **1996,** *105* (22), 9912-9920; (b) Okazaki, N.; Rábai, G.; Hanazaki, I., Discovery of Novel Bromate−Sulfite pH Oscillators with Mn2+ or MnO4- as a Negative-Feedback Species. *The Journal of Physical Chemistry A* **1999,** *103* (50), 10915-10920; (c) Rábai, G.; Kaminaga, A.; Hanazaki, I., Mechanism of the Oscillatory Bromate Oxidation of Sulfite and Ferrocyanide in a CSTR. *The Journal of Physical Chemistry* **1996,** *100* (40), 16441-16442.

2.   (a) Hu, G.; Pojman, J. A.; Scott, S. K.; Wrobel, M. M.; Taylor, A. F., Base-Catalyzed Feedback in the Urea–Urease Reaction. *J. Phys. Chem. B* **2010,** *114* (44), 14059-14063; (b) Wrobel, M. M.; Bánsági Jr., T.; Scott, S. K.; Taylor, A. F.; Bounds, C. O.; Carranzo, A.; Pojman, J. A., pH Wave-Front Propagation in the Urea-Urease Reaction. *Biophysical J.* **2012,** *103*, 610–615.

3.   Pritchard, C. D.; O'Shea, T. M.; Siegwart, D. J.; Calo, E.; Anderson, D. G.; Reynolds, F. M.; Thomas, J. A.; Slotkin, J. R.; Woodard, E. J.; Langer, R., An injectable thiol-acrylate poly(ethylene glycol) hydrogel for sustained release of methylprednisolone sodium succinate. *Biomaterials* **2011,** *32* (2), 587-597.

4.   Norling, P. M. Time-Lapse Free-Radical Polymerizable Composition. 4,000,150, 1977.

5.   Hu, G.; Pojman, J. A.; Bounds, C.; Taylor, A. F., Time-Lapse Thiol-Acrylate Polymerization Using a pH Clock Reaction. *J. Polym. Sci. Part A: Polym. Chem.* **2010,** *48*, 2955-2959.

6.   Oliveira, A. P.; Faria, R. B., The Chlorate−Iodine Clock Reaction. *J. Am. Chem. Soc.* **2005,** *127*, 18022–18023.

7.   Epstein, I. R.; Pojman, J. A., *An Introduction to Nonlinear Chemical Dynamics: Oscillations, Waves, Patterns and Chaos.* Oxford University Press: New York, 1998.

8.   (a) Williamson, F. S.; King, E. L., The Kinetics of the Reaction of Sulfite and Bromate1-2. *Journal of the American Chemical Society* **1957,** *79* (20), 5397-5400; (b) Higginson, W. C. E.; Marshall, J. W., 82. Equivalence changes in oxidation-reduction reactions in solution: some aspects of the oxidation of sulphurous acid. *Journal of the Chemical Society (Resumed)* **1957,** (0), 447-458; (c) Szirovicza, L.; Boga, E., The Kinetics of the Bromate-Sulfite Reaction System. *Int. J. Chem. Kinet.* **1998,** *30*, 869-874.

9.   Noyes, R. M.; Field, R. J.; Körös, E., Oscillations in Chemical Systems. I. Detailed Mechanism in a System Showing Temporal Oscillations. *J. Am. Chem. Soc.* **1972,** *94* (4), 1394-1395.

10.   Rábai, G.; Bazsa, G.; Beck, M. T., Kinetic investigation of the bromate–ascorbic acid–malonic acid system. *International Journal of Chemical Kinetics* **1981,** *13* (12), 1277-1288.

11.   Edblom, E. C.; Orbán, M.; Epstein, I. R., A New Iodate Oscillator: The Landolt Reaction with Ferrocyanide in a CSTR. *J. Am. Chem. Soc.* **1986,** *108*, 2826-2830.

12.   Edblom, E. C.; Gyorgyi, L.; Orban, M.; Epstein, I. R., Systematic design of chemical oscillators. 40. A mechanism for dynamical behavior in the Landolt reaction with ferrocyanide. *Journal of the American Chemical Society* **1987,** *109* (16), 4876-4880.

13.   Gaspar, V.; Showalter, K., The oscillatory Landolt reaction. Empirical rate law model and detailed mechanism. *Journal of the American Chemical Society* **1987,** *109* (16), 4869-4876.

14.   Noyes, R. M., A Generalized Mechanism for Bromate-Driven Oscillators. *J. Am. Chem. Soc.* **1980,** *102*, 4644-4649.

15.   Edblom, E. C.; Luo, Y.; Orbán, M.; Kustin, K.; Epstein, I. R., Kinetics and Mechanism of the Oscillatory Bromate-Sulfite-Ferrocyanide Reaction. *J. Phys. Chem.* **1989,** *93*, 2722-2727.

16.   Keresztessy, A.; Nagy, I. P.; Bazsa, G.; Pojman, J. A., Traveling Waves in the Iodate-Sulfite and Bromate-Sulfite Systems. *J. Phys. Chem.* **1995,** *99*, 5379-5384.

17.   Nagy, I. P.; Keresztessy, A.; Pojman, J. A., Periodic Convection in the Bromate - Sulfite Reaction: a "Jumping Wave". *J. Phys. Chem.* **1995,** *99*, 5385-5388.

18.   Rabai, G.; Kaminaga, A.; Hanazaki, I., Chaotic pH oscillations in the hydrogen peroxide-sulfite-ferrocyanide-hydrogen carbonate flow system. *Chemical Communications* **1996,** (18), 2181-2182.

19.   Szántó, T. G.; Rábai, G., pH Oscillations in the BrO3-−SO32-/HSO3- Reaction in a CSTR. *The Journal of Physical Chemistry A* **2005,** *109* (24), 5398-5402.

20.   Lloyd, D. R.; Burns, C. M., Coupling of Acrylic Polymers and Collagen by Use of a Water-Soluble Carbodiimide. I. Optimization of Reaction Conditions. *Journal of Polymer Science: Polymer Chemistry Edition* **1979,** *17*, 3459-3472.

21.   Lloyd, D. R.; Burns, C. M., Coupling of Acrylic Polymers and Collagen by Use of a Water-Soluble Carbodiimide. II. Investigations of the Coupling Mechanism. *Journal of Polymer Science: Polymer Chemistry Edition* **1979,** *17*, 3473-3483.

22.   (a) Wagner, K.; Block, H. D.; Schafer, W., Polyisocyanates which contain carbodiimide groups and which are stable in storage. Google Patents: 1981; (b)

Imashiro, Y.; Takahashi, I.; Horie, N.; Yamane, T.; Suzuki, S., Carbodiimide crosslinking agent, process for preparing the same, and coating material comprising the same. Google Patents: 2000; (c) Hamon, R. C., Carbodiimide driers for resin coating compositions. Google Patents: 1986; (d) West, M. W. J., Carbodiimides and processes therefor. Google Patents: 1994; (e) Brown, W. T., Wear-resistant coating composition and method of producing a coating. Google Patents: 2003.

23. Han, Z.-J.; Yabuuchi, N.; Hashimoto, S.; Sasaki, T.; Komaba, S., Cross-Linked Poly(acrylic acid) with Polycarbodiimide as Advanced Binder for Si/Graphite Composite Negative Electrodes in Li-Ion Batteries. *ECS Electrochemistry Letters* **2013,** *2* (2), A17-A20.

24. Balasubramanian, A.; Ponnuraj, K., Crystal Structure of the First Plant Urease from Jack Bean: 83 Years of Journey from Its First Crystal to Molecular Structure. *Journal of Molecular Biology* **2010,** *400* (3), 274-283.

25. Sumner, J. B., THE ISOLATION AND CRYSTALLIZATION OF THE ENZYME UREASE: PRELIMINARY PAPER. *Journal of Biological Chemistry* **1926,** *69* (2), 435-441.

26. Wöhler, F., Ueber künstliche Bildung des Harnstoffs. *Annalen der Physik* **1828,** *87* (2), 253-256.

27. (a) Laidler, K. J.; Hoare, J. P., The Molecular Kinetics of the Urea-Urease System. I. The Kinetic Laws. *Journal of the American Chemical Society* **1949,** *71* (8), 2699-2702; (b) Gorin, G.; Chin, C. C., Urease. VI. A new method of assay and the specific enzymic activity. *Anal Biochem* **1966,** *17* (1), 49-59; (c) Krajewska, B.; Zaborska, W., The effect of phosphate buffer in the range of pH 5.80–8.07 on jack bean urease activity. *Journal of Molecular Catalysis B: Enzymatic* **1999,** *6* (1–2), 75-81; (d) Blakeley, R. L.; Webb, E. C.; Zerner, B., Jack bean urease (EC 3.5.1.5). A new purification and reliable rate assay. *Biochemistry* **1969,** *8* (5), 1984-1990.

28. Qin, Y.; Cabral, J. M. S., Kinetic studies of the urease-catalyzed hydrolysis of urea in a buffer-free system. *Appl Biochem Biotechnol* **2014,** *49* (3), 217-240.

29. Weber, M.; Jones, M. J.; Ulrich, J., Optimisation of isolation and purification of the jack bean enzyme urease by extraction and subsequent crystallization. *Food and Bioproducts Processing 86* (1), 43-52.

30. (a) Blakeley, R. T.; Dixon, N. E.; Zerner, B., Jack bean urease VII. Light scattering and nickel(II) spectrum Thiolate → nickel(II) charge-transfer peaks in the spectrum of the β-mercaptoethanol-urease complex. *Biochimica et Biophysica Acta (BBA) - Protein Structure and Molecular Enzymology* **1983,** *744* (2), 219-229; (b) Benini, S.; Rypniewski, W. R.; Wilson, K. S.; Miletti, S.; Ciurli, S.; Mangani, S., A new proposal for urease mechanism based on the crystal structures of the native and inhibited

enzyme from Bacillus pasteurii: why urea hydrolysis costs two nickels. *Structure* **1999,** *7* (2), 205-16.

31.   (a) Upadhyay, L. S. B., Urease inhibitors: A review. *Indian Journal of Biotechnology* **2012,** *11* (October 2012), 381-388; (b) Krajewska, B.; Zaborska, W., Jack bean urease: the effect of active-site binding inhibitors on the reactivity of enzyme thiol groups. *Bioorganic chemistry* **2007,** *35* (5), 355-65.

32.   Krajewska, B.; Ciurli, S., Jack bean (Canavalia ensiformis) urease. Probing acid– base groups of the active site by pH variation. *Plant Physiol. Biochem.* **2005,** *43*, 651- 658.

33.   Jee, E.; Bánsági, T.; Taylor, A. F.; Pojman, J. A., Temporal Control of Gelation and Polymerization Fronts Driven by an Autocatalytic Enzyme Reaction. *Angew. Chem.* **2016,** *128* (6), 2167-2171.

34.   Zadorin, A. S.; Rondelez, Y.; Galas, J.-C.; Estevez-Torres, A., Synthesis of Programmable Reaction-Diffusion Fronts Using DNA Catalyzers. *Phys. Rev. Lett.* **2015,** *114* (6), 068301.

35.   Miguez, D. G.; Vanag, V. K.; Epstein, I. R., Fronts and pulses in an enzymatic reaction catalyzed by glucose oxidase. *Proc Natl Acad Sci U S A* **2007,** *104* (17), 6992- 7.

36.   Padirac, A.; Fujii, T.; Estévez-Torres, A.; Rondelez, Y., Spatial Waves in Synthetic Biochemical Networks. *J. Amer. Chem. Soc.* **2013,** *135* (39), 14586-14592.

37.   Bauer, G. J.; McCaskill, J. S.; Otten, H., Traveling Waves of *in vitro* evolving RNA. *Proc. Natl. Acad. Sci. USA* **1989,** *86*, 7937-7941.

38.   Semenov, S. N.; Markvoort, A. J.; de Greef, T. F.; Huck, W. T., Threshold sensing through a synthetic enzymatic reaction-diffusion network. *Angewandte Chemie (International ed. in English)* **2014,** *53* (31), 8066-9.

39.   Shiraki, Y.; Yoshida, R., Autonomous intestine-like motion of tubular self- oscillating gel. *Angewandte Chemie (International ed. in English)* **2012,** *51* (25), 6112-6.

40.   Lagzi, I.; Kowalczyk, B.; Wang, D.; Grzybowski, B. A., Nanoparticle oscillations and fronts. *Angewandte Chemie (International ed. in English)* **2010,** *49* (46), 8616-9.

41.   Kurin-Csorgei, K.; Epstein, I. R.; Orban, M., Systematic design of chemical oscillators using complexation and precipitation equilibria. *Nature* **2005,** *433* (7022), 139-42.

42.   Pojman, J. A.; Varisli, B.; Perryman, A.; Edwards, C.; Hoyle, C., Frontal Polymerization with Thiol-Ene Systems. *Macromolecules* **2004,** *37*, 691-693.

43.   Mota-Morales, J. D.; Gutierrez, M. C.; Sanchez, I. C.; Luna-Barcenas, G.; del Monte, F., Frontal polymerizations carried out in deep-eutectic mixtures providing both the monomers and the polymerization medium. *Chem. Comm.* **2011,** *47* (18), 5328-5330.

44.   Pojman, J. A. What is Frontal Polymerization? http://www.pojman.com/FP/FP-info.html (accessed March 7, 2013).

45.   Viner, V. G.; Pojman, J. A.; Golovaty, D., The effect of phase change materials on the frontal polymerization of a triacrylate. *Physica D: Nonlinear Phenomena* **2010,** *239*, 838-847.

46.   Chechilo, N. M.; Khvilivitskii, R. J.; Enikolopyan, N. S., On the Phenomenon of Polymerization Reaction Spreading. *Dokl. Akad. Nauk SSSR* **1972,** *204* (N5), 1180-1181.

47.   Chechilo, N. M.; Enikolopyan, N. S., Structure of the Polymerization Wave Front and Propagation Mechanism of the Polymerization Reaction. *Dokl. Phys. Chem.* **1974,** *214* (5), 174-176.

48.   Chechilo, N. M.; Enikolopyan, N. S., Effect of the Concentration and Nature of Initiators on the Propagation Process in Polymerization. *Dokl. Phys. Chem.* **1975,** *221* (5), 392-394.

49.   Chechilo, N. M.; Enikolopyan, N. S., Effect of Pressure and Initial Temperature of the Reaction Mixture during Propagation of a Polymerization Reaction. *Dokl. Phys. Chem.* **1976,** *230*, 840-843.

50.   Scognamillo, S.; Bounds, C.; Luger, M.; Mariani, A.; Pojman, J. A., Frontal cationic curing of epoxy resins. *Journal of Polymer Science Part A: Polymer Chemistry* **2010,** *48* (9), 2000-2005.

51.   Hu, T.; Chen, S.; Tian, Y.; Pojman, J. A.; Chen, L., Frontal free-radical copolymerization of urethane-acrylates. *J. Poly. Sci. Part A. Polym. Chem.* **2006,** *44*, 3018-3024.

52.   Mariani, A.; Fiori, S.; Chekanov, Y.; Pojman, J. A., Frontal Ring-Opening Metathesis Polymerization of Dicyclopentadiene. *Macromolecules* **2001,** *34*, 6539-6541.

53.   Fiori, S.; Mariani, A.; Ricco, L.; Russo, S., First Synthesis of a Polyurethane by Frontal Polymerization. *Macromolecules* **2003,** *36*, 2674-2679.

54.   Fiori, S.; Mariani, A.; Ricco, L.; Russo, S., Interpenetrating polydicyclopentadiene/polyacrylate networks obtained by simultaneous non-interfering frontal polymerization. *e-Polymers* **2002,** *29*, 1-10.

55.   Mariani, A.; Alzari, V.; Monticelli, O.; Pojman, J. A.; Caria, G., Polymeric nanocomposites containing polyhedral oligomeric silsesquioxanes prepared via frontal polymerization. *Journal of Polymer Science Part A: Polymer Chemistry* **2007,** *45* (19), 4514-4521.

56.   Pojman, J. A., Frontal Polymerization. In *Nonlinear Dynamics with Polymers: Fundamentals, Methods and Applications*, Pojman, J. A.; Tran-Cong-Miyata, Q., Eds. WILEY-VCH Verlag GmbH & Co. KGaA: Weinheim, 2010; pp 45-68.

57.   (a) Lewis, L. L.; DeBisschop, C. S.; Pojman, J. A.; Volpert, V. A., Isothermal Frontal Polymerization: Confirmation of the Mechanism and Determination of Factors Affecting Front Velocity, Front Shape, and Propagation Distance with Comparison to Mathematical Modeling. *J. Polym. Sci. Part A Polym. Chem.* **2005,** *43*, 5774-5786; (b) Pojman, J. A., Frontal Polymerization. In *Polymer Science: A Comprehensive Reference*, Matyjaszewski, K.; Möller, M., Eds. Elsevier BV: Amsterdam, 2012; Vol. 4, pp 957–980.

58.   Lewis, L. L.; Massey, K. N.; Meyer, E. R.; McPherson, J. R.; Hanna, J. S., New insight into isothermal frontal polymerization models: Wiener's method to determine the diffusion coefficients for high molecular-weight poly(methyl methacrylate) with neat methyl methacrylate. *Optics and Lasers in Engineering* **2008,** *46* (12), 900-910.

59.   Nuvoli, D.; Alzari, V.; Pojman, J.; Sanna, V.; Ruiu, A.; Sanna, D.; Malucelli, G.; Mariani, A., Synthesis and characterization of functionally gradient materials obtained by frontal polymerization. *ACS Appl. Mater. Interfaces* **2015,** *7*, 3600−3606.

60.   Mather, B. D.; Viswanathan, K.; Miller, K. M.; Long, T. E., Michael addition reactions in macromolecular design for emerging technologies. *Prog. Polym. Sci.* **2006,** *31*, 487-531.

61.   Parlato, M., Reichert, S., Barney, N., Murphy, W.L., Poly(ethylene glycol) Hydrogels with Adaptable Mechanical and Degradation Properties for Use in Biomedical Applicaitons. *Macromol. Biosci.* **2014,** *14* (5), 687-698.

62.   Bouten, P. J. M., Zonjee, M., Bender, J., Yauw, S. T.K., van Goor, H., van Hest, J. C.M., Hoogenboom, R., The chemistry of tissue adhesive materials. *Progress in Polymer Science* **2014,** *39*, 1375-1405.

63.   Duarte, A. P., Coelho, J.F., Bordado, J.C., Cidade, M.T., Gil, M.H., Surgical adhesives: Systematic review of the main types and development forcast. *Progress in Polymer Science* **2012,** *37*, 1031-1050.

64.   Xu, K.; Cantu, D. A.; Fu, Y.; Kim, J.; Zheng, X.; Hematti, P.; Kao, W. J., Thiol-ene Michael-type formation of gelatin/poly(ethylene glycol) biomatrices for three-dimensional mesenchymal stromal/stem cell administration to cutaneous wounds. *Acta biomaterialia* **2013,** *9* (11), 8802-8814.

65.   Lutolf, M. P.; Weber, F. E.; Schmoekel, H. G.; Schense, J. C.; Kohler, T.; Muller, R.; Hubbell, J. A., Repair of bone defects using synthetic mimetics of collagenous extracellular matrices. *Nat Biotech* **2003,** *21* (5), 513-518.

66.   Young, J. L.; Engler, A. J., Hydrogels with time-dependent material properties enhance cardiomyocyte differentiation in vitro. *Biomaterials* **2011,** *32* (4), 1002-9.

67.   Jiang, Y., Chen, J., Deng, C., Suuronen, E. J., Zhong, Z., Click hydrogels, microgels and nanogels: Emerging platforms for drug delivery and tissue engineering. *Biomaterials* **2014,** *35,*

4969-4985.

68.   Kharkar, P. M., Rehmann, M.S., Skeens, K.M., Maverakis, E., Kloxin, A.M., Thiol-ene Click Hydrogels for Therapeutic Delivery. *ACS Biomater. Sci. Eng.* **2016,** *2*, 165-179.

69.   Heuser, T.; Steppert, A.-K.; Molano Lopez, C.; Zhu, B.; Walther, A., Generic Concept to Program the Time Domain of Self-Assemblies with a Self-Regulation Mechanism. *Nano Letters* **2015,** *15* (4), 2213-2219.

70.   Lutolf, M. P.; Tirelli, N.; Cerritelli, S.; Cavalli, L.; Hubbell, J. A., Systematic Modulation of Michael-Type Reactivity of Thiols through the Use of Charged Amino Acids. *Bioconjugate Chemistry* **2001,** *12* (6), 1051-1056.

71.   Lutolf, M. P., Hubbell, J. A., Synthesis and Physicochemical Characterization of End-Linked Poly(ethylene glycol)-co-peptide Hydrogels Formed by Michael-Type Addition. *Biomacromolecules* **2003,** *4*, 713-722.

72.   Chatani, S.; Sheridan, R. J.; Podgórski, M.; Nair, D. P.; Bowman, C. N., Temporal Control of Thiol-Click Chemistry. *Chem. Mater.* **2013,** *25*, 3897−3901.

73.   (a) Wu, D.-C.; Liu, Y.; He, C.-B., Thermal- and pH-Responsive Degradable Polymers. *Macromolecules* **2008,** *41* (1), 18-20; (b) Siegel, R. A., Stimuli sensitive polymers and self regulated drug delivery systems: A very partial review. *J. Control. Release* **2014,** *190* (0), 337-351.

74.   Szirovicza, L.; Boga, E., The kinetics of the bromate–sulfite reaction system. *International Journal of Chemical Kinetics* **1998,** *30* (12), 869-874.

75.   (a) Lloyd, D. R.; Burns, C. M., Coupling of acrylic polymers and collagen by use of a water-soluble carbodiimide. II. Investigations of the coupling mechanism. *Journal of Polymer Science: Polymer Chemistry Edition* **1979,** *17* (11), 3473-3483; (b) Lloyd, D. R.; Burns, C. M., Coupling of acrylic polymers and collagen by use of a water-soluble carbodiimide. I. Optimization of reaction conditions. *Journal of Polymer Science: Polymer Chemistry Edition* **1979,** *17* (11), 3459-3472.

76.   Vlek, P. L. G.; Stumpe, J. M., Effects of Solution Chemistry and Environmental Conditions on Ammonia Volatilization Losses From Aqueous Systems1. *Soil Science Society of America Journal* **1978,** *42* (3).

77.   (a) Richetti, P.; Kepper, P.; Roux, J. C.; Swinney, H. L., A crisis in the Belousov-Zhabotinskii reaction: Experiment and simulation. *Journal of Statistical Physics 48* (5), 977-990; (b) Gao, Y.; Foersterling, H.-D.; Noszticzius, Z.; Meyer, B., HPLC Studies on the Organic Subset of the Oscillatory BZ Reaction 1. Products of the Ce4+-Malonic Acid Reaction. *The Journal of Physical Chemistry* **1994,** *98* (34), 8377-8380; (c) Försterling, H.-D.; Murányi, S.; Noszticzius, Z., Evidence of Malonyl Controlled Oscillations in the Belousov-Zhabotinsky Reaction (Malonic Acid-Bromate-Cerium System). *J. Phys. Chem.* **1990,** *94*, 2915-2921; (d) Försterling, H.-D.; Noszticzius, Z., An Additional Negative Feedback Loop in the Classical Belousov-Zhabotinsky Reaction: Malonyl Radical as a Second Control Intermediate. *J. Phys. Chem.* **1989,** *93*, 2740-2748.

78.   Hoiberg, C. P.; Mumma, R. O., Preparation of sulfate esters. Reactions of various alcohols, phenols, amines, mercaptans, and oximes with sulfuric acid and dicyclohexylcarbodiimide. *Journal of the American Chemical Society* **1969,** *91* (15), 4273-4278.

79.   Vermonden, T., Censi, R., Hennink, W.E., Hydrogels for Protein Delivery. *Chemical Reviews* **2012,** *112*, 2853-2888.

80.   Boekhoven, J.; Poolman, J. M.; Maity, C.; Li, F.; van der Mee, L.; Minkenberg, C. B.; Mendes, E.; van EschJan, H.; Eelkema, R., Catalytic control over supramolecular gel formation. *Nat Chem* **2013,** *5* (5), 433-437.

81.   (a) Ortega, I.; Jobbágy, M.; Ferrer, M. L.; del Monte, F., Urease Functionalized Silica: A Biohybrid Substrate To Drive Self-Mineralization. *Chemistry of Materials* **2008,** *20* (24), 7368-7370; (b) Rauner, N.; Meuris, M.; Dech, S.; Godde, J.; Tiller, J. C., Urease-induced calcification of segmented polymer hydrogels – A step towards artificial biomineralization. *Acta Biomaterialia* **2014,** *10* (9), 3942-3951; (c) Gutiérrez, M. C.; Jobbágy, M.; Ferrer, M. L.; del Monte, F., Enzymatic Synthesis of Amorphous Calcium Phosphate−Chitosan Nanocomposites and Their Processing into Hierarchical Structures. *Chemistry of Materials* **2007,** *20* (1), 11-13; (d) Yadav, V.; Pavlick, R. A.; Meckler, S. M.; Sen, A., Triggered Detection and Deposition: Toward the Repair of Microcracks. *Chemistry of Materials* **2014,** *26* (15), 4647-4652.

82.   Heuser, T.; Weyandt, E.; Walther, A., Biocatalytic Feedback-Driven Temporal Programming of Self-Regulating Peptide Hydrogels. *Angewandte Chemie (International ed. in English)* **2015,** *54* (45), 13258-62.

83.   Bychkova, V.; Shvarev, A.; Zhou, J.; Pita, M.; Katz, E., Enzyme logic gate associated with a single responsive microparticle: scaling biocomputing to microsize systems. *Chemical communications (Cambridge, England)* **2010,** *46* (1), 94-6.

84.   Yan, X.-Z.; Nijhuis, A. W. G.; van den Beucken, J. J. J. P.; Both, S. K.; Jansen, J. A.; Leeuwenburgh, S. C. G.; Yang, F., Enzymatic Control of Chitosan Gelation for Delivery of Periodontal Ligament Cells. *Macromol. Biosci.* **2014,** *14* (7), 1004-1014.

85.   Bissette, A. J.; Fletcher, S. P., Mechanisms of Autocatalysis. *Angewandte Chemie International Edition* **2013,** *52* (49), 12800-12826.

86.   Ludlow, R. F.; Otto, S., Systems chemistry. *Chem Soc Rev* **2008,** *37* (1), 101-8.

87.   (a) Chekanov, Y.; Pojman, J. A., Frontal Curing of Epoxy Resin: Comparison of Mechanical and Thermal Properties to Batch Cured Materials. *Proc. Amer. Chem. Soc. Div. Poly. Mater. Sci. Eng.* **1997,** *76*, 290-291; (b) Scognamillo, S.; Bounds, C.; Luger, M.; Mariani, A.; Pojman, J. A., Frontal cationic curing of epoxy resins. *J. Polym. Sci. Part A: Polym. Chem.* **2010,** *48* (9), 2000-2005.

88.   Robertson, I. D.; Hernandez, H. L.; White, S. R.; Moore, J. S., Rapid Stiffening of a Microfluidic Endoskeleton via Frontal Polymerization. *ACS Appl. Mater. Interfaces* **2014,** *6* (21), 18469-18474.

89.   Masere, J.; Lewis, L. L.; Pojman, J. A., Optical Gradient Materials Produced Via Low-Temperature Isothermal Frontal Polymerization. *J. Appl. Polym. Sci.* **2001,** *80*, 686-691.

90.   Nair, D. P.; Podgórski, M.; Chatani, S.; Gong, T.; Xi, W.; Fenoli, C. R.; Bowman, C. N., The Thiol-Michael Addition Click Reaction: A Powerful and Widely Used Tool in Materials Chemistry. *Chem. Mater.* **2014,** *26* (1), 724-744.

91.   Metters, A.; Hubbell, J., Network Formation and Degradation Behavior of Hydrogels Formed by Michael-Type Addition Reactions. *Biomacromolecules* **2004,** *6* (1), 290-301.

92.   Rydholm, A. E.; Anseth, K. S.; Bowman, C. N., Effects of neighboring sulfides and pH on ester hydrolysis in thiol-acrylate photopolymers. *Acta biomaterialia* **2007,** *3* (4), 449-455.

93.   (a) Nagy, I. P.; Pojman, J. A., Multicomponent Convection Induced by Fronts in the Chlorate-Sulfite Reaction. *J. Phys. Chem.* **1993,** *97*, 3443-3449; (b) Pojman, J. A.; Craven, R.; Khan, A.; West, W., Convective Instabilities In Traveling Fronts of Addition Polymerization. *J. Phys. Chem.* **1992,** *96*, 7466-7472; (c) Pojman, J. A.; Epstein, I. R., Convective Effects on Chemical Waves. 1. Mechanisms and Stability Criteria. *J. Phys. Chem.* **1990,** *94*, 4966-4972; (d) Pojman, J. A.; Epstein, I. R.; McManus, T.; Showalter, K., Convective Effects on Chemical Waves. 2. Simple Convection in the Iodate-Arsenous Acid System. *J. Phys. Chem.* **1991,** *95*, 1299-1306; (e) Pojman, J. A.; Epstein, I. R.; Nagy, I., Convective Effects on Chemical Waves. 3. Multicomponent Convection in the Iron(II)-Nitric Acid System. *J. Phys. Chem.* **1991,** *95*, 1306-1311.

94.   Temenoff, J. S.; Athanasiou, K. A.; Lebaron, R. G.; Mikos, A. G., Effect of poly(ethylene glycol) molecular weight on tensile and swelling properties of oligo(poly(ethylene glycol) fumarate) hydrogels for cartilage tissue engineering. *Journal of biomedical materials research* **2002,** *59* (3), 429-437.

95.   Kjellander, R.; Florin, E., Water structure and changes in thermal stability of the system poly(ethylene oxide)-water. *Journal of the Chemical Society, Faraday Transactions 1: Physical Chemistry in Condensed Phases* **1981,** *77* (9), 2053-2077.

96.   (a) Hasa, J.; Janáček, J., Effect of Diluent Content during Polymerization on Equilibrium Deformational Behavior and Structural Parameters of Polymer Network. *Journal of Polymer Science Part C: Polymer Symposia* **1967,** *16* (1), 317-328; (b) Baker, J. P.; Hong, L. H.; Blanch, H. W.; Prausnitz, J. M., Effect of Initial Total Monomer Concentration on the Swelling Behavior of Cationic Acrylamide-Based Hydrogels. *Macromolecules* **1994,** *27* (6), 1446-1454.

97.   Noszticzius, Z.; McCormick, W. D.; Swinney, H. L., Effect of Trace Impurities on a Bifurcation Structure in the Belousov-Zhabotinskii Reaction and Preparation of high-Purity Malonic Acid. *J. Phys. Chem.* **1987,** *91*, 5129-5134.

98.   Metters, A. T.; Anseth, K. S.; Bowman, C. N., Fundamental studies of biodegradable hydrogels as cartilage replacement materials. *Biomedical sciences instrumentation* **1999,** *35,* 33-8.

99.   Lin, C.-C.; Metters, A. T., Hydrogels in controlled release formulations: Network design and mathematical modeling. *Adv. Drug Deliv. Rev.* **2006,** *58* (12–13), 1379-1408.

VITA

Elizabeth Nicole Pohlmann Jee was born in Kenner, Louisiana in February 1987. Elizabeth attended Grace King High School, graduating in the top 10% of her class of ~450 students in 2005. She attended The University of Southern Mississippi from 2005 – 2007, changing her major 5 times trying to figure out what career she could envision for herself. She started out with dreams of being an actress, but quickly realized her talents were not strong enough to make a viable career out of it. The theatre still remains her passion today.

In the spring of 2007 Elizabeth decided to return to Louisiana to be near her family. At this point she wondered whether her childhood dreams of being a pediatrician were still worth pursuing. So she enrolled as a chemistry major to get an edge over the biology students applying to medical school. During her career at Southeastern Louisiana University the kind, caring professors at SELU convinced her that being a scientist was "where it was at" in life. She graduated from SELU with her Bachelor's degree in chemistry (biochemistry concentration) in May 2010. During her last year at Southeastern she applied to the chemistry graduate program at LSU and was accepted.

In August 2010 she started her career as a graduate student at the Louisiana State University and in January 2011 she joined the Pojman Research Team. In February 2011 Elizabeth and husband David welcomed their beautiful daughter, Amalie, into the world. Thanks to her vast support network of family, friends, and professors she has learned some great chemistry and had fun doing it. Elizabeth is a candidate to receive a Doctorate of Philosophy in Chemistry, specializing in Macromolecular Chemistry, in August 2016.